

# Modeling Intra-abdominal High Grade Serous Ovarian Cancer of Human Origin in Nude Mice

Sarah Saeed Alghamdi, MBBS  
Dr. Telleria's Research Laboratory  
Department of Pathology  
McGill University  
Montreal, Quebec, Canada

June, 2018

A thesis submitted to McGill University in partial fulfillment  
of the requirements for the degree of  
Master of Science (MSc) in Pathology

© Sarah Saeed Abdulwahed Alghamdi

2018

# Table of Contents

|  |    |
|--|----|
| List of Tables .....   | 4  |
| List of Figures .....  | 5  |
| Abstract .....   | 7  |
| 1. Introduction .....  | 15 |
| 1.1 Ovary as an organ: Anatomy and histology .....   | 15 |
| 1.2 Ovarian cancer .....   | 17 |
| 1.2.1 Classification of epithelial ovarian cancer .....  | 17 |
| 1.2.2 Challenges in Screening .....  | 25 |
| 1.2.3 Staging .....  | 27 |
| 1.2.4 Challenges in treatment .....  | 31 |
| 1.2.5 Prognosis .....  | 34 |
| 1.3 High grade ovarian serous carcinoma (HGSOC) .....  | 36 |
| 1.3.1 Pathogenesis, histopathology and molecular background .....  | 36 |
| 1.3.2 Previous experimental models .....   | 37 |
| 2. Hypothesis and Specific aims .....  | 42 |
| 2.1 Hypothesis .....   | 43 |
| 2.2 Aim 1: To study the expression of biomarkers of HGSOC in established human cell lines<br>with genetic fidelity of HGSOC according to TCGA studies .....  | 43 |
| 2.3 Aim 2: To investigate the macroscopic and microscopic intra-abdominal disease in nude<br>mice inoculated with genetically defined human HGSOC cells..... | 44 |
| 2.4 Aim 3: To evaluate the degree of heterogeneity among various genetically defined<br>HGSOC cell lines in functional studies .....                         | 44 |
| 3. Material and Methods .....  | 45 |
| 3.1 Cell culture .....   | 45 |
| 3.2 Immunocytochemistry .....  | 45 |
| 3.3 Immunohistochemistry .....   | 45 |

|  |     |
|--|-----|
| 3.4 Mouse xenografts .....   | 47  |
| 3.5 Tissue collection .....  | 48  |
| 3.6 Migration assay .....  | 48  |
| 3.7 Invasion assay .....   | 49  |
| 3.8 Double staining with Alexa Fluor 594 Phalloidin and Sytox Green .....  | 49  |
| 3.9 Microscopy .....   | 50  |
| 3.10 Statistical analysis .....  | 50  |
| 3.11 Study Approval .....  | 50  |
| 3.12 Cell line authentication .....  | 51  |
| 4. Results .....   | 52  |
| 4.1 In Vitro properties of ovarian cancer (OC) cell lines .....  | 52  |
| 4.2 Characterization of HGSOc cell lines using immunocytochemistry (ICC) .....                                     | 54  |
| 4.3 In vivo tumor growth and characterization .....  | 63  |
| 4.3.1 Tumor latency and disease presentations .....  | 63  |
| 4.3.2 Macroscopic and microscopic pathological assessment of the tumor .....                                       | 66  |
| 4.3.3 Immunohistochemistry evaluation of the in vivo tumor growth .....  | 79  |
| 4.3.4 Higher cell loads of PEO14 showed more aggressive behavior without significant change in tumor latency ..... | 88  |
| 4.4. In vitro functional characterizations of the OC cell lines .....  | 96  |
| 5. Discussion .....  | 105 |
| 6. Conclusion and future directions .....  | 116 |
| 7. References .....  | 117 |
| 8. Appendix .....  | 123 |

## **List of tables**

Table (1) Comparison between type I and type II OC

Table (2) Comparison among type I epithelial OC

Table (3) Stages of ovarian cancer

Table (4) Low-grade versus high-grade serous OC

Table (5) Lists of the antibodies used in the study

Table (6) Summary of the immunohistochemical biomarkers expressed in different OC cell lines

Table (7) Tumor latency, presenting symptoms and ascites components among the tested animals

Table (8) The common site of tumor dissemination recorded within the abdominal and pelvic cavity for each cell line.

Table (9) Advantages and limitations of patient-derived cells and cell lines

Table (10) Comparison between xenograft model and genetically engineered model

Table (11) Advantages and limitations for two types of immunodeficient mice

Table (12) Comparison between in vivo and in vitro biomarker expression using immunohistochemistry

## **List of figures**

Figure 1. Illustration of the ovarian structures

Figure 2. Histological types of epithelial ovarian cancer

Figure 3. Ovarian cancer staging

Figure 4. Mechanism of action of Bevacizumab

Figure 5. The 5-year survival rate of epithelial ovarian cancer

Figure 6. Ranking of the cell lines according to their HGSOC suitability

Figure 7. Bright field images of five different ovarian cancer cell lines (In culture)

Figure 8. P53 and PAX8 expression in different ovarian cancer cell lines

Figure 9. Expressions of different biomarkers in ovarian cancer cell lines (HGSOC)

Figure 10. Expressions of biomarkers in ovarian cancer cell lines (unlikely HGSOC)

Figure 11. Presentations of the disease and ascites components in different animals

Figure 12. Macroscopic disease developed within the peritoneal cavity of nude mice

Figure 13. Microscopic disease developed after the injection of OVCAR-4 cells

Figure 14. Microscopic disease developed within the animal injected with low load of PEO-14 cells

Figure 15. Microscopic disease developed within the animal injected with OVSAHO cells

Figure 16. Histopathology features of the tumors developed within the three cell lines (HGSOC)

Figure 17. Microscopic disease developed within A2780 animals

Figure 18. IHC evaluation of the tumor developed within animals injected with OVCAR-4 cells

Figure 19. IHC evaluation of the tumor developed in animals injected with low load of PEO14 cells

Figure 20. IHC evaluation of the tumor developed within animals injected with OVSAHO cells

Figure 21. IHC evaluation of the tumor developed within animals upon i.p. injection of A2780 cells

Figure 22. Disease presentation and macroscopic appearance of animals injected with high load cells of PEO14 intraperitoneally (i.p.)

Figure 23. Microscopic disease developed within the animal injected with high load of PEO14 cells

Figure 24. Immunohistochemical evaluation of the tumor developed with high load PEO14 cells

Figure 25. WT-1 expression of the tumor developed from high load of PEO14 cells

Figure 26. The expression of a human nuclear antigen in multiple tissues

Figure 27. Unique metastatic site in the lung

Figure 28. Comparison of migratory capacity among three cell lines that represent HGSOc

Figure 29 Comparison of the migratory capacity between five ovarian cancer cell lines

Figure 30 Comparison of the invasion capacity among the three cell lines that represent HGSOc

Figure 31 Comparison between five ovarian cancer cell lines in terms of their invasive capacities

## Abstract

**Background:** Ovarian cancer is the deadliest disease of the female reproductive tract. At the time of diagnosis, in most cases the disease has already progressed beyond the confines of the ovaries and into adjacent pelvic structures and various other sites within the peritoneal cavity. High-grade serous ovarian cancer (HGSOC) is the most common reported subtype, accounting for almost 70% of all ovarian cancer cases. Having a HGSOC mouse model with a phenotype of disease as close as it develops in humans, should allow a better assessment of preclinical therapeutic options as well as better understanding of the progression of the disease. Orthometastatic mouse models of peritoneal HGSOC are poorly described in the literature. Most of the ovarian cell lines studied in immunocompromised mice have been implanted subcutaneously instead of intraperitoneally thus not reflecting the nature of the disease, and, consequently, not allowing for a clear assessment of treatment responses. Moreover, most studies published utilized ovarian cancer cell lines that have low genetic fidelity with HGSOC. Hence, we created mouse models of HGSOC using cell lines with genetic fidelity to HGSOC aiming to allow better assessment of preclinical therapeutic options as well as better understanding of the progression of the disease.

**Methods:** Athymic nude mice were injected intraperitoneally with one of the following cell lines: OVCAR-4, PEO14, or OVSAHO. The three cell lines showed expression of ARID1A, PAX8 and mutant p53, with variable expression of CA125 and WT1. We contrasted among the models the time needed for the disease to develop, the tissues being targeted, and the histopathological abnormalities detected. We also ran functional assays to test and compare the ability of the cell lines for migration and invasion.

**Results:** The elapsed time for the disease to develop for all cell lines ranged from 4 to 11 months. This result stands in contrast with the less than 3 months it takes for the disease to evolve in the peritoneal cavity when injecting cells of unlikely HGSOc fidelity, such as SKOV-3 or A2780. Within the three cell lines used, we found commonalities and differences in terms of in vivo behavior. Among the commonalities, all cells homed to the omental-spleen-pancreatic area, liver base, mesentery and diaphragm. Among the differences, PEO14 cells developed sizable masses not invading the abdominal organs. OVSAHO cells developed more discrete masses closely surrounding yet not invading the organs. Finally, OVCAR-4 cells caused full invasiveness within the organs of the abdominal cavity in addition to developing micro-metastases in the lung. Animals injected with OVCAR-4 cells showed abundant bloody ascites heavily populated with multicellular structures (MCS). Animals injected with OVSAHO or PEO14 cells accumulated reduced volume of ascites fluid. In functional studies, OVCAR-4 has the highest migration and invasion capacity concordant with the in vivo behavior. Other cell lines have variable degree of heterogeneity of their invasion capacity when compared to their in vivo behavior.

**Conclusion:** Despite having used three cell lines with high genetic fidelity of HGSOc, they were heterogeneous in terms of disease progression when implanted intraperitoneally in nude mice.

## **Abstract (FRENCH)**

**Contexte:** Le cancer de l'ovaire est la maladie la plus mortelle de l'appareil reproducteur féminin. Au moment du diagnostic, dans la plupart des cas, la maladie a déjà progressé au-delà des ovaires, dans les structures pelviennes adjacentes et divers autres sites dans la cavité péritonéale. Le cancer ovarien séreux de haut grade (HGSOC) est le sous-type le plus commun, représentant près de 70% de tous les cas de cancer de l'ovaire. Avoir un modèle de souris HGSOC avec un phénotype de la maladie aussi proche qu'il se développe chez les humains, devrait permettre une meilleure évaluation des options thérapeutiques précliniques ainsi qu'une meilleure compréhension de la progression de la maladie. Les modèles de souris orthométastatiques de HGSOC péritonéale sont mal décrits dans la littérature. La plupart des lignées de cellules ovariennes étudiées chez des souris immunodéprimées sont implantées par voie sous-cutanée plutôt qu'intra-péritonéale, ne reflétant ainsi pas la nature de la maladie et, par conséquent, ne permettant pas une évaluation claire des réponses au traitement. De plus, la plupart des études publiées utilisaient des lignées cellulaires de cancer de l'ovaire qui ont une faible fidélité génétique avec HGSOC. Par conséquent, nous avons créé des modèles murins de HGSOC en utilisant des lignées cellulaires avec une fidélité génétique à HGSOC, visant à permettre une meilleure évaluation des options thérapeutiques précliniques ainsi qu'une meilleure compréhension de la progression de la maladie.

**Méthodes:** Des souris nudes athymiques ont été injectées par voie intrapéritonéale avec l'une des lignées cellulaires suivantes: OVCAR-4, PEO14 ou OVSAHO. Les trois lignées cellulaires ont montré l'expression de ARID1A, PAX8 et mutant p53, avec une expression variable de CA125 et WT1. Nous avons comparé entre les modèles le temps nécessaire pour que la maladie se développe, les tissus ciblés et les anomalies histopathologiques détectées. Nous avons également

effectué des tests fonctionnels pour tester et comparer la capacité des lignées cellulaires pour la migration et l'invasion.

**Résultats:** Le temps écoulé pour que la maladie se développe pour toutes les lignées cellulaires allait de 4 à 11 mois. Ce résultat est en contraste avec les moins de 3 mois nécessaires à l'évolution de la maladie dans la cavité péritonéale lors de l'injection de cellules de fidélité HGSOC improbable, telles que SKOV-3 ou A2780. Au sein des trois lignées cellulaires utilisées, nous avons trouvé des points communs et des différences en termes de comportement in vivo. Parmi les points communs, toutes les cellules se sont dirigées vers la zone omentale-rate-pancréatique, la base hépatique, le mésentère et le diaphragme. Parmi les différences, les cellules PEO14 ont développé des masses considérables qui n'envahissaient pas les organes abdominaux. Les cellules OVSAHO ont développé des masses plus discrètes, entourant étroitement les organes sans les envahir. Enfin, les cellules OVCAR-4 ont provoqué une invasivité totale dans les organes de la cavité abdominale en plus de développer des micro-métastases dans les poumons. Les animaux ayant reçu une injection de cellules OVCAR-4 présentaient une ascite sanglante, abondante, fortement peuplée de structures multicellulaires (MCS). Les animaux injectés avec des cellules OVSAHO ou PEO14 ont accumulé un volume réduit de liquide d'ascite. Dans les études fonctionnelles, OVCAR-4 a la capacité de migration et d'invasion la plus élevée concordant avec le comportement in vivo. D'autres lignées cellulaires ont un degré variable d'hétérogénéité

**Conclusion:** En dépit d'avoir utilisé trois lignées cellulaires avec une haute fidélité génétique de HGSOC, elles étaient hétérogènes en termes de progression de la maladie lorsqu'elles ont été implantées, par voie intrapéritonéale, chez des souris nude.

## **Acknowledgements**

“Thinking outside the box” is definitely an outstanding skill that is hard to acquire! During the two years of my Master’s degree, I found myself developing this skill on a daily basis. Of course, this would not have been possible without the tremendous amount of help and support I received from many people during this unforgettable journey. I joined Dr. Telleria’s research laboratory at McGill in May 2016, as my first ever learning experience away from home. This experience was preceded with many doubts, questions and sometimes fear! In my first meeting with Dr. Zorychta, Dr. Telleria and Dr. Goyeneche, I already felt at home! With all the encouragement and support I had received during my first few weeks, I was able to adapt myself to the new environment, navigate the system and build new lifelong career friends.

I first would like to specially thank our laboratory manager Dr. Goyeneche, who was the warm hug through all my ups and downs. She was never late when offering help and her office was always open whenever I ran into a trouble spot or had a question about my project. She always calmed me down whenever I was anxious or overwhelmed with my personal and professional lives. She tirelessly taught me ABC laboratory and kept doing the same until the last day. As a working mother, she always shared her experiences with me as a smart working mother of five smart kids. All of her kind gestures will not be forgotten! Moreover, she contributed to my project by running the animal experiments prior to my starting date and that was of great help to me to proceed faster in my project.

I also extend my thanks to my supervisor Dr. Telleria, whose maddening attention to details drove me to learn to be careful and precise when working and writing. I am so grateful for his

guidance during my journey, his interesting lectures during my courses and his paternal advice to improve my work. All of his efforts and time are appreciated!

I am also thankful for Dr. Zorychta, our program director, who was always there whenever I had any questions. Since the moment I decided to join McGill, she was always with me, step by step until I adapted myself to the system. She was never late when I had any inquiry or needed a letter of support. She also did her best to help me during my transition both when I joined McGill and when I left for Ontario. She is truly a leader who helps her team members to achieve their goals. Extended thanks also to Dr. Ling, our program coordinator for her help during our journey and for her contribution to bring so much fun and joy to our journeys. I would like to thank her specially for the Chinese tea that always comes at the right time.

Special thanks also go to my research advisors Dr. Lili Fu and Dr. Gao for their comments and meaningful contribution to this work. The time they took to listen to the presentations and to make corrections is highly appreciated.

Every journey comes with those people who always cheer you up. Thanks to my laboratory mates who always played that role. Thanks to the smiling lady (Sabrina) -who is also my coffee partner- for her ears that listen to my stories, complaints and non-sense words. As we shared many experiments together (part of the migration and the invasion assays), she was always the best to teach me every detail while keeping a smile on her face. I also would like to thank her specifically for the time she took to make editorial corrections for the English and the French texts in this thesis. I am also thankful for the scientist mother (Subeha Mahbuba) for inspiring me during her talk and when presenting to us. She has a wise counsel and sympathetic ears that I always needed. Thanks also to Michael and Robert, the two energetic young scientists of our laboratory.

Thanks to McGill, a prestigious institution, where I am super proud to be a student and graduate. Montreal was a terrific city in which I enjoyed my time with family and Canada was a great place to pursue my higher education.

This work could not have been done without the financial support of the government of Saudi Arabia- Ministry of Education and the departmental support of the Saudi Arabia Cultural Bureau. Thanks for my academic mentor (Majda Saleh) whose guidance I was lucky to be supervised by, thanks for her support and encouragement during my journey. She answered and is still answering my endless number of phone calls and she is never late to find a solution for any obstacle I encounter.

Last but not least, I must express my profound gratitude to my parents (Saleha Raddah and Saeed Alghamdi), my ultimate role models, whose love and prayers are with me in whatever I pursue. Most importantly, I wish to thank my loving husband (Naif) for providing me with unfailing support and continuous encouragement throughout my years of study and through the process of my project to writing this thesis. He blessed me with life full of support in the hours when it was all dark. This accomplishment would not have been possible without him being around. Thanks to GOD who sent me an angel and the sugar cube of my life, my little daughter (Loulwah) who brought so much joy and fun to my life.

## ***Dedication***

I dedicate this thesis to,

My mother: Saleha Raddah and My father: Saeed Alghamdi

For making me be who I am

My husband: Naif

For his unconditional love and support

My daughter: Loulwah (Luli)

The sweetest little sunshine ever!

# 1. Introduction

## 1.1 Ovary as an organ: Anatomy and histology

Each female has two ovaries, each one is of oval shape and measures 2-4 cm long. Ovaries are kept in position by the broad ligaments and the mesovarium. The ovaries lie against the lateral wall of the pelvis in an ovarian fossa; however, some variabilities of their position are seen in pregnancy when the ovaries are pulled up and, post-partum, when the broad ligaments are lax and the ovaries may prolapse into the pouch of Douglas (4).

The ovarian artery is a branch of the abdominal aorta at the level of the first lumbar vertebra while it drains into the ovarian vein. On the right side, the right ovarian vein drains into the inferior vena cava and the left ovarian vein drains into the left renal vein. In the sexually mature female, the ovary is the organ responsible for the production of the female sex hormones - estrogen and progesterone- and for the production of the female germ cell cells; the ova (4).

Histologically, the ovary consists of cortex and stroma, each with specific type of structures and cells. The ovarian cortex is divided into superficial cortex and deep cortex; the deep cortex has scattered numerous follicles that contain female gametes in various stages of development (Figure 1). The superficial cortex is a thin fibrous layer, which is covered externally by a modified peritoneal layer misleadingly called germinal epithelium, as it was thought that this layer may give rise to ova; current research called this flat to cuboidal epithelium the ovarian surface epithelium or ovarian mesothelium (5).

The ovarian stroma consists of spindle-shaped cells, collagen fibers, and ground substance. Bundles of smooth muscle cells are also located within the stroma. The central zone of the stroma is the medulla, which is a highly vascular component (4).

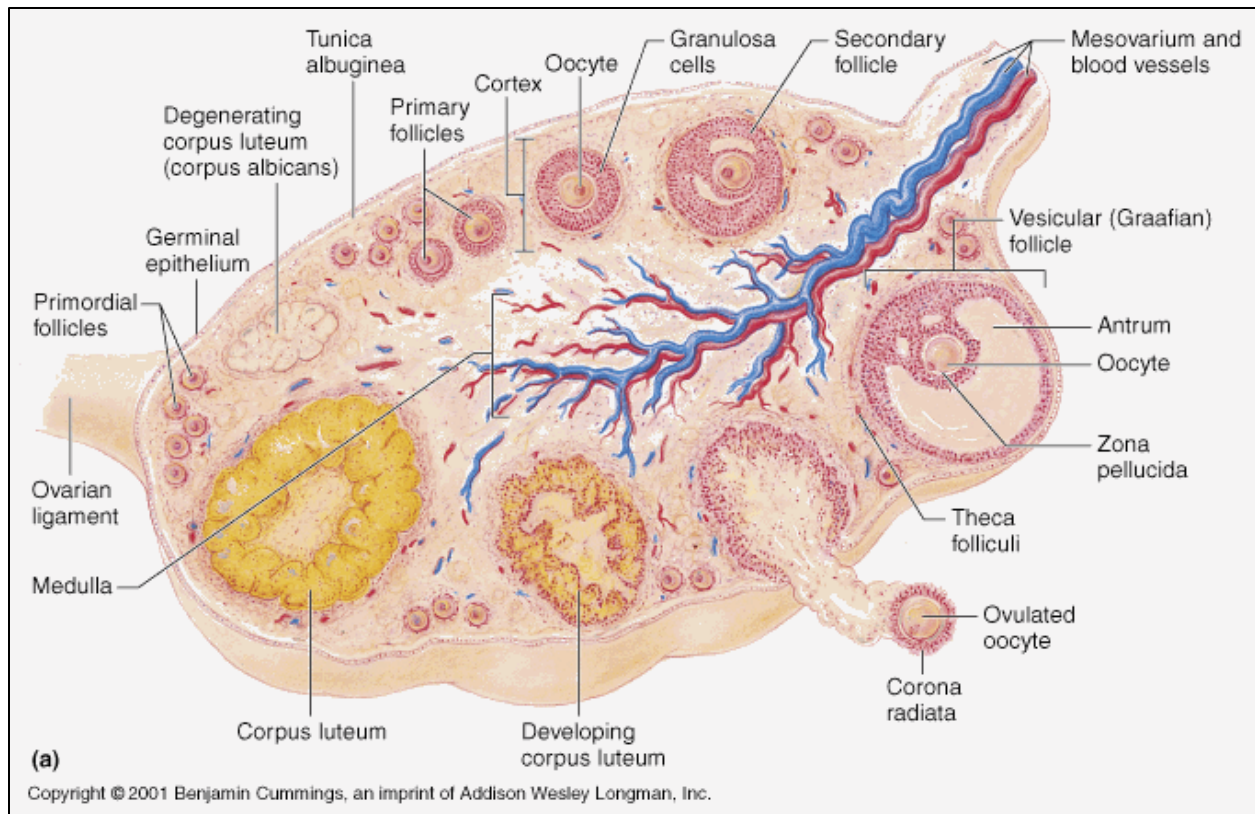


Figure 1. Illustration of the ovarian structures.

## **1.2 Ovarian Cancer**

Ovarian cancer is the deadliest disease of the female reproductive tract. In Canada, it remains the fifth leading cause of death in female patients diagnosed with cancer (6). Primary ovarian cancer can be classified broadly into three categories; epithelial ovarian cancer, germ cells tumor and sex cord stromal tumors. In this thesis, we will focus on epithelial ovarian cancer and, specifically, on high-grade serous ovarian carcinoma (HGSOC).

Epithelial ovarian cancer (EOC) is the most common type of ovarian cancer of all ages (7). The mean age of diagnosis is 63 years, and, most cases are diagnosed in women between 55 and 64 years of age. EOC occurs more frequently in white women in the industrialized countries of northern and western Europe and North America while it is least common in India and Asia (8).

Few studies in the literature correlate the symptoms and signs of this disease with specific histological types of EOC. In a large population-base study that correlates the patient's presentation with the histological type and/or the grade, patients diagnosed with serous ovarian carcinoma were more likely to experience bowel symptoms, in comparison to distended abdomen in mucinous ovarian carcinoma, and vaginal bleeding in endometrioid ovarian carcinoma. In patients with asymptomatic high-grade serous ovarian carcinoma who were diagnosed incidentally in the clinic, the majority of cases had already advanced disease; this fact proves that serous ovarian carcinoma is a "silent" disease compared to other histological types (9, 10).

### **1.2.1 Classification of epithelial ovarian tumors (EOT)**

Epithelial ovarian cancer was thought to originate from the ovarian surface epithelium (OSE) (11). Benign EOTs lack any invasiveness to the ovarian stroma and have benign-looking

cells. Tumors are considered borderline when they have atypical proliferation without invasiveness. Malignant EOTs are the most common and aggressive tumors of the ovary, accounting for approximately 90% of all malignant ovarian carcinomas.

EOTs were classified based on the histological features into five main categories; Serous (low and high grade), Mucinous, Clear cell, Endometrioid and transitional cell tumor of the ovary (Figure 2). For each histotype, there are specific gross, microscopic, immunohistochemical and molecular features that help to differentiate it from other histotypes. High grade Serous OC will be discussed in the following section.

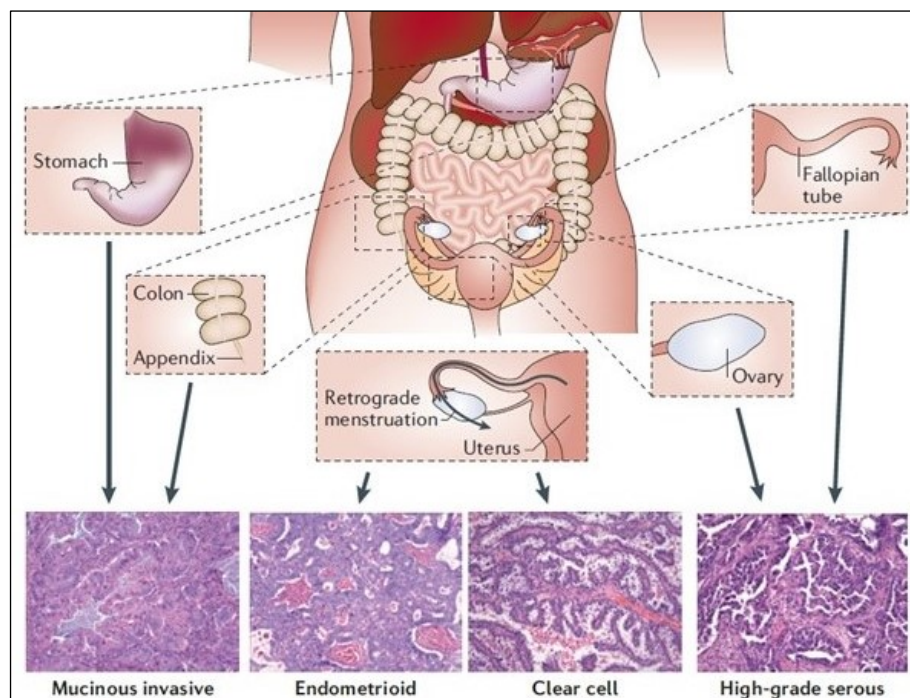


Figure 2. Histological types of epithelial ovarian cancer.(3) Low-grade serous and transitional tumors are not shown.

#### A- Low grade serous OC:

A 2-tier grading system is applied for serous OC to classify it into high and low grade serous OC. Low grade serous OC has been hypothesized to arise from cystadenomas and then progress in step-wise manner. Morphologically, it forms micropapillary branches lined by cells that have uniform round to oval nuclei with evenly distributed chromatin. The mitotic figures are usually 10 or less per high power field and the tumor usually has many psammoma bodies, while necrosis is usually absent (12). Low grade serous is characterized by mutations of any of the three following genes: Kirsten rat sarcoma viral oncogene homolog (KRAS), BRAF or Erbb2. Mutations in any of the three genes result in the constitutive activation of mitogen-activated protein kinase (MAPK), which leads to uncontrolled cell proliferation.(13)

#### B- Mucinous OC:

By definition, OC is of mucinous type when most or all epithelial cells have mucins. It mimics the gastrointestinal type of epithelium or the endocervical epithelium. Unlike HGSOC, it is more common in teenagers and rarely occurs after menopause. Most of the cases (up to 80%) are benign, and the incidence of invasive mucinous carcinoma is rare; in two large population-based studies, the incidence was near 3% (14, 15). When diagnosing mucinous OC, differentiation between primary or secondary (metastatic) disease is vital for the patient. It is not uncommon to misinterpret the two diseases. In a series of 35 cases of secondary ovarian tumors, more than two-thirds of the cases of metastatic colonic cancers were initially diagnosed as primary mucinous OCs (16). There are some helpful features that distinguish the primary mucinous OC from the secondary disease. Surface epithelial involvement and/or involvement of both ovaries are favoring secondary disease. Primary mucinous OC, grossly, is usually confined to one ovary, has more cystic spaces than other types, and the tumor is filled with gelatinous

material rich in glycoproteins (12). In immunohistochemical studies, mucinous OC are cytokeratin (CK) CK2+/CK20+, CDX2+ (as for most of the colonic origin tumors) and CEA + (17). Most of the diagnosed cases of mucinous OC (40% - 50%) have KRAS mutation (18) and 19% have human epidermal growth factor receptor-2 (HER-2) gene amplification (19). In invasive carcinoma, mucinous OC has worse prognosis than the serous type (20).

#### C- Clear cell OC (CCOC):

CCOC is the second most common OC subtype after HGSOC. For unknown reasons, the incidence is higher in Asia compared to western countries (21). Atypical endometriosis and atypical adenofibroma are both reported to be precursor lesions for CCOC (22). Unlike HGSOC, CCOC is usually diagnosed at early stage (stage I). In a large randomized clinical trial (RCT) conducted by The Japanese Gynecology Oncology Group to test the effects of different combinations of chemotherapy agents, 66.4% of the patients with CCOC had stage I disease (23). Histologically, the tumor organizes in solid, cystic, tubular-cystic or papillary configuration with a hyalinized papillary core. The tumor cells are large with hobnail nuclei (nuclei projection into the cystic lumen) and clear cytoplasm containing fat or glycogen (12). In immunohistochemical studies, CCOC is typically CK7+/CK20- and, in contrast to HGSOC, is negative for estrogen (ER)/progesterone (PR) receptors, and Wilms-tumor suppressor 1 (WT-1). Hepatocyte nuclear factor-1 beta (HNF1 $\beta$ ) has positive predictive value to diagnose CCOC and differentiate it from other OC subtypes. A reduction in HNF1 $\beta$  expression in CCOC induced cell apoptosis, making this molecular marker a potential target for therapy (24). Genetic studies of CCOC have shown AT-rich interactive domain 1A (ARID1A) mutation and higher frequency of the phosphatidylinositol- 4,5-bisphosphate 3-kinase catalytic subunit  $\alpha$  (PIK3C) mutation leading

to activation of the PI3K-AKT-mTOR pathway (25). KRAS mutation was reported to trigger the transformation of atypical endometriosis to CCOC (26).

#### D- Endometroid OC:

It accounts for 10-15% of all primary OCs. Simultaneous malignancies of the endometrium and the ovaries occur in 15-20 % of the ovarian tumors and in 5% of the endometrial carcinomas (27). Endometroid OC is most commonly diagnosed as a low-grade tumor, arising from an endometriotic cyst (27), and up to 42% of the cases are accompanied by ipsilateral pelvic or ovarian endometriosis (28). Histologically, it resembles the uterine counterparts; it forms a villoglandular pattern or glandular confluency. In 50% of the cases, there is squamous differentiation. High-grade endometroid OC is morphologically indistinguishable from HGSOC making the diagnosis of this subtype very challenging (28). Genetic studies have shown that the most common two somatic mutations associated with endometroid OC are  $\beta$ -catenin and PTEN (29). Ovarian endometroid carcinoma has a similar frequency of  $\beta$ -catenin mutation seen in uterine endometroid carcinoma but lower frequency of PTEN mutation and microsatellite instability (MI) (30).

#### E- Transitional cell tumor (TCT) of the ovary

TCT of the ovary includes two distinct categories; transitional cell carcinomas (TCC) and Brenner tumors (BT). Despite their commonalities in some histopathological features, there are considerable differences between them. Malignant BT is less aggressive than TCC and it is usually diagnosed at early stage (stage I) without extraovarian metastasis; 19% of malignant BT present in late stage compared to 69% of TCC (31). On gross examination, TCC showed focal calcification not seen in cases of malignant BT. Microscopically, malignant BT shows focal areas of well-differentiated transitional cells which are not present in TCC. Instead, TCC forms

malignant sheets of cells throughout (31). In immunohistochemical studies, TCC shares some features seen in HGSOC, for example, it diffusely expresses P53, ER and WT-1; it also shows diffuse expression of P16. In contrast, malignant BT is negative for these markers (31). In genetic studies, malignant BT tends to overexpress Ras, Cyclin D1 and epidermal growth factor receptor (EGFR). This molecular pattern was not seen in TCC (32).

Many years ago, *Kurman et al* (33) proposed a dualistic model to re-classify the OC based on the combination of histological features and molecular genetic analysis. They re-classified OC into two main types; type I and type II. Type I OC includes low grade serous, mucinous carcinoma, CCOC, endometrioid carcinoma and malignant BT. These tumors develop from a well-known precursor, their progression is slow, so they are mostly diagnosed at an early stage when the disease is only confined to the ovaries. Type II includes HGSOC, carcinosarcoma and undifferentiated carcinoma. In contrast to type I, the precursors of these tumors are rarely identifiable, they are highly aggressive and usually diagnosed in late stage (stages III or IV). The molecular alterations are very distinctive between the two types supporting the proposed dualistic model. Type I is associated significantly with mutation in BRAF and KRAS oncogenes and rarely demonstrates P53 mutation. Unlike type I, type II OC tumors are almost always P53 mutant (Table 1).

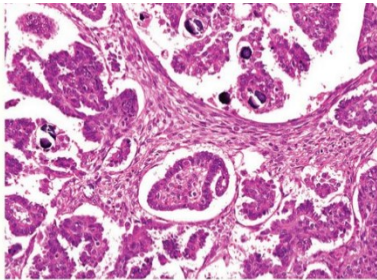
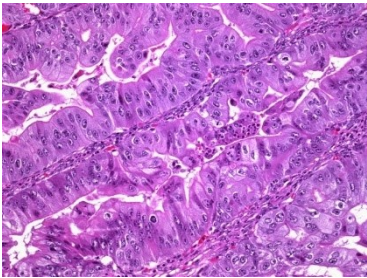
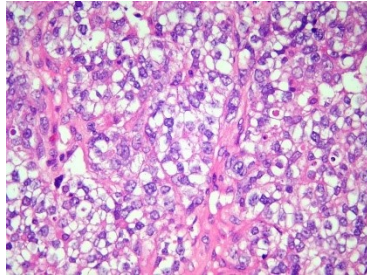
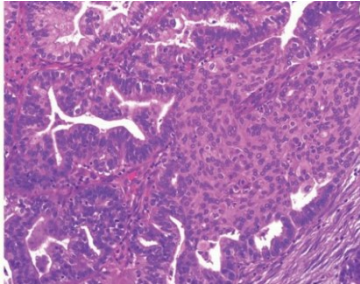
Ten years later, *Kurman et al* (10) published a revised dualistic model which provides further molecular classification and clinical integration. The revised model added seromucinous carcinoma as an additional subtype of type I OC. In type II, HGSOC was divided into four categories based on the molecular analysis: immunoreactive, differentiated, proliferative and mesenchymal. The main molecular differences between type I and type II OCs are the genetic instability and the frequency of TP53 mutations that are common in type II but not in type I.

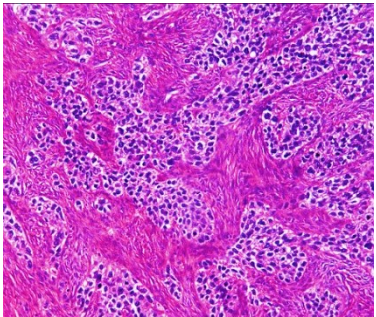
Other somatic mutations that are frequently seen in type I but not in type II are: PIK3C/PTEN, catenin  $\beta$ , and KRAS/BRAF protooncogene.

Table 1. Comparison between type I and type II OC

| Type I  | Type II  |
|---|--|
| Low grade tumor   | High grade tumor   |
| Usually detected early  | Usually late detection; advanced stage   |
| Step-wise progression   | Rapid aggressive progression   |
| Rarely presents with ascites  | Usually presents with ascites  |
| Chromosomally stable  | High DNA copy number variation   |
| Infrequent P53 mutation   | Almost always P53 mutation   |
| <ul style="list-style-type: none"> <li>- Mucinous OC</li> <li>- Endometrioid OC</li> <li>- Clear cell OC</li> <li>- TCC</li> <li>- Low-grade serous OC</li> </ul> | <ul style="list-style-type: none"> <li>- High-grade serous OC</li> <li>- Carcinosarcoma</li> </ul> |

Table 2. Comparison among type I epithelial OCs (28, 34, 35).

| Histological type   | Microscopy  | Molecular alterations  |
|---------------------|---|--|
| Low-grade serous OC |   | <ul style="list-style-type: none"> <li>- KRAS</li> <li>- BRAF</li> <li>- Erbb2</li> </ul>      |
| Mucinous OC         |   | <ul style="list-style-type: none"> <li>- KRAS</li> <li>- HER-2</li> </ul>                      |
| Clear Cell OC       |  | <ul style="list-style-type: none"> <li>- ARID1A</li> <li>- PIK3C</li> <li>- KRAS</li> </ul>    |
| Endometrioid OC     |  | <ul style="list-style-type: none"> <li>- <math>\beta</math>-catenin</li> <li>- PTEN</li> </ul> |

|                         |   |  |
|-------------------------|---|--|
| Malignant Brenner Tumor |  | <ul style="list-style-type: none"> <li>- Ras</li> <li>- Cyclin D1</li> <li>- EGFR</li> </ul> |
|-------------------------|---|--|

### 1.2.2 Ovarian cancer; challenges in screening

Most of the cases of OC are sporadic. However, family history of breast and/or ovarian cancer is a strong factor increasing the incidence of OC. Hereditary cases of epithelial OC account for 10% of all cases, and most of them have BRCA mutations (usually HGSOC) (8), while a small portion have Lynch syndrome (endometrioid and CCOC) (36). Over decades, several epidemiological studies consistently reported the inverse relationship between the use of the oral contraceptive pills and the incidence of OC (8). Moreover, the protective effects increase with the increased number of years of using the pills and persists even after cessation of usage. Parity has also a protective effect for OC; parous women have 30-60% lower risk than nulliparous of getting OC (8). Obesity has been linked to several malignancies including OC. In a meta-analysis of 28 observational studies, obese and even overweight women were at greater risk to develop OC compared to women of normal weight (37).

The screening and the detection of early epithelial OC have always been challenging. Several factors contribute to the difficulty associated with screening, including: i) limited data for the molecular mutations that lead to malignancies; ii) the lack of knowledge of the time it takes for the disease to develop or to progress to an advanced stage; and iii) a relatively lower prevalence of the disease when compared to other malignancies (38). In order for any screening

method to be optimal, it must be un-expensive, time-efficient, have tolerable or no side effects, and have high sensitivity, specificity, and positive and negative predictive values. Several tools have been used to detect OC in early stages: serum CA125, ultrasound, combined tests and combined screenings; yet, none proved to be of high sensitivity or specificity for early disease diagnosis.

#### A- Serum CA125:

Carbohydrated antigen 125 also known as Mucin 16 (or MUC16) is a mucinous glycoprotein with high molecular weight (39). The protein core of CA125 is divided into three parts: a short cytoplasmic tail, a transmembrane domain, and a large glycosylated extracellular structure (39). CA125 is expressed by most epithelial OCs and detected by OC125 monoclonal antibodies. However, CA125 has poor sensitivity and specificity as an ovarian cancer biomarker. A retrospective study conducted by *Moss et al.* that enrolled 751 female patients, CA125 was used as a tool to investigate a wide range of vague symptoms and signs; 80% of cases of abnormal CA125 values were not a consequence of OC. This large number of false positive results indicates poor specificity of CA125 for OC diagnosis. The sensitivity of the test increases, however, in advanced cases when the disease is already located beyond the confines of the ovaries and mostly in an incurable status (40).

#### B- Ultrasound:

Ultrasound is a radiological modality to non-invasively image the ovaries and the adjacent structures. The trans-vaginal ultrasound (TVUS) is preferable because it allows for visualization of specific details that could be evaluated for possible detection of early OC stage. These details include, but are not limited to, size of the ovaries, presence of ovarian cysts, cystic wall thickness and septation, presence of pelvic or abdominal accumulation of fluid, and blood flow

within the masses if present. In the general population, TVUS has poor specificity and predictive value (38). An important limitation of the TVUS is the considerable intra-observer variation among radiologists interpreting and scoring the images (38).

#### C- Combined modalities:

A very recent systematic review of four trials of OC was reported upon screening in women with average risk and evaluated via TVUS, CA125 or the combination of both, and compared to usual or no screening. In all trials conducted among asymptomatic women, OC mortality did not significantly differ between screened women and those with no screening. Moreover, screening can harm patients, including the consequences of non-necessary surgeries in women found not to have cancer (41).

### **1.2.3 Staging of ovarian cancer**

The surgical procedure in ovarian cancer patients not only anticipates treatment, but also allows staging of the cancer. The International Federation of Gynecology and Obstetrics (FIGO) and the American Joint Committee on Cancer (AJCC) staging system are used to stage OC. FIGO was published in 1973, first revised in 1988, and lastly revised in January 2014 (1). The latest FIGO revision was done upon progression of the understanding of OC pathogenesis. The AJCC staging system is based on the size of the tumor, lymph node involvement and distant metastasis; hence, the other name is TNM staging. Table 3 lists the stages of OC using FIGO and AJCC staging systems (1) .

Table 3. Stages of ovarian cancer

| TNM               | FIGO | Description  |
|-------------------|------|--|
| Primary Tumor (T) |      |  |
| TX                |      | Primary tumor cannot be assessed   |
| T0                |      | No evidence of primary tumor   |
| T1                | I    | Tumor is limited to the ovary (one or two)   |
| T1a               | IA   | Tumor limited to one ovary; capsule intact, no tumor on ovarian surface; no malignant cells in ascites or peritoneal washings.                                 |
| T1b               | IB   | Tumor limited to both ovaries; capsules intact, no tumor on ovarian surface; no malignant cells in ascites or peritoneal washings.                             |
| T1c               | IC   | Tumor limited to one or both ovaries with any of the following: capsule ruptured, tumor on ovarian surface, malignant cells in ascites or peritoneal washings. |
| T2                | II   | Tumor involves one or both ovaries with pelvic extension.  |
| T2a               | IIA  | Extension and/or implants on the uterus and/or tube(s); no malignant cells in ascites or peritoneal washings.  |
| T2b               | IIB  | Extension to and/or implants in other pelvic tissues; no malignant cells in ascites or peritoneal washings.  |
| T2c               | IIC  | Pelvic extension and/or implants (T2a or T2b) with malignant cells in ascites or peritoneal washings.  |

|                          |      |  |
|--------------------------|------|--|
| T3                       | III  | Tumor involves one or both ovaries with microscopically confirmed peritoneal metastasis outside the pelvis.            |
| T3a                      | IIIA | Microscopic peritoneal metastasis beyond the pelvis (no macroscopic tumor).  |
| T3b                      | IIIB | Macroscopic peritoneal metastasis beyond the pelvis 2 cm or less in greatest dimension.                                |
| T3c                      | IIIC | Macroscopic peritoneal metastasis beyond the pelvis >2 cm in greatest dimension and/or regional lymph node metastasis. |
| Regional lymph nodes (N) |      |  |
| NX                       |      | Regional lymph nodes cannot be assessed  |
| N0                       |      | No regional lymph node metastasis  |
| N1                       | IIIC | Regional lymph node metastasis   |
| Distant metastasis (M)   |      |  |
| M0                       |      | No distant metastasis  |
| M1                       | IV   | Distant metastases (excludes peritoneal metastases).   |

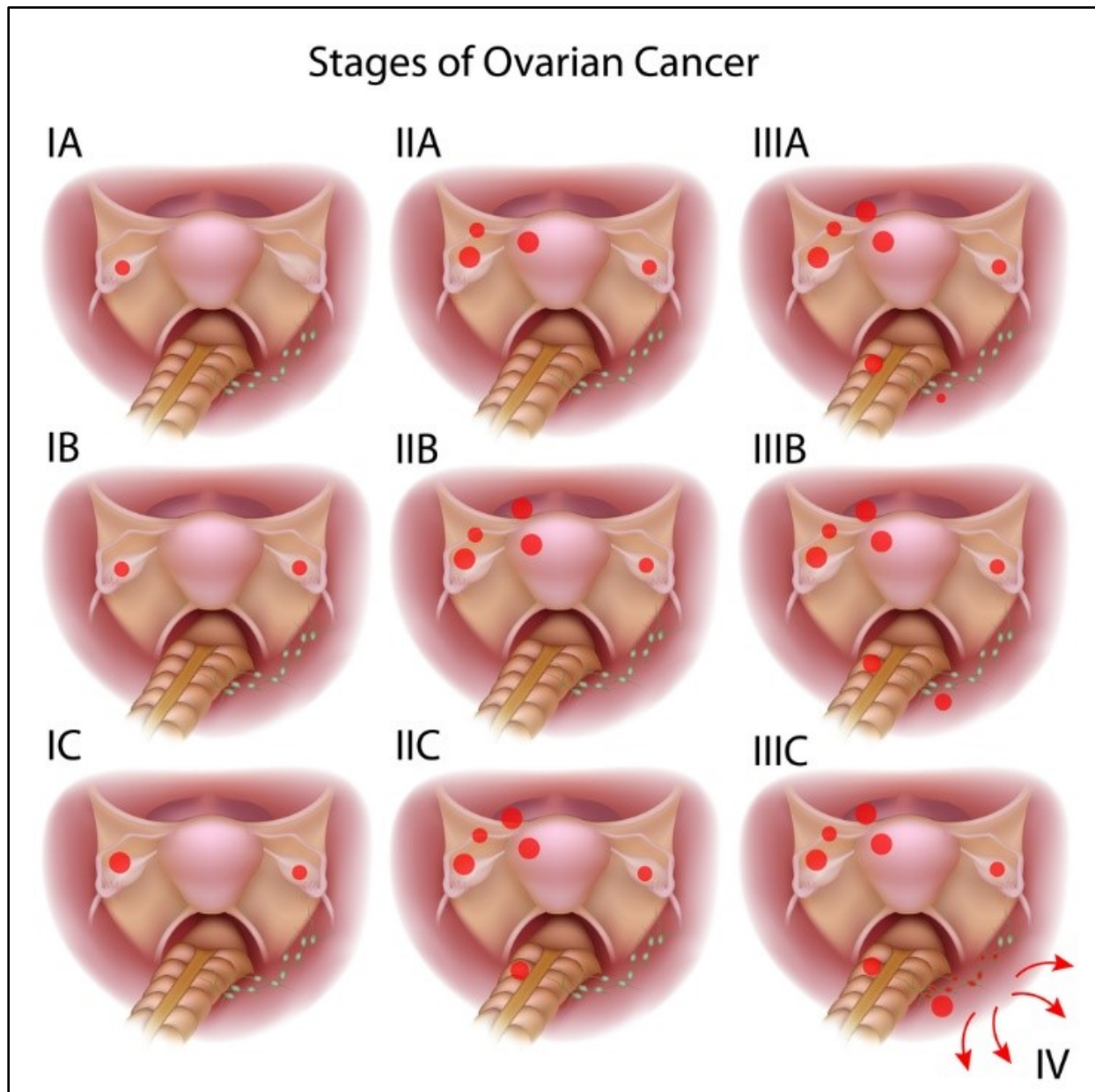


Figure 3. Ovarian cancer staging (1)

### 1.2.4 Current treatment modalities for OC

#### A- Treatment options for primary OC

The current standard of treatment for patients with OC is cytoreductive surgery followed by chemotherapy. Cytoreductive surgery (case-dependent) may involve a removal of the affected ovary or both, an affected fallopian tube or both, the uterus, part of the diaphragm, part of the intestine, liver or spleen. It helps to accurately stage the disease, remove all or most of the tumor implants that measure > 1-2 centimeters and alter the microenvironment of the remaining microscopic disease to magnify the effect of adjuvant therapy (42, 43). The goal of the optimal cytoreductive -debulking- surgery is to reduce the tumor volume to no visible tumor deposits. The removal of a great amount of the tumor has been associated with improved survival outcomes (42, 44).

Taxane-platinum-based chemotherapy (i.e. combined paclitaxel and carboplatin) is the current standard chemotherapeutic approach provided as first-line adjuvant therapy (45). Carboplatin is preferable to cisplatin as the former is better tolerated by the patients and easier to deliver in an outpatient setting (42). The question of which is more efficient, intravenous (IV) or intraperitoneal (IP) delivery of chemotherapy, is still debatable (45). A meta-analysis of six randomized controlled trials showed an increased overall survival and progression-free survival in patients who received IP chemotherapy compared to the IV route of administration (46). However, there are several limitations to the use of IP administration. Patients with residual implants of more than two centimeters, older patients and those with declining renal function, are poor candidates for IP administration and the IV route remains the standard of care in these groups (45).

The role of neoadjuvant chemotherapy -i.e. administration of the chemotherapeutic agents prior to the debulking surgery- remains uncertain, especially in terms of survival outcomes (47, 48). It remains an appropriate choice when the patient is expected to develop morbidity or mortality as a consequence of the debulking surgery but it cannot replace the optimal primary debulking (45).

#### B- Treatment for recurrent OC

Despite the initial response to the first-line of treatment that is seen in up to 80% of the cases, two-thirds of the cases have disease recurrence (49, 50). The platinum-free interval or PFI defined by the period of the last platinum cycle to the evidence of disease progression, is a predictor of the response to further treatment (45). The Gynecology Oncology Group (GOG) uses the PFI to categorize the disease recurrence as follows:

- platinum-refractory disease: the tumor fails to respond to first-line regimens and exhibits immediate further progression.
- platinum-resistant disease: the disease has a PFI of less than six months following platinum-based therapy.
- platinum-sensitive disease: the disease has a PFI of greater than six months after a platinum-based regimen.

Patients with platinum refractory disease have poor prognosis and their overall survival is for less than a year (51). Platinum-resistant patients are usually treated with single agent non-platinum-based chemotherapy (52). Platinum-sensitive groups have better prognosis than other groups as they usually respond to multiple platinum-based combined chemotherapies (52).

### C- Novel agents to treat OC

Angiogenesis – i.e. formation of new blood vessels- has a fundamental function in OC formation, progression and metastasis as it modulates the tumor microenvironment (53). The angiogenesis process is initiated by signals from the vascular endothelial growth factor VEGF, platelet-derived growth factor PDGF, angiopoietins, and other factors (54). Based on this fact, Bevacizumab – a humanized VEGF-neutralizing monoclonal antibody – has now been added to the combined taxane-platinum based chemotherapeutic approach at specific dosages (52). Two randomized clinical trials conducted by the GOG and by the International Collaboration on Ovarian Neoplasms (ICON7) group compared the progression-free survival (PFS) between two groups of patients with or without adding bevacizumab. Newly-diagnosed patients with advanced epithelial OC who received bevacizumab in addition to chemotherapy showed prolonged PFS by about four months in the GOG study (55). Similar results were obtained from the ICON7 study, where the PFS at 42 months was 24.1 months in patients who received bevacizumab compared to 22.4 months in patients without it (56).

BRCA germ-line mutations were found in up to 17.1% of patients diagnosed with HGSOc (57). These mutations lead to deficiency in homologous recombination repair (HRD) of DNA damage. Mutant BRCA cells, to repair their damaged DNA, depend on base-excision repair pathways that can be suppressed by blocking Poly-ADP Ribose Polymerase (PARP) enzyme activity (58). Thus, PARP inhibitors lead to unrepaired single strand DNA-breaks. PARP inhibitors also promote cell death by another mechanism called “PARP tapping” in which the PARP enzyme attaches to the broken DNA and blocks the DNA repair process, so the PARP-DNA complex itself becomes a cytotoxic complex. There are three Food and Drug administration (FDA)-approved PARP inhibitors: Olaparib, Niraparib and Rucaparib (approved

in 2014, 2016, and 2017, respectively). The benefits of PARP inhibitors as maintenance therapy in clinical trials were seen in patients with platinum-sensitive and BRCA-mutant disease associated with HGSOC (59).

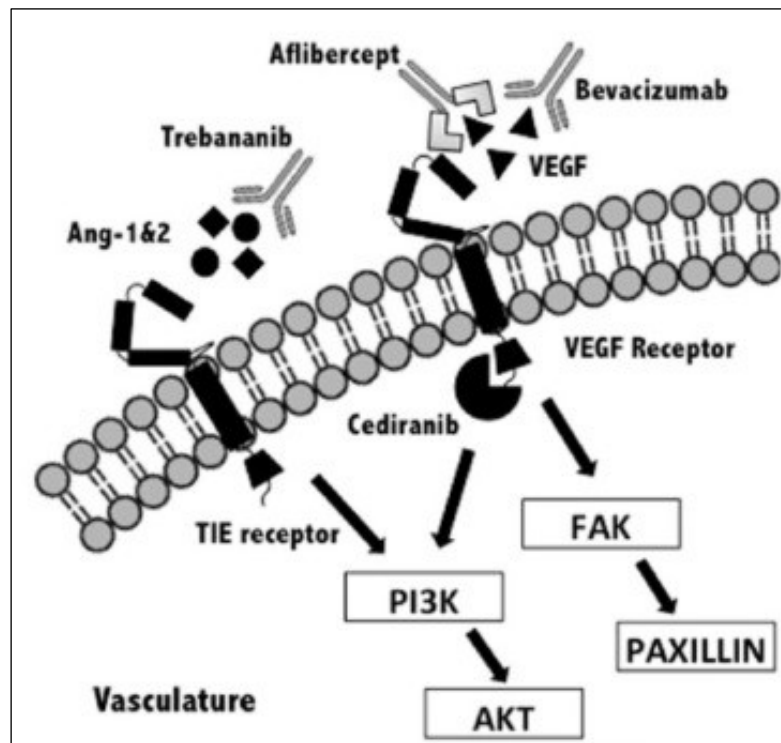


Figure 4, Mechanism of action of Bevacizumab. One of the new modalities for treating OC.

### 1.2.5 Prognosis

Despite the advances in medicine and the treatment modalities, the prognosis of epithelial OC remains poor in comparison to other cancers, for example; breast cancer. The survival rate has not changed in more than two decades. Figure 5 shows that the 5-year-survival rate of epithelial OC has never been more than 40% over the past twenty years.(3)

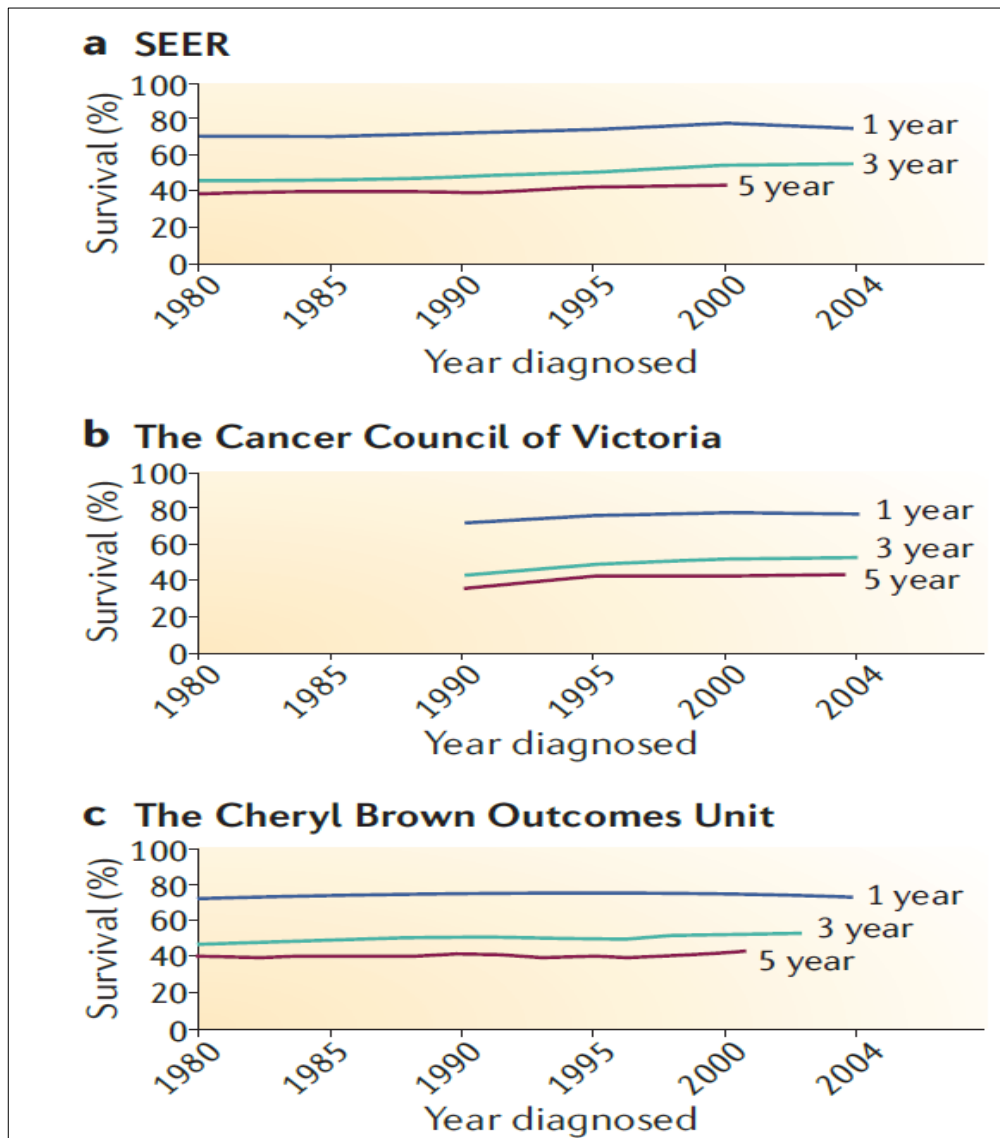


Figure 5. Data from three different large centers; A) USA, B) Australia and C) Canada. Data showed a 5-year survival rate of no more than 40% in the last two decades.(3)

### **1.3 High grade serous ovarian carcinoma (HGSOC)**

HGSOC accounts for 60%-80% of all OC cases and for most deaths related to OC (60). One of the recent advances in understanding the pathogenesis of HGSOC is the recognition of serous tubal epithelial carcinoma (STIC) as a precursor lesion for HGSOC (10). STIC is defined as proliferation and stratification of the fallopian tube secretory epithelium with a P53 signature consistent with P53 mutation. The basement membrane invasiveness of the STIC and the dissemination to the ovary seem to trigger the development of invasive HGSOC (61).

At very early stage of the disease, the tumor cells shed from the primary site and can be detected in peritoneal lavages. In addition to hematogenous spread -which is rare- the peritoneal fluid works as a carrier to transfer the tumor cells from the pelvis to the abdominal cavity. This mode of cell dissemination and the dynamic movement of the peritoneal fluid facilitate the adhesion of the cancer cells to the omentum and to various serous linings within the peritoneal cavity (62). The peritoneal fluid is a rich environment in tumor-promoting factors and other host cells that contribute to further tumor cell proliferation and progression (63). Moreover, several data from in vitro and in vivo experimentation suggests that constitutive autocrine production of TNF- $\alpha$  by the epithelial tumor cell itself leads to tumor growth and spread by promoting the synthesis of various other cytokines within the tumor microenvironment (64).

#### **1.3.1 HGSOC: histological and molecular background**

As mentioned before, HGSOC is a type II OC in which the disease is, most of the time, diagnosed at late stages. In addition to the clinical history and the radiological images, HGSOC is diagnosed extensively based on the gross and histological features of the tumor and some immunohistochemical markers that aid to reach an accurate decision. The tumors usually are bilateral, solid, and may have some areas of necrosis or hemorrhage. Histologically, the tumor

usually forms branching papillary fronds, has glandular complexity and slit-like fenestrations, in addition to a nucleus with features consistent with high grade. High-grade nuclear features include marked nuclear atypia, pleomorphism, prominent nucleoli, stratification, and extensive mitosis (>10/ high power field). Various psammoma bodies can also be found (12). In immunohistochemical studies, pathologists often use P53, WT-1 and PAX8 as a biomarker panel to help diagnose HGSOC.

Unlike low-grade serous OC, the major challenges in terms of early diagnosis and treatment of HGSOC are the genomic instability of the disease and the heterogeneity of the tumor. Despite the advances that have been made in the treatments of many cancers, ovarian cancer -specifically the most aggressive type, HGSOC,- falls behind others and retains a consistent 5-year survival rate of approximately 40% over the past two decades (3). As mentioned in the treatment of OC in general, while most patients with HGSOC show initial response, most of them relapse with platinum-resistance disease. One of the accepted explanations of the resistance is the presence of a heterogenous population of cells, including some that are genetically different from the dominant population. It is accepted that after clearance of the dominant chemo-sensitive groups, the small population of chemoresistant cells grows and progresses (65). *Cooke et al.* genetically characterized three series of cell lines generated before and after chemotherapy to address whether the inter-tumor genetic heterogeneity is present de novo, or instead, it is acquired after chemotherapy. Multiplex fluorescence in situ hybridization (M-FISH) is a 24-color karyotyping technique used mainly to study interchromosomal rearrangement (66). Array comparative genomic hybridization (CGH) is used to study copy number variations. Using M-FISH and Array CGH, they found that the cell lines had extensive karyotyping divergence and that the sensitive and resistant sub-clones are not

linearly related. This observation supports the explanation of the intrinsic pre-existence of genetically different sub-clones within the tumor before initiation of chemotherapy (65).

The disease aggressiveness and the lack of a well-established genomic profile for HGSOC drove the Cancer Genome Atlas (TCGA) to evaluate 489 samples of HGSOC stage II – IV before receiving chemotherapy. Surprisingly, the results of the genetic analysis were unpretentious. In more than 96% of the samples, TP53 mutation was detected, 22% of the cases showed somatic or germline BRCA1 or BRCA2 mutation and, noticeably, very high copy number variations (67).

Table 4. Low-grade versus high-grade serous OC

|                            | Low-grade serous OC      | High-grade serous OC                                     |
|----------------------------|--------------------------|--|
| Precursor lesions          | Adenofibroma/cystadenoma | Serous tubal intraepithelial carcinoma                   |
| Main molecular alterations | KRAS<br>BRAF<br>ERBB2    | TP53   |
| Chromosomal instability    | Low                      | High   |
| Main microscopic finding   | Micropapillary structure | Large papillary growth, solid, with glandular complexity |
| Nuclear grade              | Low                      | High   |
| Necrosis                   | Absent                   | Usually present  |
| Mitosis                    | Low (Less than 10/HPF)   | High (More than 10/HPF)                                  |

### 1.3.2 Experimental model of HGSOC

There are many in vitro and in vivo models currently used in ovarian cancer biology. Cell lines derived from the tumor are the most commonly utilized model in this area of cancer biology. However, this model comes with some limitations including the choice of the cell lines and the animal types into which the cells are injected to develop experimental tumors.

#### A- The choice of cell line

The choice of a good cell line that closely mimic the disease is vital in experimentation as the data acquired from the model will help understand disease development, progression and sometimes response to therapeutic agents. After the cancer genome atlas (TCGA) study on HGSOC (67), *Domcke et al.* (2) evaluated 47 cell lines that were often used in the literature as models for HGSOC including the most prevalent SKOV-3, A2780, OVCAR-3, CAO3 and IGROV1 cells. They compared the genomic profile to the actual patient samples that were published by the TCGA study of 485 patients with HGSOC(67). They ranked the cell lines by suitability to represent HGSOC based on the correlation between the copy number variation, the presence of TP53 mutation, and the absence of other genes recurrently altered in other ovarian cancer subtypes. Based on this ranking, the 47 cell lines studied were divided into three categories: good, moderate or bad models for HGSOC (Figure 6). The striking result was that SKOV3 and A2780 cells, the most popular in the literature, were at the bottom of the list, i.e., unlikely to represent HGSOC (2). This study helped to optimize the choice of cell lines in HGSOC experimentation to the top category that is highly likely representative of the disease.

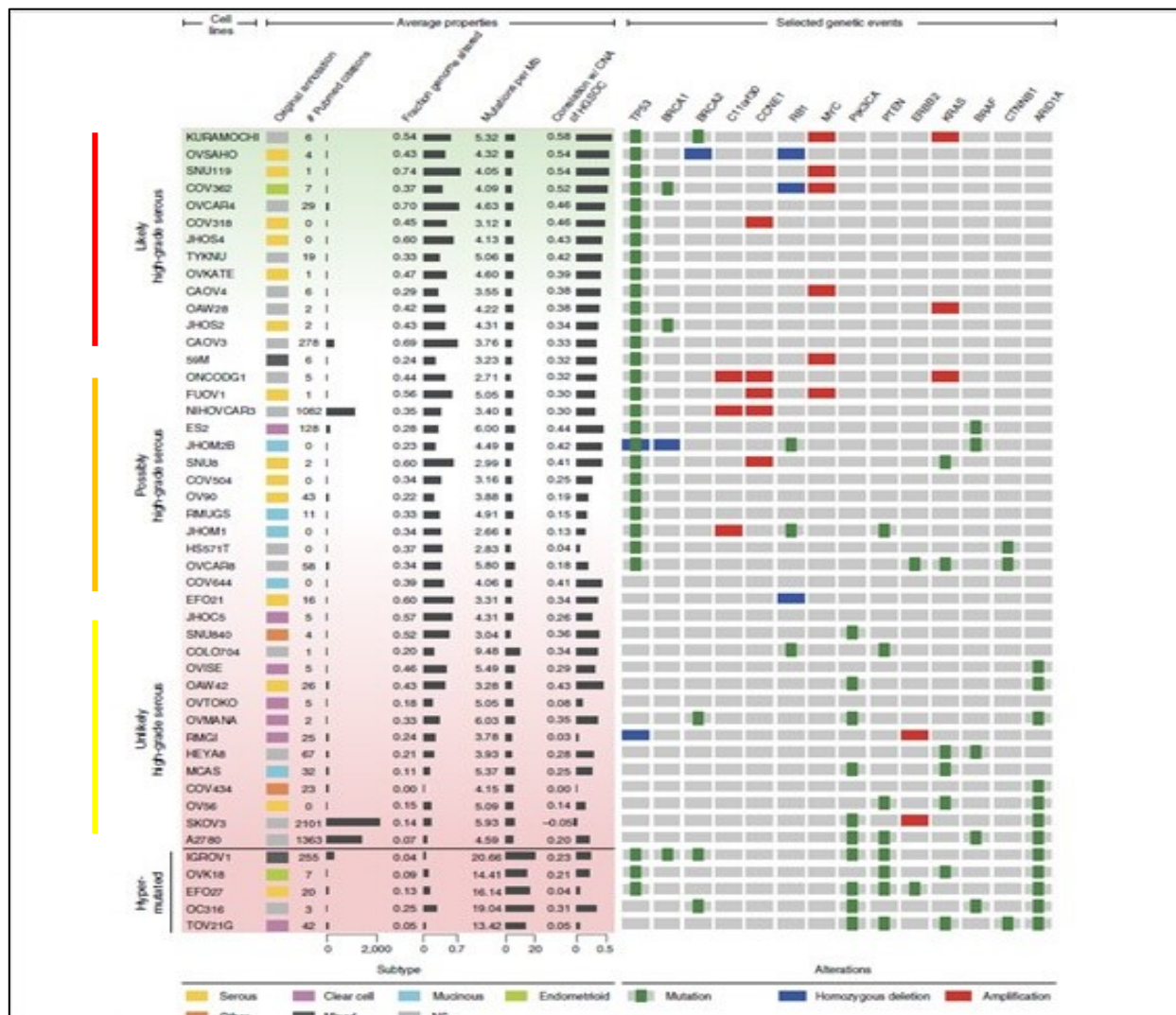


Figure 6. Ranking of the cell lines according to their suitability to represent HGSOC. Red line: likely represents HGSOC. Orange line: Possibly represents HGSOC. Yellow line: Unlikely represents HGSOC. (2)

## B- The choice of mouse type

Xenograft mouse models have been used commonly in the literature. The question is whether humanized transgenic mice, nude mice or severe combined immunodeficiency (SCID) mice are preferable. There are immunological differences among the three types; these differences make each model suitable for particular studies. Humanized transgenic mice have a deletion of the H2-Ab1 gene, which blocks the expression of Major Histocompatibility Complex MHC class molecules A and E. This type of mouse is also engrafted by human T-cell clones and is very suitable for modeling autoimmune diseases (68). SCID mice have defects generating T or B lymphocytes; these defects make them good candidates as host recipients for transplants of human cells and organs. Nude mice have a mutation at the *Foxn1* gene, leading to inactivation of thymus-derived T cells. However, they have increased natural killer cell response and they are commonly used for human tumor xenografts (69).

Previous experimental models described in the literature utilized cell lines that are unlikely to represent HGSOV, such as SKOV-3, IGROV-1 or A2780 cells. Moreover, most of them used SCID mice which allow for rapid tumor growth, yet did not represent the physiological microenvironment of the cancer itself and did not allow for appropriate assessment of the treatment response due to the absolute absence of immune response. In addition, the tumor latency that has been reported in the literature was never more than three months regardless of animal model utilized. All previous mentioned factors lead to a poor representation of the HGSOV progression thus not allowing for clear assessment of the treatment response. The lack of a well-characterized representative model of HGSOV in the literature drove us to define an *in vivo* model of HGSOV utilizing existing human ovarian cancer cell lines having the genetics, histology, and biomarker expression recreated in the host.

## ***2. Hypothesis and Specific Aims***

Ovarian cancer (OC) is the fifth leading cause of cancer-related death among women in Canada (2016) (6). Most deaths (70%) are encountered in patients with advanced-stage (stage III and IV) high-grade serous ovarian carcinoma (HGSOC) (67) when the disease has already reached the peritoneal cavity. The current standard of treatment in this group of patients is cytoreductive surgery following by adjuvant platinum (Pt) and taxane (Tx) based chemotherapy (52). However, over the past 30 years, the survival rate has not improved for OC in comparison to other solid cancers (3).

OC cell lines are frequently used for both experimental in vivo models and in vitro studies. However, most of the OC cell lines used globally are not genomically representative of HGSOC, specifically A2780 and SKOV-3, the most two cited in the literature. Several other OC cell lines, however, have been recently identified to be genetically suitable to represent HGSOC (2). Thus, it is of great clinical relevance to use these HGSOC cell lines—that represent the most aggressive subtype of OC—in an in vivo experimental model of the disease.

Having a HGSOC mouse model with fidelity of the disease as close as possible to development in humans will allow better assessment of preclinical therapeutic options as well as better understanding of the progression of the disease. This model will also allow investigators to utilize a reliable, easy to access mouse strain (the nude mouse) with the least disturbance of the immune system among the immunosuppressed mice available. The central *hypothesis* of this work is that **intra-abdominal (i.e., orthotopic) administration of human cancer cell lines with genetic fidelity of HGSOC will develop, in the widely available female nude mouse, peritoneal carcinomatosis resembling anatomical and histopathological features of**

**advanced disease encountered in stage III/IV patients.** Three specific aims were developed to examine the hypothesis.

**Aim 1: To study the expression of biomarkers of HGSOC in established human cell lines with genetic fidelity of HGSOC according to ‘The Cancer Genomic Atlas’ (TCGA) studies.**

The genomic analysis and the expression of the biomarkers are both significant in terms of determining the histological type of the OC and the biological properties of a histological subtype, regardless of the cell of origin or the histological similarities between different tumor subtypes (70). We used an immunohistochemical approach to study the expression of biomarkers of HGSOC in three cell lines with demonstrated high genetic fidelity to the disease (2, 65, 67): OVCAR-4, OVSAHO and PEO14. We compared them to the OC cell lines that are the least likely to represent HGSOC: A2780 and SKOV-3 (71). We determined the biomarkers based on the histotype prediction using the calculation of the subtype prediction (COSP) that was developed by a group of scientists, pathologists and gynecologists from the University of British Columbia (70). Moreover, with the aid of gynecological pathologists, we included other biomarkers used for differential diagnosis for HGSOC in the clinic. At the end, the total number of markers used to achieve this aim consisted of the following nine biomarkers:

Nuclear biomarkers: P53, WT-1, PAX-8, HNF-1 $\beta$ , ARID1A and ER

- Membranous biomarkers: CA125 and E-cadherin
- Cytoplasmic biomarker: Vimentin

**Aim 2: To investigate macroscopic and microscopic intra-abdominal disease in nude mice inoculated with genetically defined human HGSOC cells.**

We studied the development of abdominal disease in nude mice upon injecting intraperitoneally HGSOC cells; we compared them against the disease developed when injecting the non-HGSOC, A2780 and SKOV-3 cells. We monitored the disease progression until the animals reached a humane end point. For each animal, we recorded the time of necropsy, the number of tumors developed, the presence of ascites and the cellular components within it, as well as the affected diseased organs within the animal. Tissues then were collected systematically for histological analysis to document the capability of the specific OC cells to migrate, invade and form a tumor. Before the tissue collection, we documented the gross anatomical disease within the abdominal cavity using a high-power stereoscopic microscope. The differences and similarities between disease manifestation among the cell lines were recorded and analyzed.

**Aim 3: To evaluate the degree of heterogeneity among various genetically defined HGSOC cell lines in functional studies**

We studied the migration and the invasion of the three OC cell lines with high genetic fidelity to HGSOC: OVCAR-4, OVSAHO and PEO14. We compared them to the least likely OC cells to represent HGSOC: SKOV-3 and A2780. To study the migration capacity of the cells, we employed Boyden chamber assays. Finally, to determine the invasive capacity of these cell lines, we performed invasion studies of the cells on extracellular matrix-coated Boyden chambers.

### ***3. Materials and Methods***

#### ***3.1 Cell culture***

All reagents were obtained from Corning Cellgro (VA, USA) unless otherwise mentioned.

OVSAHO cells were purchased from the Japanese Collection Research Bioresources (JCRB) cell bank in August-2013; OVCAR-4 were obtained from the National Cancer Institute (NCI) of the USA in August-2014; PEO-14 were from the Public health England cell line repository (ECACC) (March-2013); A2780 were obtained in October of 2003 from Dr. Stephen B. Howell, (University of California San Diego, USA); finally, SKOV-3 cells were from the American Type Culture Collection (ATCC). All the cell lines were cultured in RPMI media supplemented with 5% fetal bovine serum and 5% bovine serum, 10 mM HEPES, 4 mM L-Glutamine, 100 IU penicillin, 100 µg/ml streptomycin, 0.01 mg/ml insulin (Roche diagnostic, Indiana, USA) and 1 mM of sodium pyruvate. All cells were incubated at 37°C with 5% CO<sub>2</sub>.

#### ***3.2 Immunocytochemistry***

To study the expression of different markers on cell lines, cells were plated on 8-well slides at 50,000 cells/well in complete media. At a full confluence stage, the media was aspirated, cells were washed twice with phosphate buffer solution (PBS) followed by 4% paraformaldehyde (PFA) fixation for forty minutes; thereafter, the PFA was removed, the cells covered by PBS, and the slide lid was covered with Parafilm. The slide stayed in 4°C overnight before performing the immunocytochemistry (ICC). For the ICC, in brief, the cells were washed twice with T-PBS followed by a third wash in PBS. Permeabilization of the cells was done using 0.5 % Triton buffer (Sigma X100) for 20 minutes. After washing, normal horse serum 2.5% (Vector, S-2012) was used for 20 minutes to block the non-specific bindings. Cells were then incubated with

primary antibodies for 30 minutes. Prior to 30 minutes incubation with secondary antibodies ImmPRESS, whether anti-mouse IgG (Vector – MP-7402) or anti-Rabbit IgG (Vector – MP-7401), 3% hydrogen peroxidase (Sigma-216763) was used to block the endogenous peroxidase. Target staining was detected via 3,3'-diaminobenzidine (DAB, Vector). The samples were counterstained with hematoxylin. The primary polyclonal antibodies used in the study are listed below (Table 1). Analysis of the results were based on individual's observation. The expression of ER has been analyzed based on the clinical judgment of the pathologists. According to the pathologist consulted, 1% or more cells being positive renders the sample “positive” for ER.

### ***3.3 Immunohistochemistry***

Immunohistochemistry for the paraffin embedded sections was performed as for the cells except that deparaffinization and hydration were done using xylene and different concentrations of ethanol. These steps were followed by antigen retrieval using a steamer chamber. Bloxall (Vector, SP-6000) was used prior to the primary antibody in tissue instead of 3% hydrogen peroxide to block endogenous peroxidase activities. The primary polyclonal antibodies used in the study are listed below in Table 5.

Table 5. Lists of the antibodies used in the project

| Antibody                      | Source         | Catalog No  | Dilution     | 2ry<br>Antibody | Antigen retrieval<br>buffer |
|-------------------------------|----------------|-------------|--------------|-----------------|-----------------------------|
| P53                           | DAKO           | M7001       | 1:400        | Mouse           | EDTA                        |
| WT-1                          | DAKO           | M3561       | 1:50         | Mouse           | Citrate                     |
| CA125                         | Thermo         | #MS-1151-R7 | Ready to use | Mouse           | Citrate                     |
| Vimentin                      | Cell signaling | #5741       | 1:100        | Rabbit          | Not done                    |
| E-cadherin                    | Cell signaling | #3195       | 1:400        | Rabbit          | Not done                    |
| PAX8                          | Proteintech    | #10336-1-AP | 1:1000       | Rabbit          | EDTA                        |
| A1RDA1                        | Sigma          | HPA005456   | 1:75         | Rabbit          | Not done                    |
| ER                            | DAKO           | M7047       | 1:35         | Mouse           | Not done                    |
| HNF1 $\beta$                  | Sigma          | HPA002083   | 1:100        | Rabbit          | Not done                    |
| Anti-human<br>nuclear antigen | abcam          | Ab190710    | 1:400        | Mouse           | Citrate                     |

### 3.4 Mouse xenografts

Six-seven week old female Athymic nude mice were purchased from Harlan (IN, USA). After quarantine for five days, xenografting with human OC cell lines was done by loading  $2 \times 10^6$  cells intraperitoneally (i.p.) in sterile PBS. Animal weight, abdominal distention (if present), tumor bulging and overall wellbeing were tracked weekly and, close to euthanasia, daily. The end-of-wellness endpoints criteria were: weight loss or gain >15%, presence of abdominal distention

that affects the mobility, respiratory distress, anorexia, and/or diarrhea. In case the animal did not develop any of these criteria, we waited to one year before sacrificing the animal.

### ***3.5 Tissue collection***

After euthanasia, peritoneal disease was documented either by the naked eye or by the use of a Leica stereoscopic microscope M165 FC; images of multiple tumor masses and of invasion of organs were taken using the same stereo-microscope. Ascites fluid –if present- was drained using a 14-gauge needle and then examined under an inverted microscope. The dissected tissues of interest were placed in cassettes and fixed in 4% paraformaldehyde overnight. Thereafter the tissues were placed in 70% alcohol before transferring them to the histology core facility of the Goodman Cancer Research Centre (GCRC) for processing, paraffin embedding and hematoxylin and eosin (H&E) staining.

### ***3.6 Migration***

Six well plates (Nunc) enclosing Boyden chambers of 8-micron pore size were used (Thermo-Scientific). First, cells were cultured in T75 cm<sup>2</sup> flasks in RPMI media supplemented with 5% fetal bovine serum and 5% bovine serum, 10 mM HEPES, 4 mM L-Glutamine, 100 IU penicillin, 100 µg/ml streptomycin, 0.01 mg/ml insulin (Roche diagnostic, Indiana, USA) and 1 mM of sodium pyruvate at 37°C with 5% CO<sub>2</sub>. Then, the cells were trypsinized, resuspended in serum free media, and plated in the upper chamber at a density of 200,000 cells per insert. A 10% solution containing fetal bovine and calf serum containing media was added to the lower chamber to serve as a chemoattractant. Cells were allowed 30 hours to cross the polycarbonate membrane. At 30 hours, the non-migratory cells remaining in the upper chamber were removed using a cotton swab. Then, the cells located in the lower chamber were washed twice with PBS

before being fixed in 4% paraformaldehyde for 20 minutes. After all cells had been fixed, the membranes and the attached cells were stored in PBS at 4 °C. The membranes were then stained with Alexa Fluor 594 Phalloidin and Sytox Green fluorescence dyes. The migratory cells were counted using a DMI8 Leica inverted fluorescence microscope using an average of twenty images of 20x fields per insert.

### ***3.7 Invasion***

Using the same Boyden chambers, cells were cultured and grown as described for the migration studies. However, before plating the cells, the inserts were coated with a layer of extracellular matrix (ECM) gel (Sigma, E-1270). The stock of ECM gel was thawed overnight at 4 °C and then diluted in cold serum-free media to a working concentration of 60 µg/ml per insert. Each insert was coated with 150 µl of diluted ECM gel and incubated overnight at 37 °C in a humidified atmosphere in the presence of 5% CO<sub>2</sub>. Following incubation of the gel layer, cells were plated at a density of 200,000 cells/insert and in the same manner as described for the migration studies. After allowing 30 hours for invasion, cells were fixed, stained, and quantified as previously described.

### ***3.8 Double staining with Alexa Fluor 594 Phalloidin and Sytox Green***

After storing the cells in PBS, 0.1% Triton was used as permeabilization buffer for 5 minutes. Then, cells were washed twice with PBS before incubating them for twenty minutes with 1% BSA in PBS to reduce the background staining. After washing the cells in PBS, cells were incubated again for twenty minutes with a solution containing 5 ml of stock solution of Alexa-Fluor 594 Phalloidin in 200 ml of PBS per well. During the last 10 minutes of the previous step,

4 ml of a 50 mM dilution of Sytox Green was added to each insert. Once the twenty minutes were completed, the inserts were washed twice with PBS before being stored at 4 °C.

### ***3.9 Microscopy***

Images of general cell morphology and wound healing assays were taken using a phase contrast Amscope inverted microscope with toupview software. Fluorescent images were taken using the DMI8 Leica fluorescence inverted microscope. With the same microscope, manual counting of the cells in the Boyden chamber assays was done. Bright field images of the gross diseases developed within the animals were taken using a Leica stereoscopic microscope M165 FC. H&E and IHC images of the slides were taken using the bright field properties of the Amscope microscope with toupview software.

### ***3.10 Statistical analysis***

All data are represented as mean  $\pm$  s.e.m., and statistical significance was consistently defined as  $P < 0.05$ . Student's t-test and one-way ANOVA followed by the turkey's multiple comparison test were used as appropriate.

### ***3.11 Study approval***

All animals were treated in accordance to the federal government's Canadian Council on Animal care. Animal protocol (#2017-7909) was approved on September of 2017 by the Animal Compliance Office, McGill University, Montreal, Canada. Part of the tissues used in this thesis were obtained from the University of South Dakota following an approved protocol as well.

### ***3.12 Cell line authentication***

All cell lines were authenticated in May 2017 using autosomal short tandem repeat [STR] profiling markers showing a  $\geq 80\%$  match between the cells used in this study and the original cell lines with profiles suitable for verification in references databases. The authentication was done in the cell line authentication core facility of the University of Arizona (<http://uagc.arl.arizona.edu/services/cell-line-authentication-human>).

## **4. Results**

### **4.1 *In Vitro* properties of OC cell lines**

To assess the *In Vitro* properties of HGSOC cell lines in culture, three cell lines were chosen as they have high genetic fidelity to HGSOC according to the genomic profile analysis published by *Domcke et al.* (2): OVCAR-4, OVSAHO and PEO14. The same published data ranked SKOV-3 and A2780 as unlikely to represent HGSOC. On tissue culture plates, OVCAR-4 formed sheets of adherent atypical epithelial cells. OVSAHO organized in micro-rosettes of epithelial cells, while PEO14 tended to form pockets of epithelial cells. In contrast, SKOV-3 and A2780 arranged as more spindle-shaped cells; SKOV-3 has spiked ends, which mimic the neurons dendritic ends. A2780 are smaller in size compared to other cell lines and, characteristically, have very granular nucleus and cytoplasm (Fig.7).

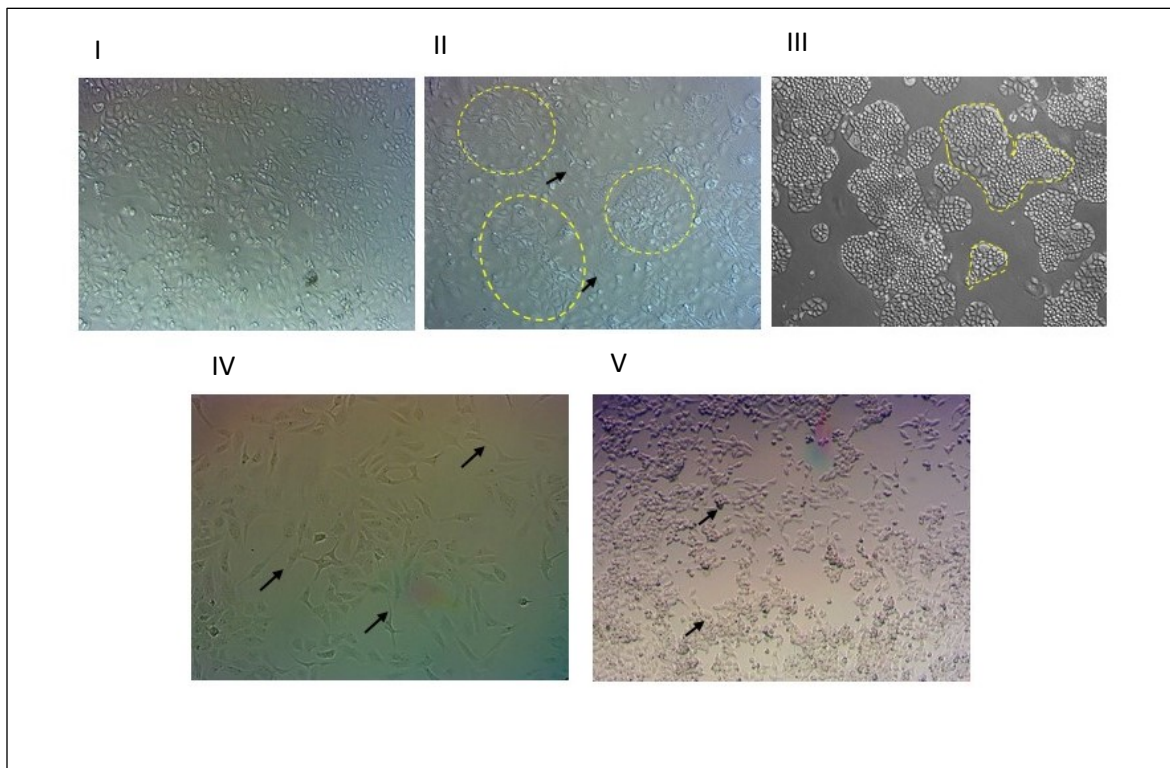


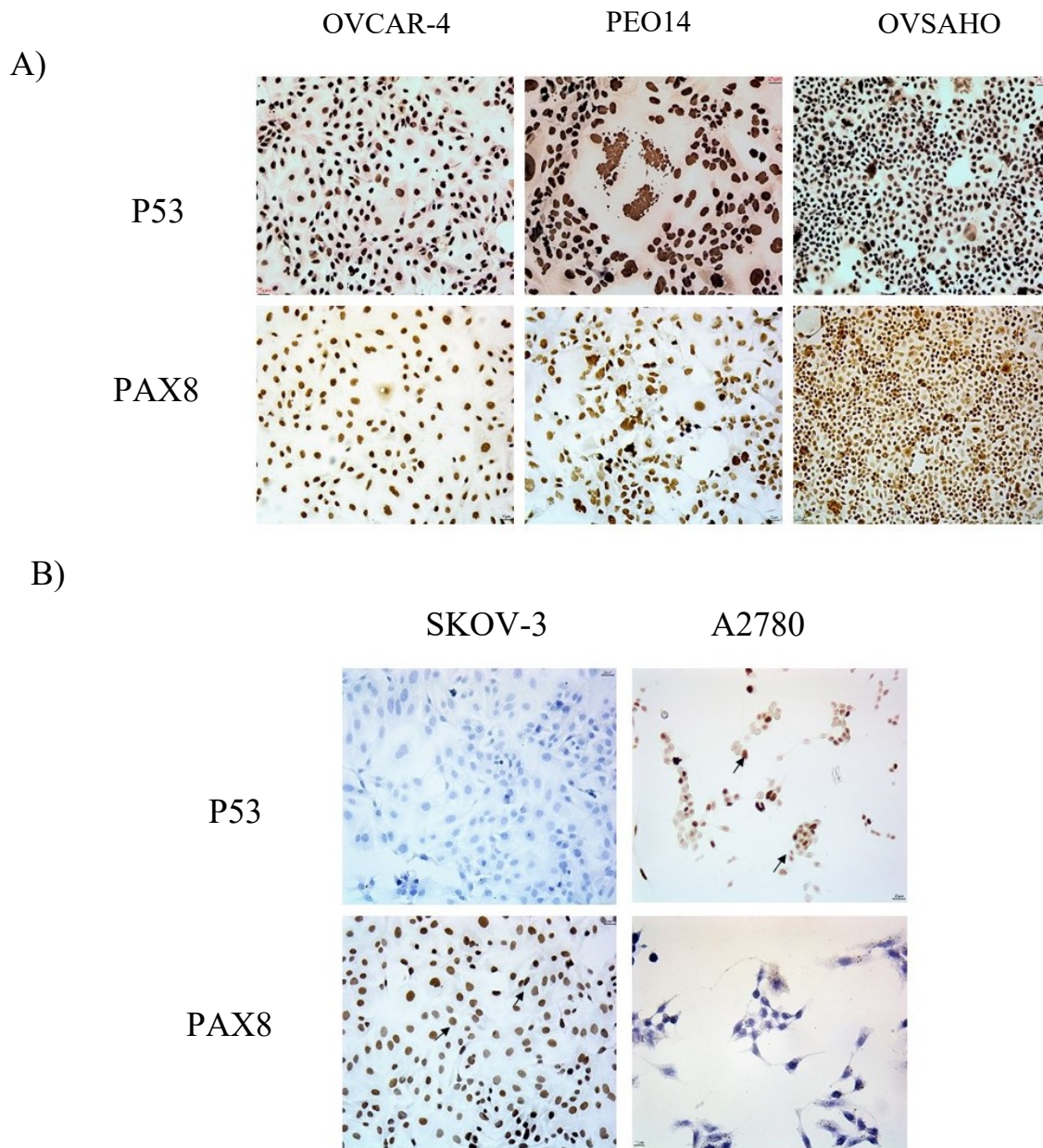
**Figure 7.** Bright field images of five different OC cell lines. All pictures x10 magnification. I) OVCAR-4 showed sheets of epithelial cells. II) PEO14 formed pockets-highlighted by the yellow dash lines-of highly epithelial cells with some other cells in between the pockets (arrows). III) OVSAHO organized in rosettes of different sizes; dashed lines point at two well-formed micro-rosettes. IV) SKOV-3 cells are spindle-shaped with spiked ends (arrows). V) A2780 cells are smaller and granular (arrows).

#### **4.2 Characterization of HGSOC cell lines using immunocytochemistry (ICC)**

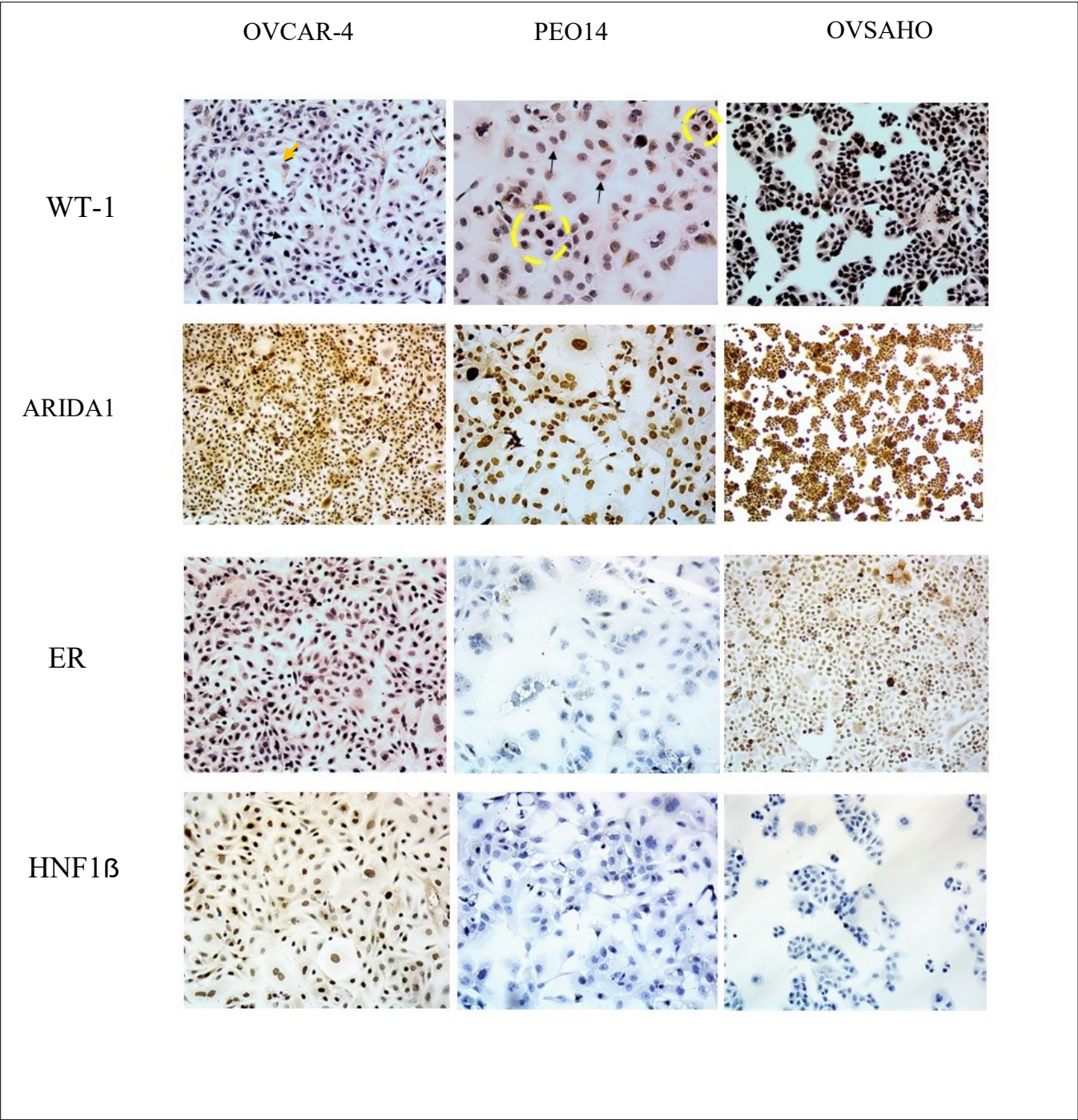
Using ICC, we tested several biomarkers to characterize HGSOC cell lines. Biomarkers were chosen according to the calculation of subtype prediction (COSP) published by *Anglesio et al.* (70) in addition to consultation with a gynecological pathologist regarding the biomarkers that are commonly used in the clinic to diagnose and differentiate HGSOC from other OC subtypes. Nine markers (P53, PAX8, WT-1, ARIDA1, ER, HNF1 $\beta$ , CA125, Vimentin and E-cadherin) were chosen to be tested in three cell lines that highly represent the HGSOC genotype, OVCAR-4, PEO14 and OVSAHO, and two other cell lines that are unlikely to genetically represent HGSOC, SKOV3 and A2780 for the purpose of contrast and comparison.

OVCAR-4, PEO14 and OVSAHO expressed abundantly and homogeneously PAX8 and accumulated abundantly mutant P53, both markers that characterize HGSOC (Fig. 8). This contrasts with SKOV-3, which showed completely negative P53 expression and various degrees of PAX8 expression. A2780 expressed what seemed to be wild type P53 and did not express PAX8 (Fig. 8). Other tested markers showed heterogeneous expression among the different cell lines of HGSOC (Fig. 9). WT-1 was expressed in around 50% of OVCAR-4 cells; in contrast PEO14 showed heterogeneous expression with around 30% of the cells in pockets with nuclear positivity, while the remainder were negative. OVSAHO showed homogenous, intense nuclear positivity; there appeared to be no negative cells. All three cell lines expressed ARIDA1 with similar intensity. ER expression was analyzed based on the clinical judgment of the consulting pathologists, who classified a sample as positive when 1% or more cells were stained. ER was expressed homogeneously and with high intensity in around 70% of OVCAR4 cells, while PEO14 was completely negative with none of the cells demonstrating nuclear staining. In OVSAHO cells, approximately 50% of the cells expressed ER in various degrees of intensity.

For HNF1 $\beta$ , OVCAR4 was the only positive cell line of the three, and almost 90% of cells expressed nuclear staining. CA125 tended to be expressed in clusters in all cell lines, with PEO14 showing the lowest number of positive clusters. Vimentin showed faint cytoplasmic expression in OVCAR-4, somewhat greater expression in PEO14, where around 70 % of the cells were positive, and no expression in OVSAHO cells. E-cadherin formed a network, mainly in pockets surrounding the cells in OVCAR-4 and PEO14, and was not expressed in OVSAHO cells. SKOV-3 and A2780 cells also showed a different panel of ICC that differentiates them from HGSOC (Fig. 10). Table 6 summarizes the results achieved from this experiment.



**Figure 8.** Light microscopy images of the three cell lines that represent HGSOc tested with P53 and PAX8 antibodies. All pictures are shown in x20 magnification; PAX8 in A2780 is shown in x100 for clarity. (A) Note the abundant accumulation of mutant P53 and the expression of PAX8 in the three HGSOc cell lines. PAX8 was homogeneously strong in its intensity among them. (B) SKOV-3 lacks any expression of P53, as expected, because it is known to carry a P53 deletion. A2780 has wild type P53, which is depicted by the fact that few cells express the protein (arrow). PAX8 was expressed in various degrees (dark and light) of intensity in SKOV-3 (arrows). A2780 cells do not show any expression of PAX8.



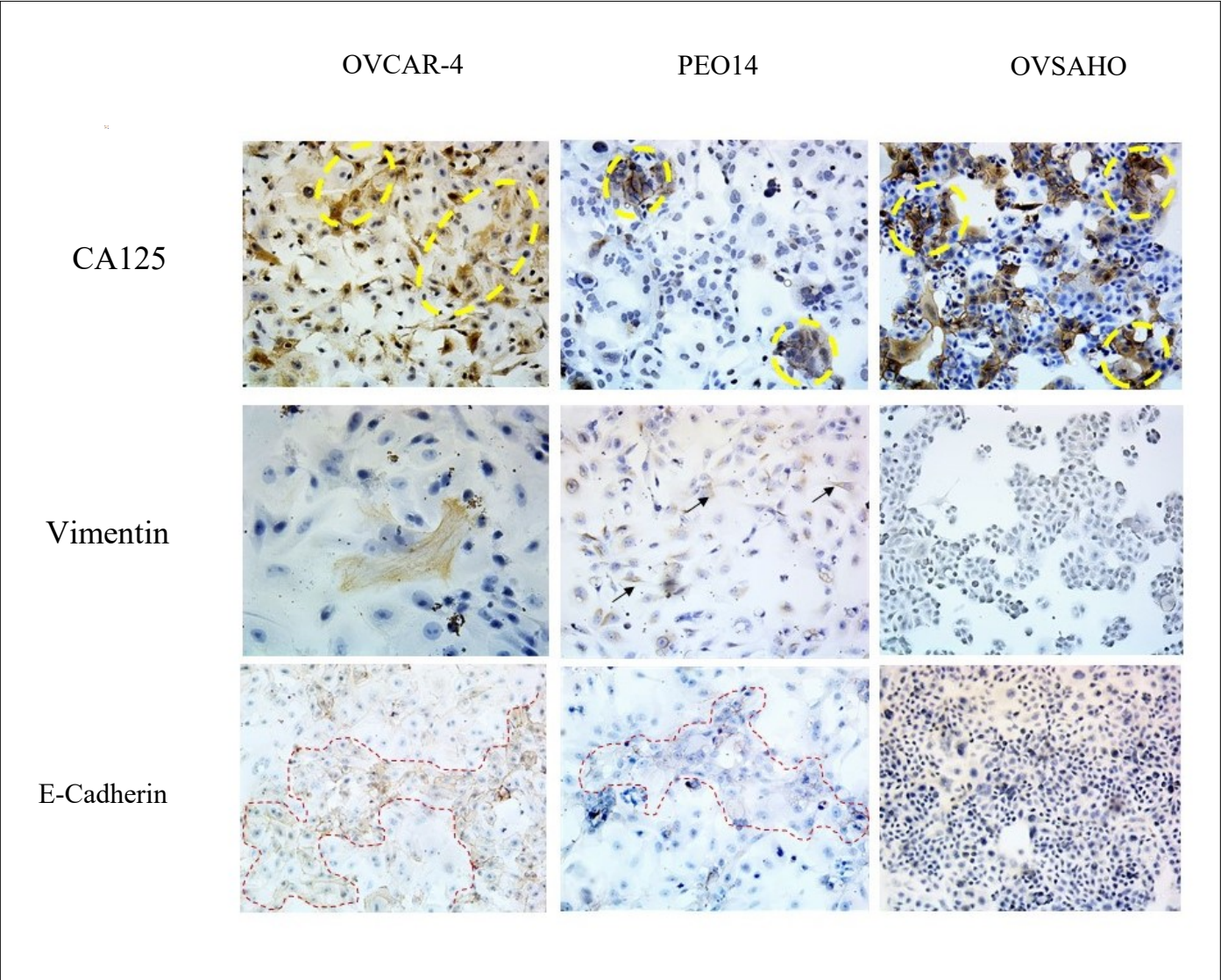
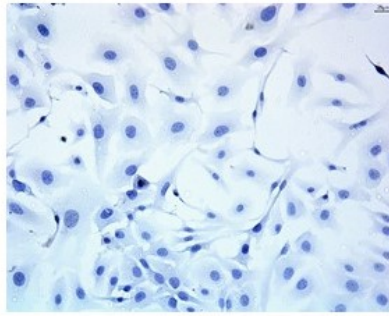


**Figure 9.** Light microscopy images of the three cell lines that represent HGSOC tested with 7 different antibodies. All pictures are shown in x20 magnification unless otherwise specified. Labels: **WT-1** positive cells have a dark brown nucleus (black arrow) when compared to negative cells (yellow arrow). For **WT-1** and **CA-125**, dashed yellow circles indicate clusters of positive cells. For **E-cadherin**, brown dashed lines indicate a network surrounding the cells, mainly in pockets.

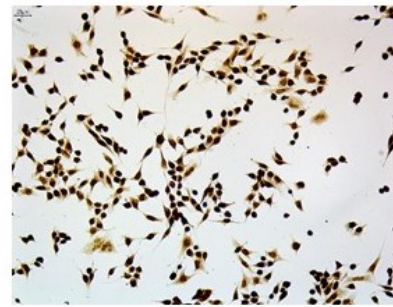
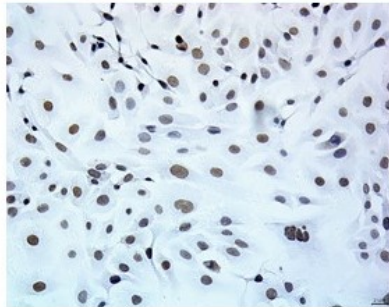
SKOV-3

A2780

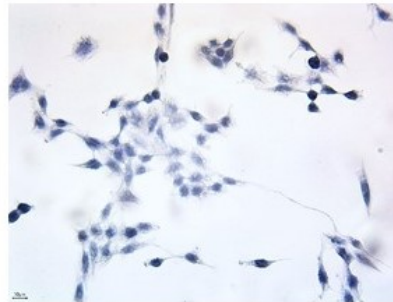
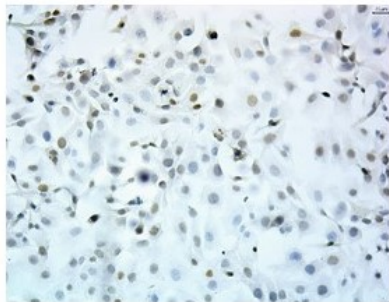
WT-1



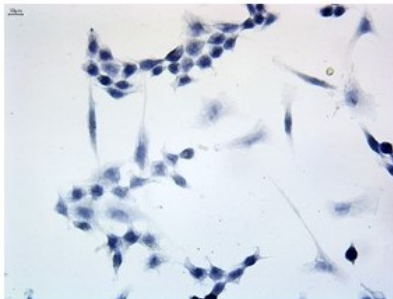
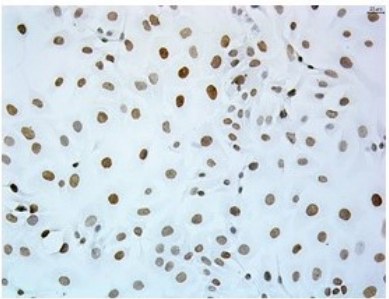
ARIDA1



ER



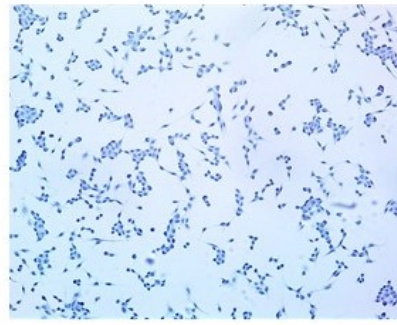
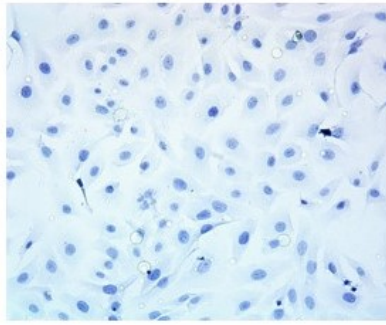
HNF1 $\beta$



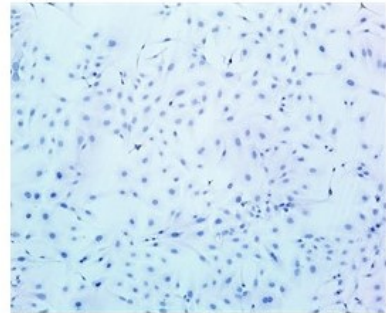
SKOV-3

A2780

CA125



Vimentin



E-Cadherin

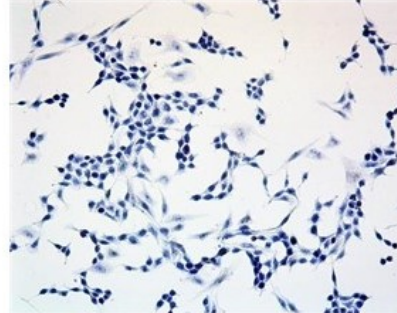
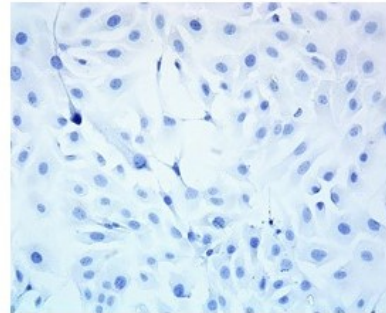


**Figure 10.** Light microscopy images of the two cell lines that unlikely represent HGSOc tested with different antibodies. All pictures are in x20 magnification unless otherwise specified. **WT-1:** SKOV-3 cell line was completely negative for WT-1 while A2780 was intensely positive (dark brown nucleus). **A1RDA1:** expressed in both cell lines, but with higher intensity seen in A2780 cells. **ER:** analyzed based on the clinical judgment of the pathologist; if 1% and more of the cells are positive, it is considered positive. ER was expressed in around 50% of SKOV3 cells (heterogenous expression- arrows) making this cell line positive for ER. A2780 is completely negative for ER as none of the cells had nuclear staining. **HNF1 $\beta$ :** SKOV-3 expressed nuclear positivity for HNF1 $\beta$  while A2780 was completely negative. **CA125:** this membranous marker was completely negative in both SKOV-3 and A2780 cells. **Vimentin:** cytoplasmic marker expressed with high intensity in A2780 cells. **E-Cadherin:** neither SKOV-3 nor A2780 express the biomarker.

Table 6: Summary of the immunohistochemical biomarkers expressed in different OC cell lines

|                               | <b>OVCAR-4</b>                            | <b>PEO14</b>                 | <b>OVSAHO</b>  | <b>SKOV-3</b>               | <b>A2780</b> |
|-------------------------------|---|------------------------------|----------------|-----------------------------|--------------|
| <b>P53</b>                    | + (100%) (mut)                            | + (100%) (mut)               | + (100%) (mut) | - (100%) (del)              | + wild type  |
| <b>PAX8</b>                   | + (100%)                                  | + (100%)                     | + (100%)       | + (100% variable intensity) | - (100%)     |
| <b>WT-1</b>                   | + (~50%)                                  | + (~30%) in pockets          | + (100%)       | - (100%)                    | + (100%)     |
| <b>ARIDA1</b>                 | + (100%)                                  | + (100%)                     | + (100%)       | + (100%)                    | + (100%)     |
| <b>ER</b>                     | +   | - (100%)                     | +              | +                           | - (100%)     |
| <b>HNF1<math>\beta</math></b> | + (~70%)                                  | - (100%)                     | - (100%)       | + (~70%)                    | - (100%)     |
| <b>CA125</b>                  | + in pockets                              | + in pockets                 | + in pockets   | - (100%)                    | - (100%)     |
| <b>Vimentin</b>               | Single cell positivity / high power field | + (~70%)                     | - (100%)       | - (100%)                    | + (100%)     |
| <b>E-Cadherin</b>             | + forming network                         | + forming network in pockets | - (100%)       | - (100%)                    | - (100%)     |

### ***4.3 In vivo tumor growth and characterization***

#### ***4.3.1 Tumor latency and disease presentation***

To assess the ability of the different cell lines to recapitulate the disease (HGSOC), xenografting followed by extensive pathological characterization were done. We hypothesized that intra-peritoneal (i.p.) administration of OC cells from different cell lines having high genetic fidelity to HGSOC will develop, in nude mice, peritoneal carcinomatosis resembling anatomical and histopathological features of advanced disease encountered in patients with advanced disease. We first studied the tumorigenicity of the three cell lines that have high genetic fidelity to HGSOC as mentioned before: OVCAR-4, PEO14 and OVSAHO. In addition, and to allow better assessment, we also tested the tumorigenicity of the tumors developed by the cell lines that have low genetic fidelity with HGSOC: SKOV-3 and A2780. For that purpose, we had five groups of mice; one group/cell line. Each group consisted of three mice; we injected 2 million cells i.p. into each experimental mouse. Two other groups of mice were injected with vehicle. The unique observation of the cell lines tested is the time that cells take to develop the disease and reach the end-of-wellness endpoint criteria. The three cell lines OVCAR-4, PEO14 and OVSAHO took an average of four to eleven months to show the disease manifestation, hence the tumor development. This is in marked contrast to the low HGSOC fidelity cell lines SKOV-3 and A2780, which developed the disease in less than three months.

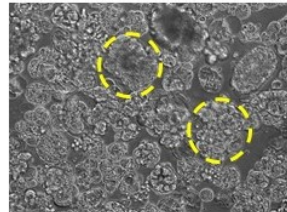
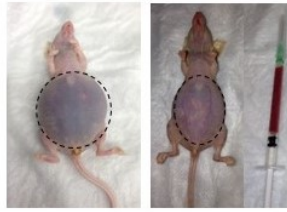
The disease presentations are markedly variable among the three cell lines that represent HGSOC. OVCAR-4 accumulated large volume bloody ascites heavily populated by multicellular aggregates. OVSAHO developed rapid weight loss over two weeks before euthanasia, with a small volume of ascites showing only scant number of multicellular structures

(MCS). The tumor burden was evident in PEO14 when the masses were bulging from the abdomen, yet none developed ascites. When compared to the low fidelity cell lines, SKOV-3 consistently developed large bulging lower pelvic masses and large abdominal distention which has very complex multicellular structures. A2780 formed bilateral large flank masses (Fig. 11). The data shown in table 7 summarize the tumor latency, presenting symptoms, and the presence or absence of ascites in animals injected with each cell line.

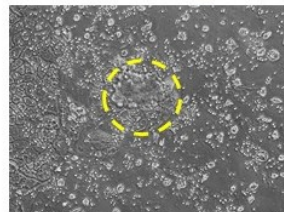
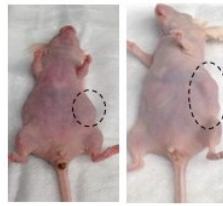
Table 7: tumor latency, presenting symptoms and ascites components

|                                   | <b>OVCAR-4</b> | <b>PEO14</b>             | <b>OVSAHO</b> | <b>SKOV-3</b>     | <b>A2780</b>           |
|-----------------------------------|----------------|--------------------------|---------------|-------------------|------------------------|
| <b>Tumor latency</b>              | ~7 months      | ~11 months               | ~5 months     | ~11 weeks         | ~30 days               |
| <b>Marked presenting symptoms</b> | Ascites        | Bulging abdominal masses | Cachexia      | Lower pelvic mass | Bilateral flank masses |
| <b>Ascites components</b>         | MCS            | No ascites               | Scant MCS     | Complex MCS       | Few MCS                |

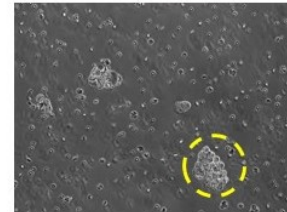
OVCAR-4



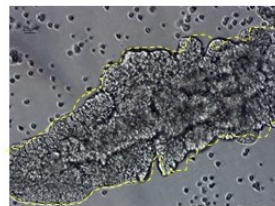
PEO14



OVSAHO



SKOV-3



A2780

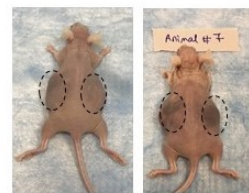


**Figure 11.** Presentations of the disease and the ascites. All pictures of bright field were taken using an inverted microscope with a x20 magnification. OVCAR-4-injected animals showed distended abdomen that was progressively developed over 7 months; the corresponding image of the ascites is full of MCS. Animals injected with PEO14 cells, after 11 months, developed masses that were bulging from the abdomen or masses that could be felt on palpation. None had ascites, however peritoneal washes performed showed few MCS. OVSAHO cells, when injected in animals, caused sudden loss of weight and the animal became cachectic as depicted by the hunched back (arrow); the abdominal wall was mildly distended, and less than 1 ml of bloody ascites was drained which had scant MCS. SKOV-3 cells caused the mice to have very distended abdomens and a large volume of hemorrhagic ascites with very complex MCS. A2780 cells distinctively developed bilateral flank masses; the small volume ascites rarely had MCS.

#### ***4.3.2 Macroscopic and microscopic pathological assessment of the tumor***

The intra-abdominal disease was examined upon each animal's sacrifice using the naked eye and a stereoscopic microscope. The disease dissemination within the pelvic, abdominal and pleural cavities was recorded to allow valid comparison among the cell lines. Macroscopically, OVCAR-4 cells formed tumors that were adherent to different organs within the abdominal cavity and even afar including the plural cavity and the diaphragm. PEO14 cells formed well-defined masses of different sizes that are separated from the organs, while OVSAHO cells developed discrete disease compared to OVCAR-4 and PEO14 cells. None of the three OC cell lines showed clear macroscopic invasion to the ovaries. SKOV-3 formed distinctive and consistent lower pelvic masses, micro-nodular masses surrounding the mesenteric fat, and very adhesive disease that occupied almost the entirety of the abdominal organs. The ovaries were very difficult to be identified in SKOV-3 injected mice, as the tumor adhesion was very dense. We assumed that the ovaries were taken within the adhesions. A2780 cells uniquely formed ovarian masses; both ovaries were consistently replaced by the tumor growth (Fig. 12). All the OC cell lines tested in this experiment were prone to metastasize to the omnetum, mesenteric fat and various parts of the gastrointestinal tract. However, the disease developed by SKOV-3 and A2780 cells was more evident and easily detectable than the ones developed by the other three cell lines with high genomic fidelity to HGSOC. Table 8 summarizes the common sites of metastasis for each cell type studied.

Microscopically, among the three cell lines that represent HGSOC, there were various degrees of invasiveness. Tumor formed by OVCAR-4 cells showed aggressive parenchymal invasion with desmoplastic reaction to every organ within the abdominal cavity and even distant

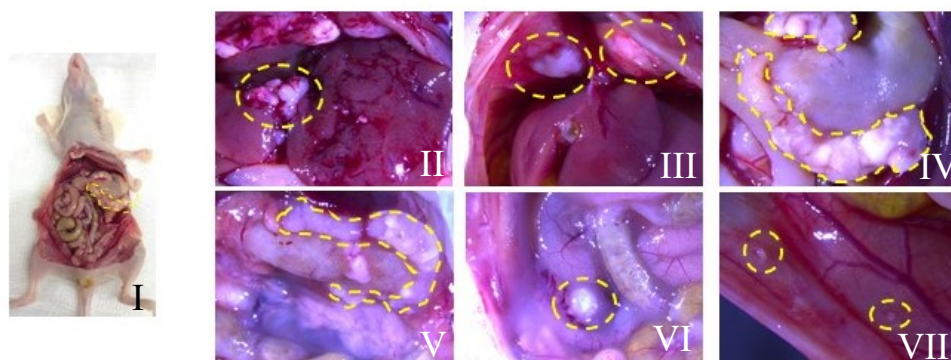
microscopic invasion to the lung (Fig. 13 & 27). PEO14 failed to invade organs within the abdominal cavity; instead the cells promoted the formation of well-defined masses scattered between the organs (Fig. 14). OVSAHO cells triggered the formation of masses that caused pushing invasiveness to various organs within the abdominal cavity including pancreas, liver and the gastric wall (Fig. 15). A2780 cells led to the formation of tumors that had the capacity to invade some but not all the organs within the abdominal cavity (Fig. 17).

Despite various degrees of microscopic invasiveness, all the tumors developed within the three cell lines that represent HGSOE displayed the same features seen in patient specimens diagnosed with this histopathological type of the disease (i.e. HGSOE) (Fig.16). Histologically, the tumor formed branching papillary fronds with slit-like fenestrations in some part of the tumors; areas of glandular complexity were identified as well. The nuclear features were consistent with high grade carcinoma, involving marked nuclear atypia, nuclear pleomorphism and prominent nucleoli. Extensive mitosis ( $>10$  mitosis/High Power Field [HPF]) was noticed within the tumor section studied. Distinctively, tumor formed by OVCAR-4 cells showed various psammoma bodies (calcium deposition with concentric laminations) (Fig. 16). Tumor developed from A2780 cells formed sheets of high grade tumor with some glandular punched out spaces that mimic high grade endometrioid carcinoma with some areas of poorly differentiated carcinoma (Fig.17).

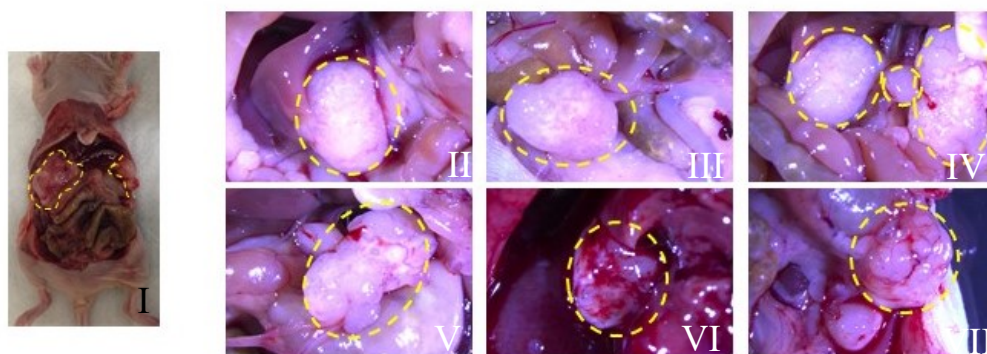
Table 8. The common site of tumor dissemination recorded within the abdominal and pelvic cavities for each cell line.

|   | OVCAR-4  | PEO14  | OVSAHO                                | SKOV-3   | A2780   |
|---|--|--|---------------------------------------|--|---|
| Macroscopic abdominal disseminations of the disease | Diaphragm, liver, stomach, omentum, pancreatic-spleen area, mesentery, mesenteric fat, pelvic fat, kidney. | Masses were close to the liver, pancreatic area, and parts of the mesentery. | Omentum, stomach and pancreatic area. | Diaphragm, adhesive mass attached to the spleen, stomach, liver and the genital tract. diaphragm, lower pelvic mass. | Diaphragm, stomach, liver, omentum-pancreatic area, mesentery, ovaries. |

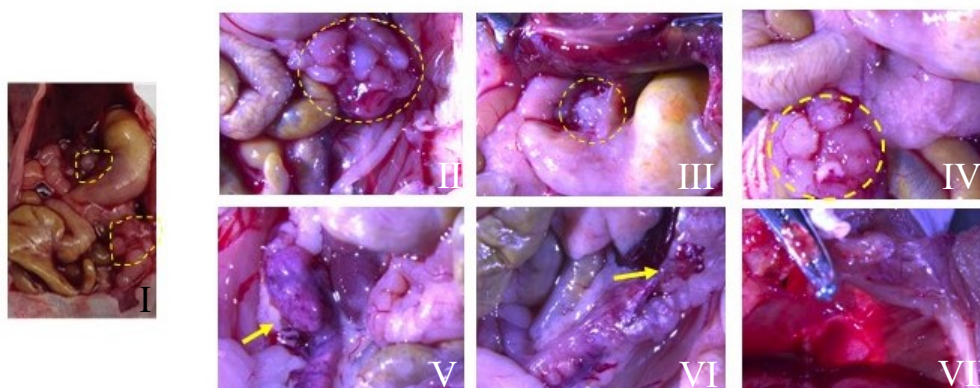
A) OVCAR-4



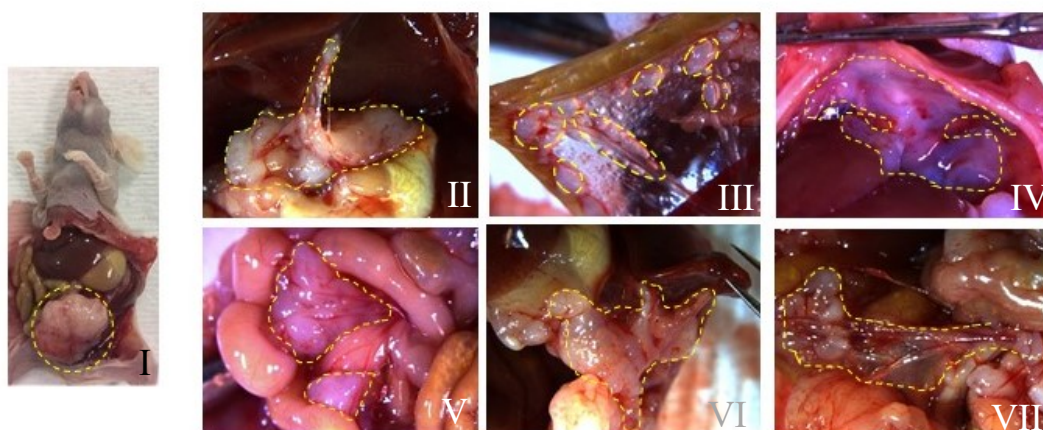
B) PEO14



C) OVSAHO



D) SKOV-3



E) A2780

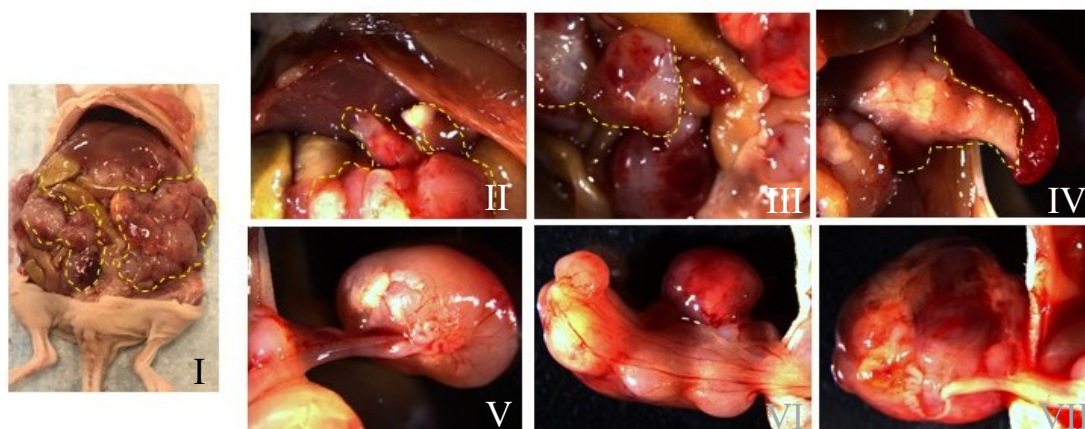


**Figure 12.** Macroscopic disease developed within the peritoneal cavity of nude mice by each cell line. **(A)** OVCAR-4 formed adherent tumors in various parts of the abdominal cavity. **(A II)** Liver and liver base: there are multiple growths of tumor masses within the liver and the liver base. Masses are white in color, lobulated and showed gross invasion to the liver parenchyma. **(A III)** Diaphragm: Multiple bulging masses occupied the diaphragm. Masses are presented as white nodular structures covered by some vascular layer. **(A IV-V)** Omentum/tissue around the stomach: a relatively large irregular nodular white growth of the tumor is seen around the stomach area; it occupied more than 2/3 of the greater curvature of the stomach. Another large irregular white mass is occupying the omentum area. **(A VI)** Mesentery: The fat tissue around the intestines show multiple small tan-gray nodules. Adherent to the intestine, there is a well-defined white mass (shown in the images). **(A VII)** Pleural cavity: Small multiple white nodules lining on the muscular wall of the pleural cavity. **(B)** PEO14 formed variable size masses distributed around the organs. **(B II)** Liver: there is a well-defined white mass pushing the liver base. **(B III)** Mesentery: Well-defined white mass with irregular surface attached but not invading the mesentery. **(B IV)** Masses at the injection site (smooth white in color) and another one attached to the stomach (irregular surface white in color). **(B V)** Omentum: there are three irregular white masses located around the stomach/omentum area. **(B VI)** Within the peritoneal cavity there is a well-defined hemorrhagic mass between the liver and the kidney. **(B VII)** Hemorrhagic well-defined mass in the left side. **(C)** OVSAHO cells formed discrete masses compared to other cell lines. **(C II)** Grape-like structure seen occupying the area of the omentum (underneath the stomach). **(C III)** Just above the lesser curvature of the stomach, there is a small white shiny mass. **(C IV)** small mass around the stomach-pancreatic area **(C V)** and **(C VI)** hemorrhagic ovaries. **(C VII)** Unremarkable diaphragm. **(D)** SKOV-3 cells consistently formed

large lower pelvic masses **(D I)** and very adhesive tumors. **(DII)** Liver base mass bilaterally attached to the liver and the stomach. **(D III)** Peri-mesenteric fat occupied by multiple small well-defined white nodules. **(D IV)** White irregular patches are seen covering the diaphragm. **(D V)** Mesenteric multiple masses formed rings around the intestine. **(D VI)** Mass attached underneath the spleen. **(D VII)** Clear view of the dense adhesion that took most parts of the tumors and attached them to various organs within the abdomen. **(E)** A2780 cells showed bulky tumors within the abdominal and pelvic cavities. **(E II)** Multiple fused tumors attached to the liver and stomach. **(E III)** Multiple masses attached to the mesentery. **(E IV)** Mass attached to the spleen. **(E V, VI and VII)** Enlarged ovarian growth.

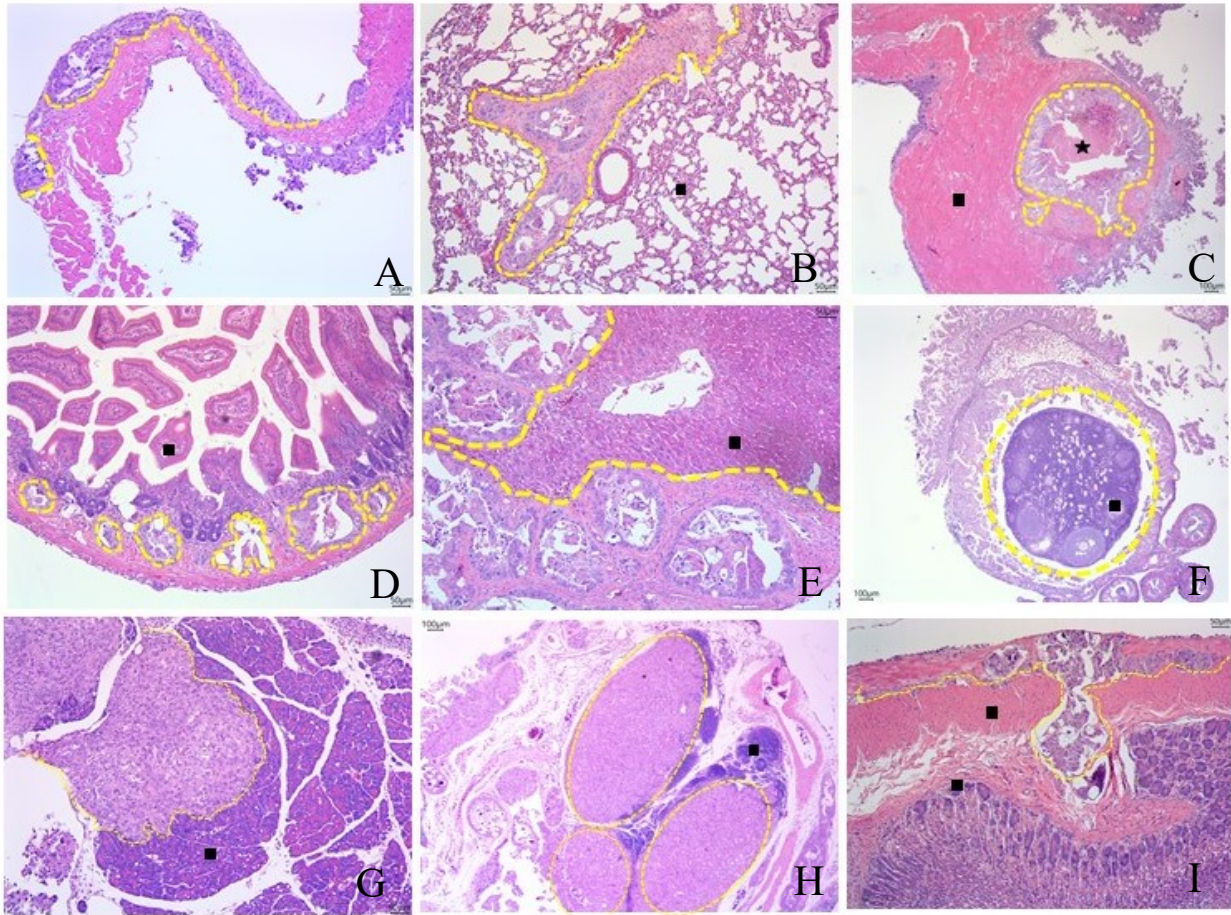


**Figure 13.** Tumors developed after the injection of OVCAR-4 cells were able to invade multiple organs within and beyond the abdominal cavity. **(A)** A tumor infiltrates the skeletal muscle of the diaphragm (yellow dashed line). **(B)** Lung parenchyma was also infiltrated by the tumor (yellow dashed line). **(C)** Skeletal muscle of the abdominal wall (square) was infiltrated by the tumor (yellow dashed line). The star points to the necrosis developed in the center of the tumor. **(D)** Submucosal infiltration (yellow dashed line) was seen in the small intestine (square). **(E)** Liver parenchyma (square) was infiltrated by the tumor. **(F)** Ovarian tissue (square) was completely surrounded by the tumor growth. **(G)** Pancreatic parenchyma (square) was infiltrated by the tumor (yellow dashed line). **(H)** A lymph node (square) is heavily infiltrated (“almost replaced”) by the tumor (yellow dashed line). **(I)** Gastric wall muscle (square) is invaded by islands of tumor tissue (yellow dashed line).

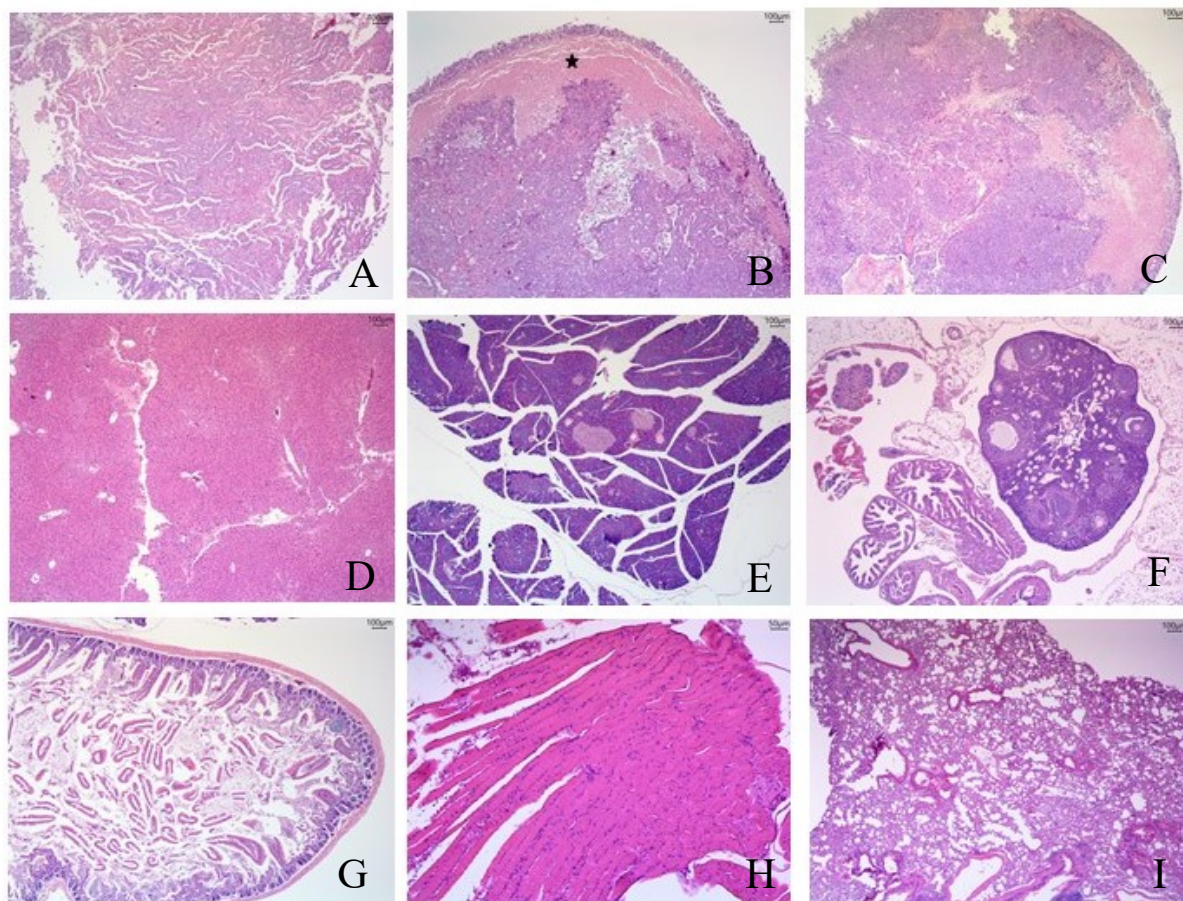


**Figure 14.** The tumors developed within the animals injected with low load of PEO-14 cells showed no invasiveness to any of the organs. **(A)**, **(B)** and **(C)** tumor masses developed within the abdominal cavity, displayed the features of HGSOc, such as papillary structures, and glandular complexity. Note in **B** the necrotic area within the tumor growth (star). Multiple sections from multiple organs showed organs-free of any growth as follows: **(D)** liver, **(E)** pancreas, **(F)** ovaries, **(G)** small intestine, **(H)** diaphragm, skeletal muscle, and **(I)** lung tissue.

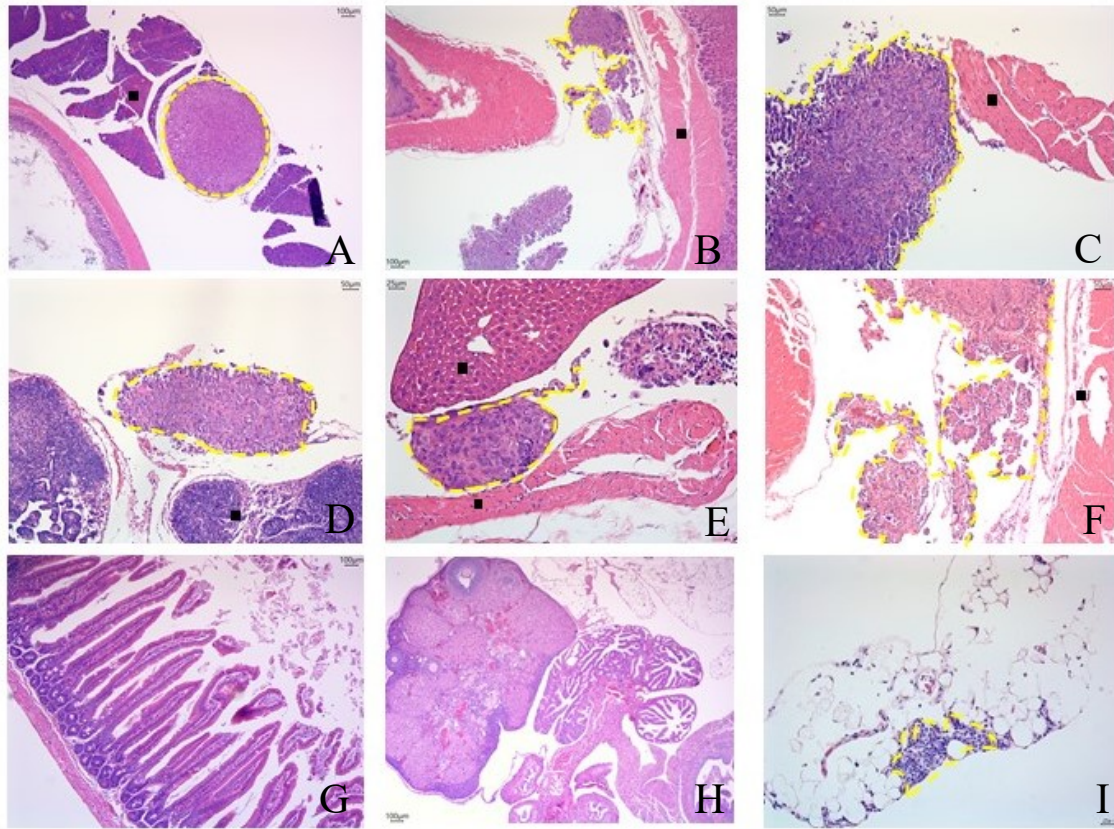


**Figure 15.** OVSAHO tumor formed pushed invasiveness into the (A) pancreas, (B) gastric wall, (C) diaphragm, (D) lymph nodes and (E) liver (F) Abdominal wall. However, some other tissues were free of tumor growth; (G) intestine; and (H) ovaries. (I) There are small inflammatory infiltrates (yellow dashed line) noticed in the fat of the omentum.

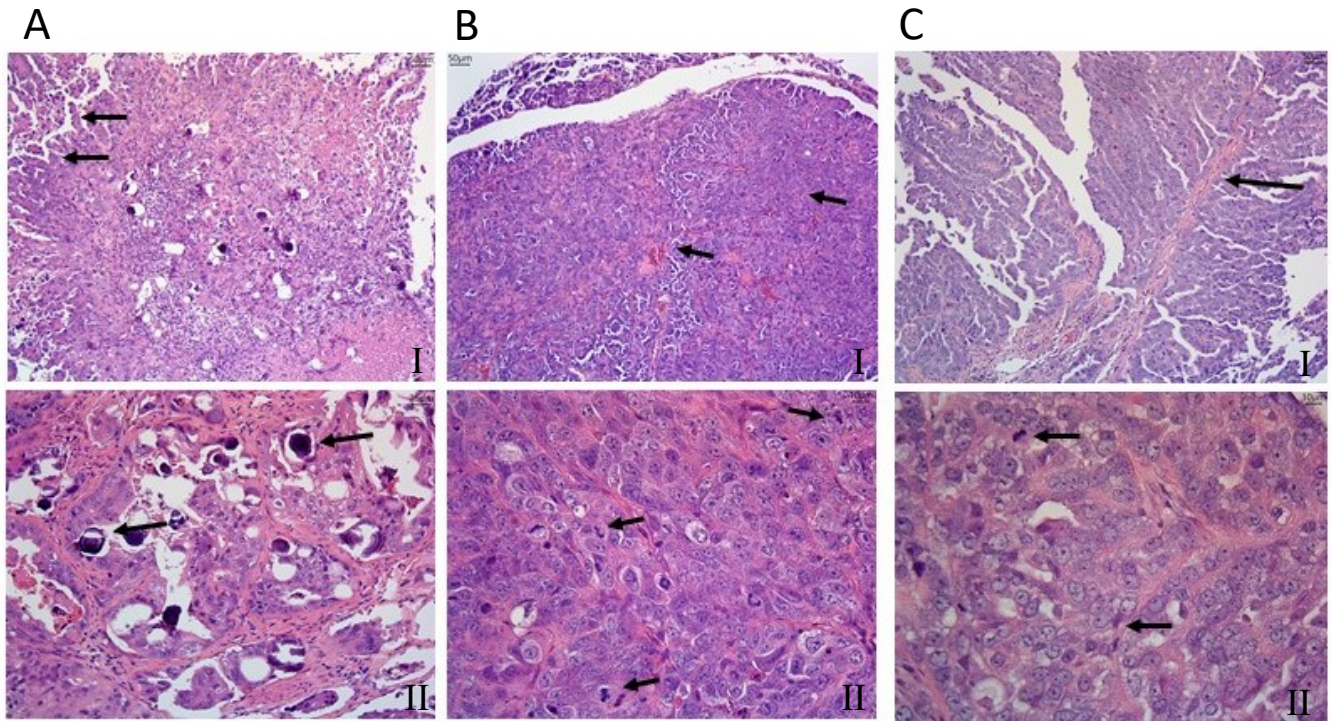
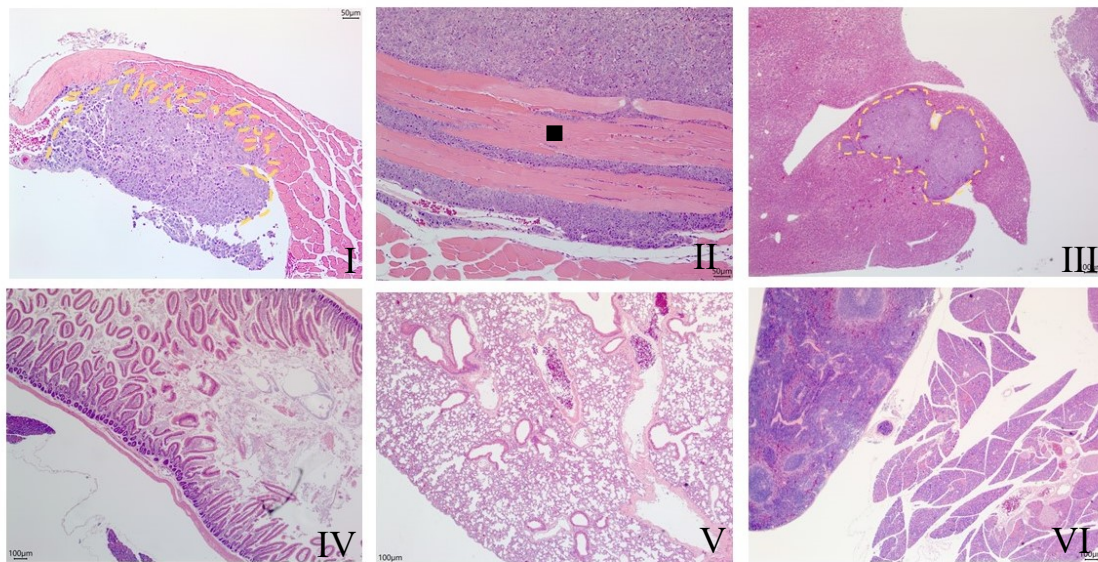
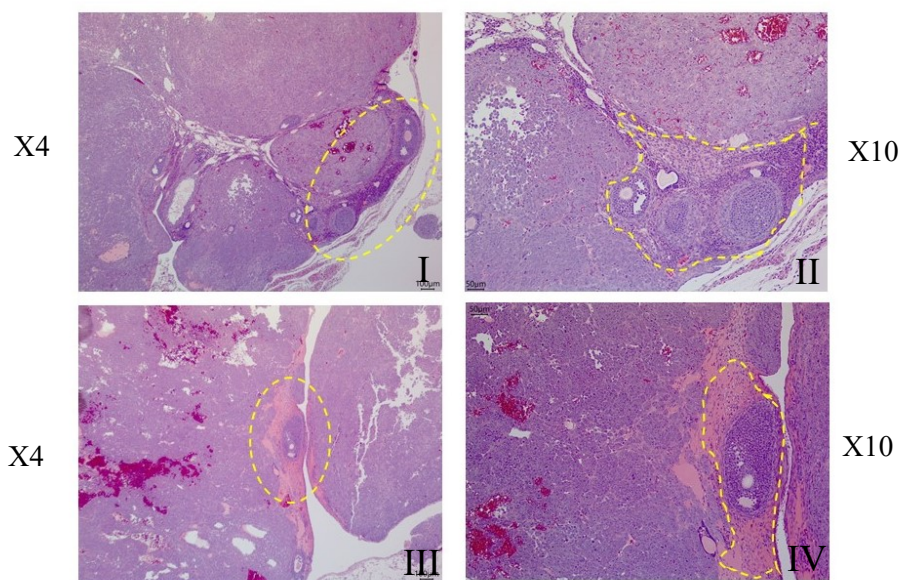


**Figure 16.** Though different cell lines had different invasive capacity within the abdominal cavity, all of them developed tumors that displayed the same histological features of HGSOC (upper panel in x10 and lower panel in x40 magnifications). **(A I)** Tumors developed within the animals carrying OVCAR-4 cells show papillary structure (arrows). **(A II)** High nuclear to cytoplasm (N/C) ratio, marked nuclear pleomorphism, prominent nucleoli, and extensive mitosis. Various psammoma bodies were noted (arrows). **(B I)** Tumor developed within the animals carrying OVSAHO cells show glandular complexity and slit-like spaces (arrows). **(B II)** High N/C ratio, marked nuclear pleomorphism, prominent nucleoli, and extensive mitoses (arrows). **(C I)** Tumors developed within the animals carrying PEO14 cells showed papillary structures (arrow). **(C II)** Marked nuclear pleomorphism, prominent nucleoli and extensive mitoses (arrows).

A



B



C

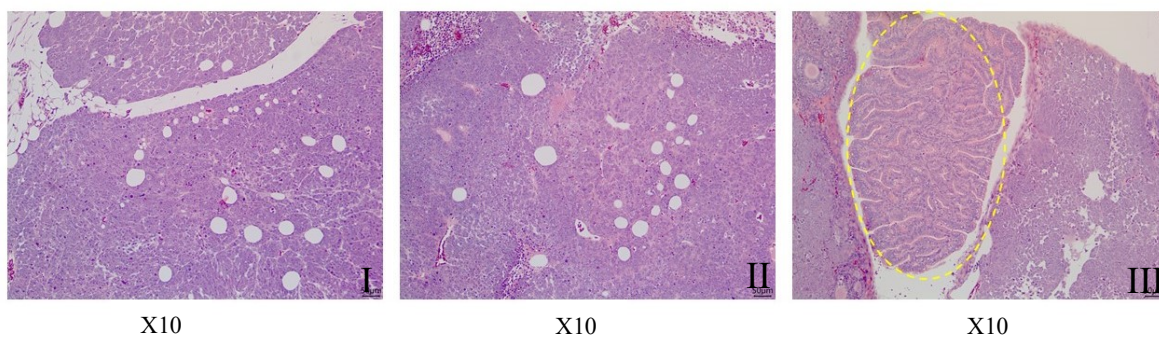
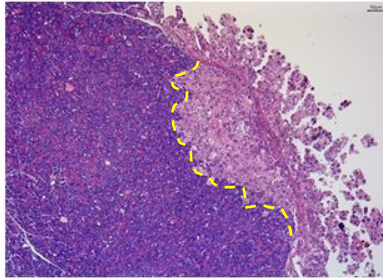


**Figure 17.** Microscopic disease developed within animals injected with A2780 cells. **(A)** All images were taken at x4 magnification except **(A II)** that was taken at x10 for better visualization. **(A-Upper panel)** Depicted is a representation of the tumor invasion to different parts within the abdominal cavity. **(A I)** Tumor cells display infiltration to the skeletal muscle of the diaphragm. **(A II)** Tumor infiltration between the skeletal muscle of the abdomen (square). **(A III)** Part of the tumor growing— dashed yellow line- embedded within the hepatic parenchymal tissue. **(A-Lower panel)** Different organs: **(A IV)** small intestine, **(A V)** lung, **(A VI)**, spleen and pancreas, all showed organs free of malignancy. **(B)** Unique metastatic site for A2780 cells. **(B I and II)** Low and high power images showing the small remaining structure of the ovary. **(B III and IV)** Low and high power images showing that the single growing follicle is the only remaining structure within the ovary; the rest of the ovary is completely replaced by tumor outgrowth. **(C)** Higher magnification depicting some regions within the tumor. **(C I and II)** Rounds punched out clear spaces. **(C III)** Small foci of tissue -dashed yellow lines- mimic high grade endometrial carcinoma.

#### ***4.3.3 Immunohistochemistry evaluation of the in vivo tumor growth***

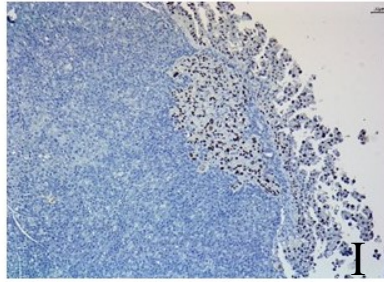
Four immunohistochemistry biomarkers were used to characterize the histopathology of the tumors developed within the peritoneal cavity of nude mice by the OC xenografts. P53, PAX8, WT-1 and CA125 were chosen as they are the most clinically used OC markers. The tumor developed from the three cell lines that genetically resemble HGSOc showed abundant nuclear expression of P53 (likely mutant) and PAX8. This observation is consistent with our in vitro finding showing the expression of both biomarkers in the cultured cells (Figs. 18, 19 and 20). WT-1 showed strong nuclear expression in OVSAHO-derived tumors and some expression in OVCAR-4-derived tumors. Interestingly, tumors developed upon i.p. injection of PEO14 cells lack WT-1 expression. All the tumors derived from the three cell lines showed characteristic expression of CA125 in the slit-like fenestrations (Figs. 18, 19 and 20). A2780 cells led to the formation of tumors that showed varied intensity of expression of P53 likely denoting the wild-type nature of this gene in these particular cells. They do not express either PAX8 or CA125. WT-1 showed diffuse expression within the A2780-derived tumor cells and such expression was non-limited to the nucleus (Fig. 21).

A

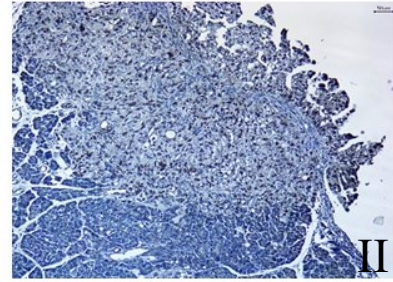


H & E

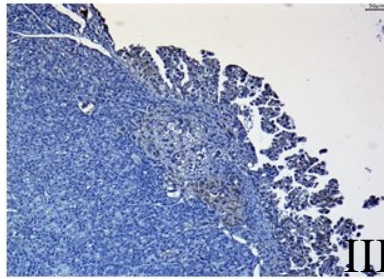
P53



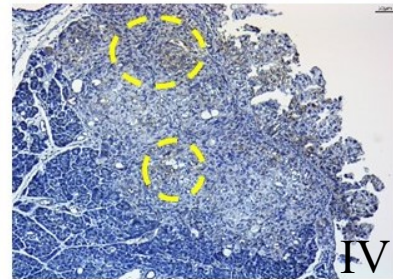
PAX8



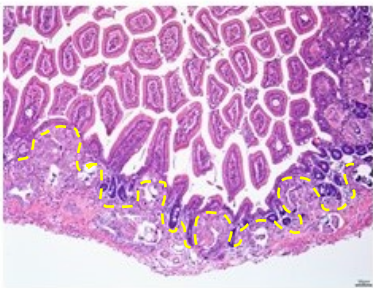
WT-1



CA125

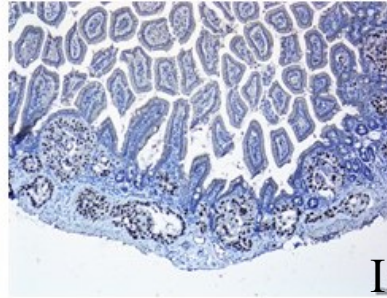


B

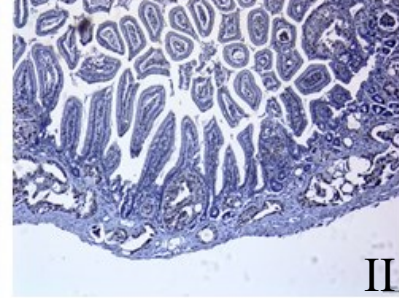


H & E

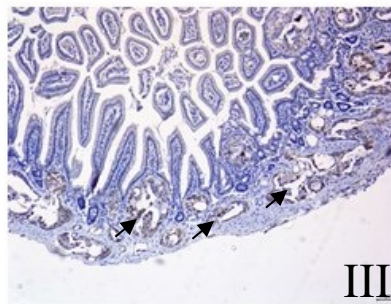
P53



PAX8



WT-1



CA125

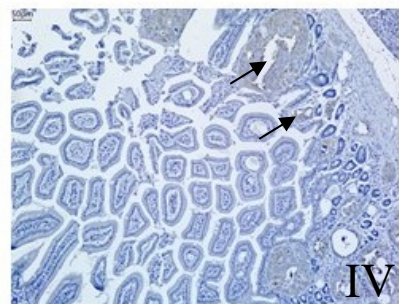
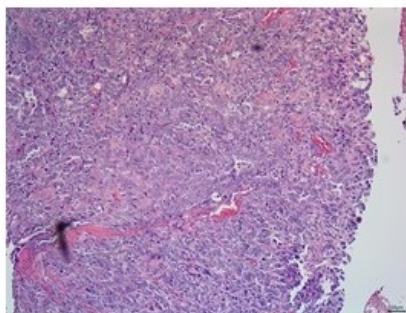
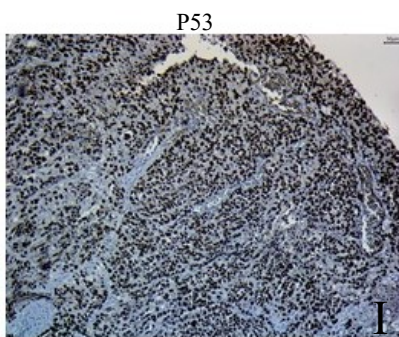


**Figure 18.** Immunohistochemistry evaluation of the tumor developed within animals injected with OVCAR-4 cells. All images were taken with a magnification of x10. **(A)** Tumor infiltrating the pancreatic parenchyma as shown by H&E staining (dashed yellow line). **(A I)** P53 showed dark nuclear stain. **(A II)** PAX8 showed dark nuclear stain. **(A III)** WT-1 showed nuclear stain. **(A IV)** Pockets of cells expressed CA125 in the open spaces within the tumor tissue. **(B)** Submucosal infiltration of the tumor within the small intestine (dashed yellow line). **(B I)** P53 showed dark nuclear stain. **(B II)** PAX8 showed dark nuclear stain. **(B III)** WT-1 showed nuclear stain in most of the cells (arrows). **(B IV)** Pockets of cells expressed CA125 in the open spaces within the tumor tissue (arrows).

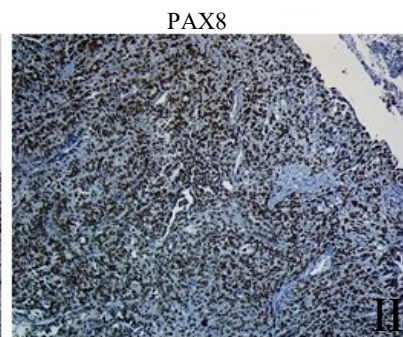
A



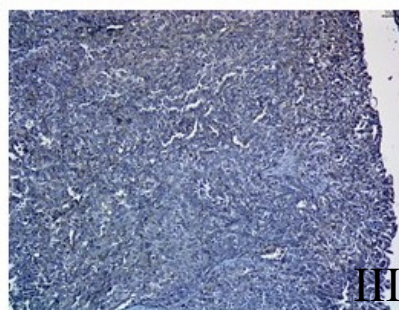
H & E



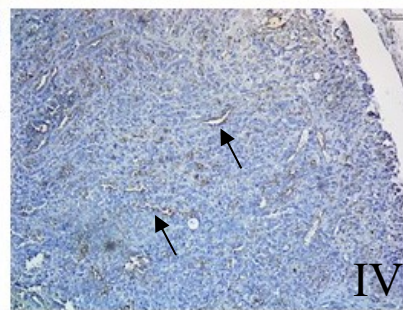
P53



PAX8



WT-1

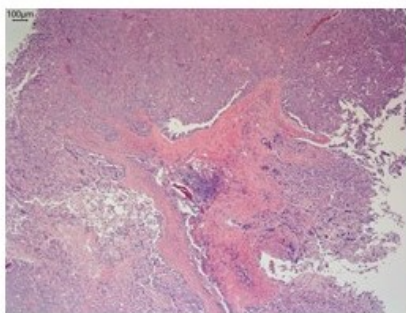


CA125

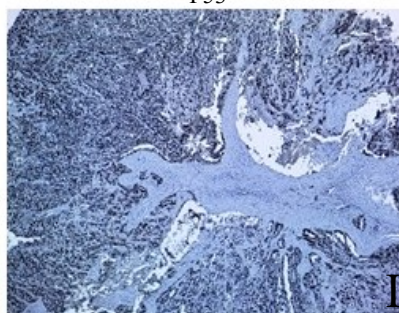
IV

III

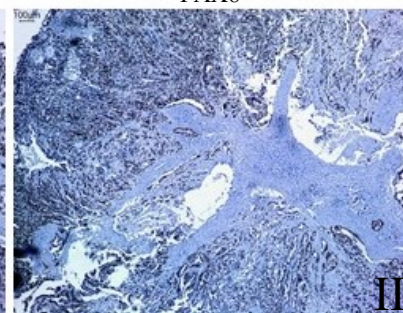
B



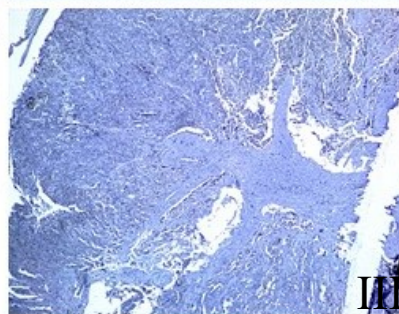
H & E



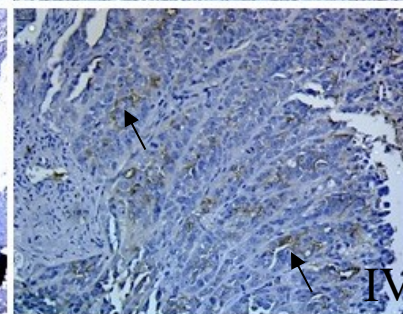
P53



PAX8



WT-1



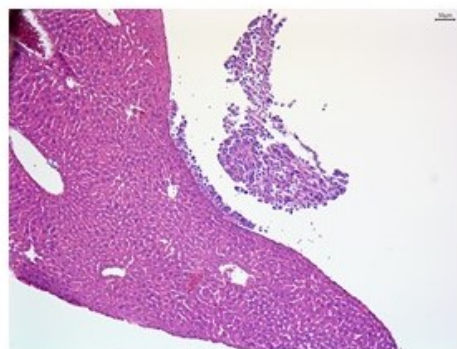
CA125

IV

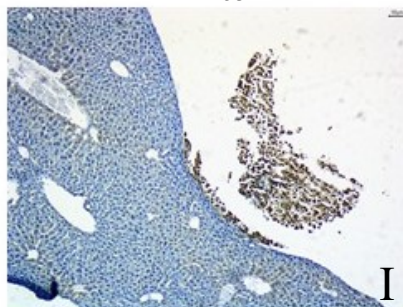
III

**Figure 19.** Immunohistochemistry evaluation of the tumor developed in animals injected with PEO14 cells. **(A)** Part of the tumor (all images captured at x10 magnification). **(AI)** P53 showed dark nuclear stain. **(AII)** PAX8 showed dark nuclear stain. **(AIII)** WT-1 did not show any expression within the tumor tissue. **(AIV)** Pockets of cells expressed CA125 in the open spaces within the tumor tissue (arrows). **(B)** Part of the tumor with connective tissue (all images were taken using a x10 magnification, except for **(BIV)** in which the image was taken at higher magnification (x20) for clarity. **(BI)** P53 showed dark nuclear stain. **(BII)** PAX8 showed dark nuclear stain. **(BIII)** WT-1 was not expressed in the tumor cells. **(BIV)** Cells expressed CA125 in the open spaces within the tumor tissue (arrows).

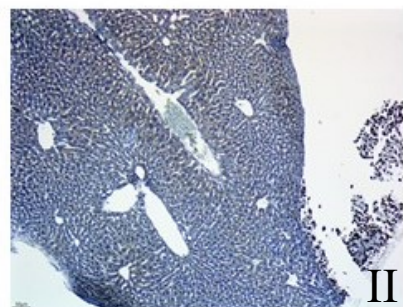
A



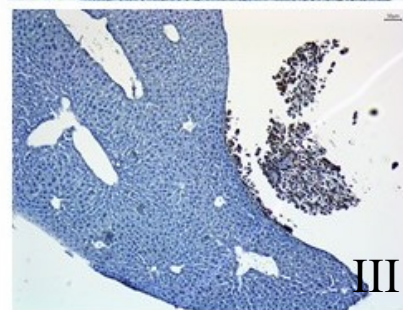
P53



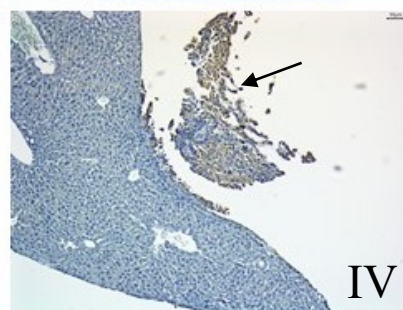
PAX8



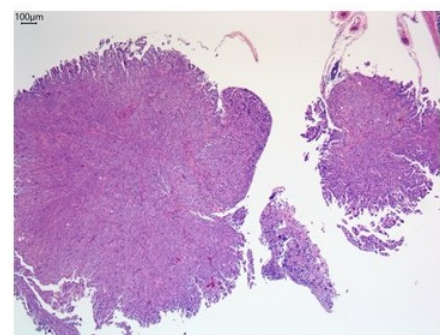
WT-1



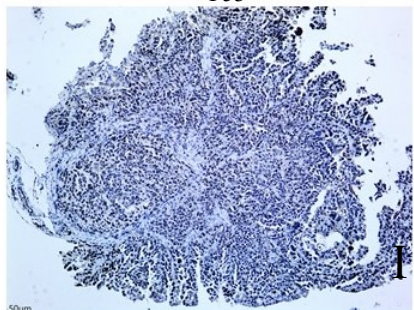
CA125



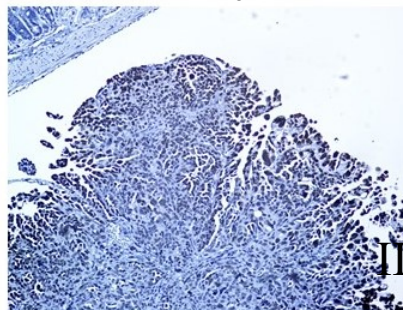
B



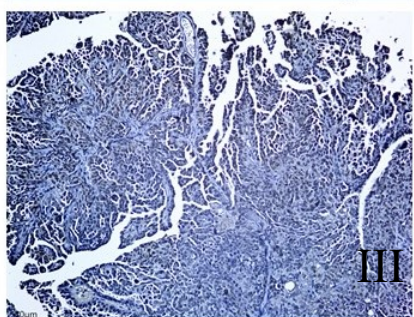
P53



PAX8



WT-1



CA125

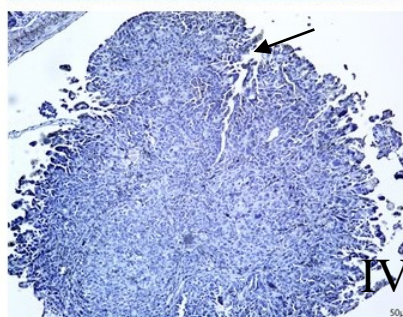
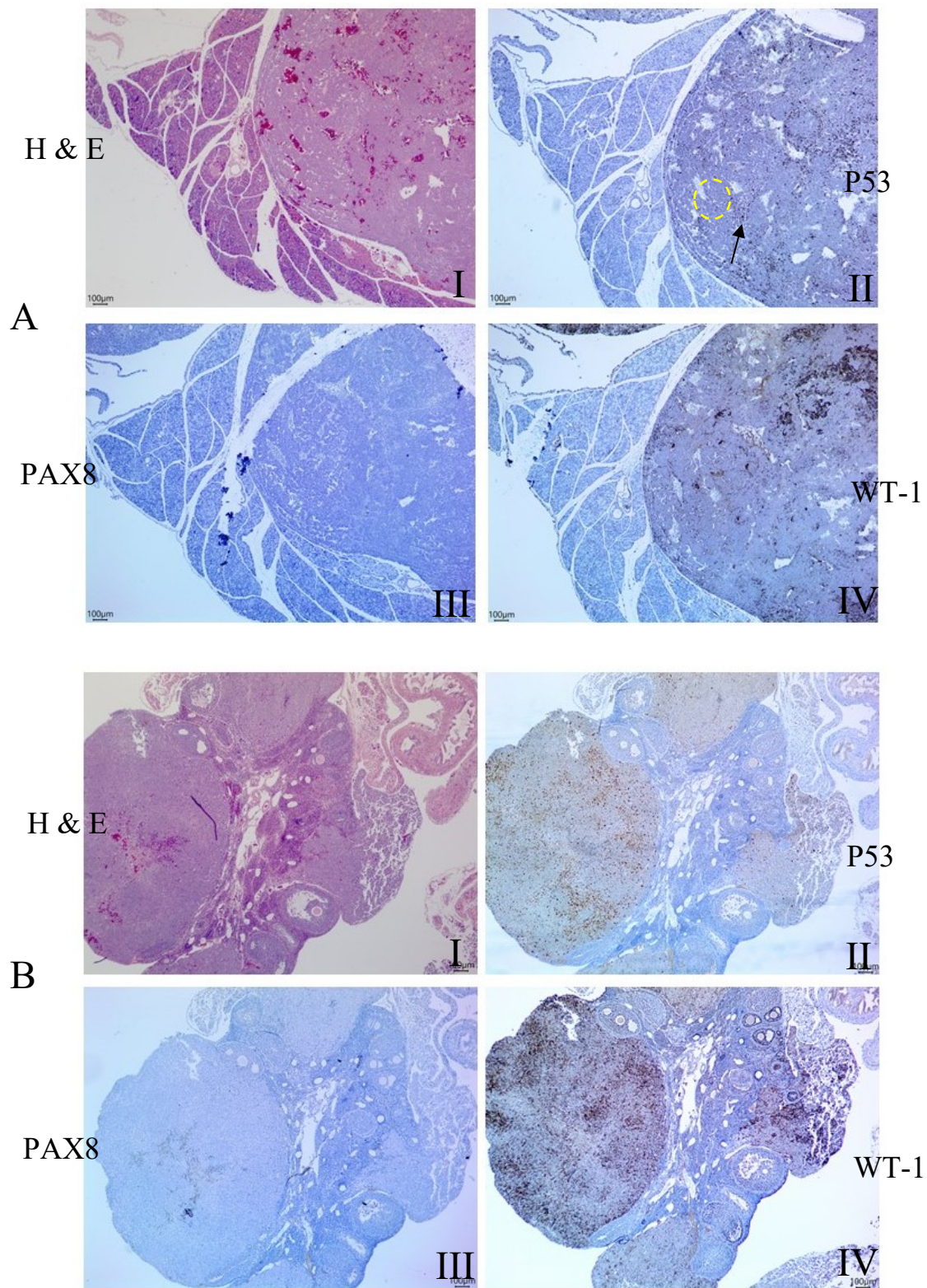
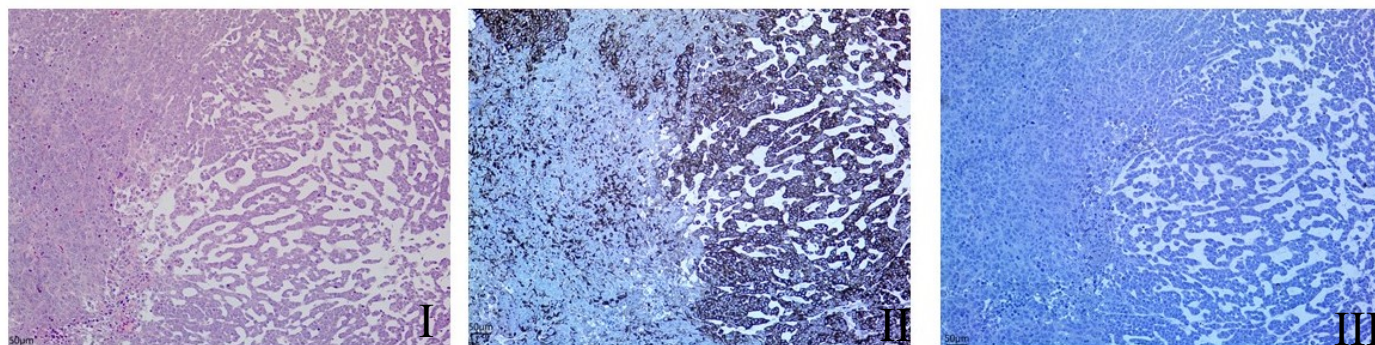


**Figure 20.** Immunohistochemistry evaluation of the tumor developed within animals injected with OVSAHO cells. All images were taken at a x10 magnification. **(A)** Part of the tumor shows invasiveness pushing into the liver. **(AI)** P53 showed dark nuclear stain. **(AII)** PAX8 showed dark nuclear stain. **(AIII)** WT-1 expressed dark nuclear stain. **(AIV)** Pockets of cells expressed CA125 in the open spaces within the tumor tissue (arrow). **(B)** Part of the tumor. **(BI)** P53 showed dark nuclear stain. **(BII)** PAX8 showed dark nuclear stain. **(BIII)** WT-1 showed dark nuclear stain. **(BIV)** Cells expressed CA125 in the open spaces within the tumor tissue (arrow).



C



H & E

WT-1

CA125

**Figure 21.** Immunohistochemical evaluation of the tumor developed within animals upon i.p. injection of A2780 cells. (A) and (B) show images taken at x4 magnification, (C) Images at x10 magnification. (A) Part of the tumor pushes the pancreatic parenchymal tissue as shown in H&E-stained sections (AI). (AII) P53 showed varied expression (likely representing wild-type expression); some cells expressed the protein (arrow) while others are completely negative (dashed yellow line). (AIII) PAX8 did not show any expression. (AIV) WT-1 showed diffuse expression not limited to the nucleus (membranous and cytoplasmic). (BI) Ovarian tumor growth that replaces the ovarian tissue. (BII) P53 showed varied expression in which there are some cells expressing the protein (BIII) PAX8 did not show any expression. (BIV) WT-1 showed diffuse expression not limited to the nucleus (membranous and cytoplasmic). (CI) Closer view for the tumor in H&E. (CII) diffuse expression of WT-1, mostly membranous. (CIII) CA125 is negative in the developed tumor.

#### ***4.3.4 Higher cell loads of PEO14 showed more aggressive behavior without significant change in tumor latency***

As animals injected with  $2 \times 10^6$  PEO14 cells did not show any organ invasion within the abdominal cavity after eleven months, we repeated the experiment with  $40 \times 10^6$  cells. Surprisingly, 20 fold increase in cellular load did not significantly change the average tumor latency. The tumor formed and the animals reached the criteria for euthanasia after six months of injection. The main presenting criteria for euthanasia were distended abdomen with small volume ascites abundantly populated by MSC. Interestingly, PEO14 cells kept forming different sizes of well-defined masses, but showed more adherence to the organs than the tumor formed from the low load cells (**Fig. 22**). Microscopically, the tumor showed high invasive capacity mimicking that of OVCAR-4 when injected in low load. Most of the abdominal organs, including liver, pancreas, gastric wall and some lymph nodes, are infiltrated by the tumor (**Fig. 23**). In immunohistochemical studies, the tumors accumulated likely-mutant P53 and expressed nuclear PAX8. CA-125 was expressed in the open spaces between the tumor cells (**Fig. 24**). Unlike the low load tumor, high load tumor showed pockets of cells having nuclear stain for WT-1 (**Fig. 25**).

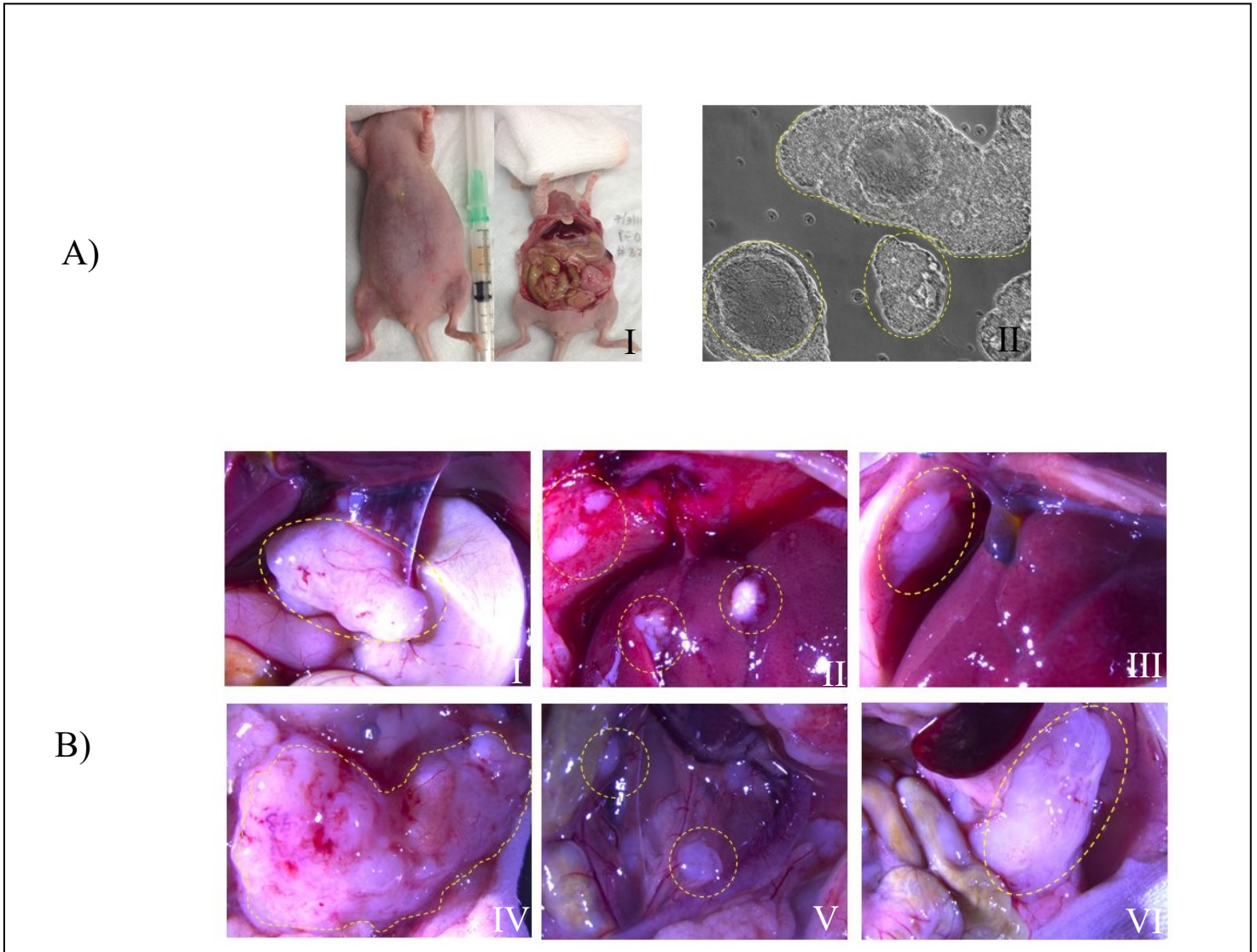


**Figure 22.** Disease presentation and macroscopic appearance within the peritoneal cavity: **(A)** typical features caused by high load injection of PEO14 cells. **(AI)** Distended abdomen; milky ascites was drained. **(AII)** Abundant MCS. **(B)** Gross disease within the abdominal cavity. **(BI)** and **(BII)** show the liver with white masses within the organ and at its base. **(BII)** The masses are grossly invading the liver parenchyma. **(BIII)** Diaphragm showing white lesions adherent to the diaphragm. **(BIV)** Omental area displaying large irregular white hemorrhagic masses **(BV)** and **(BVI)** show the mesentery displaying white masses attached to the mesenteric fat around the intestine. **(BVI)** Large irregular shaped white mass around the area of the large intestine.

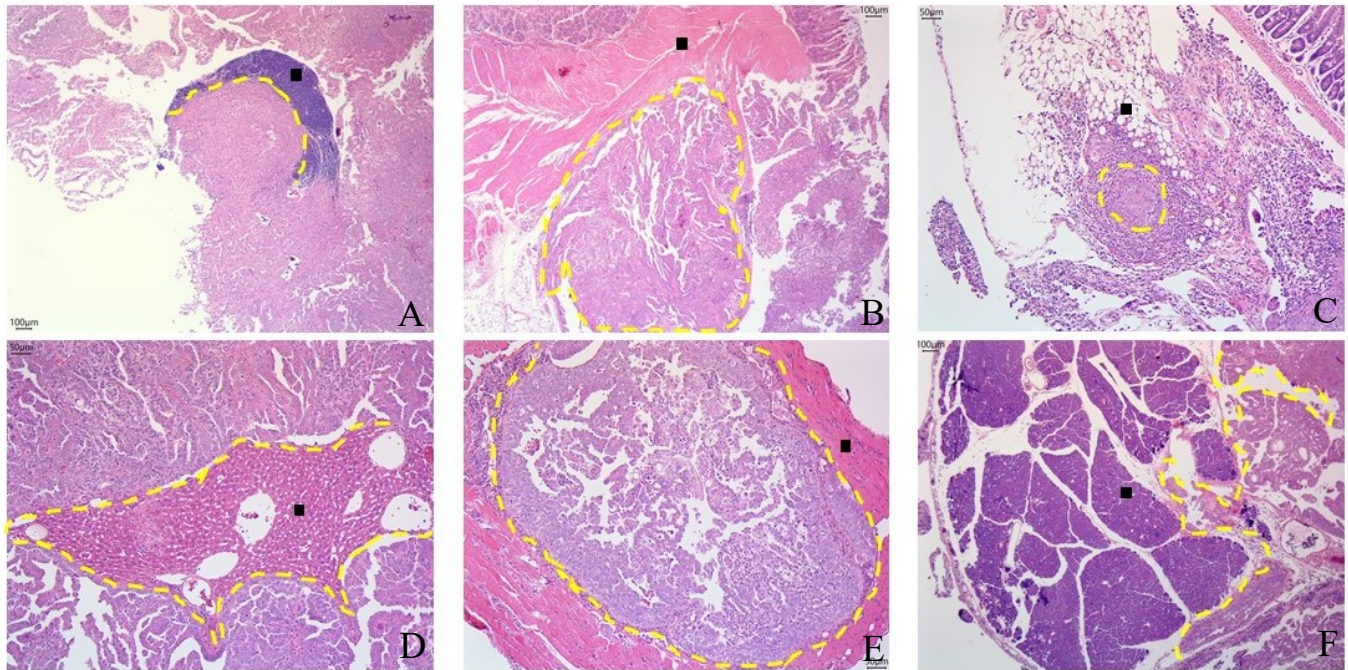
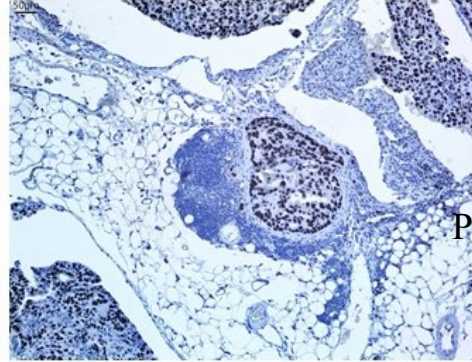
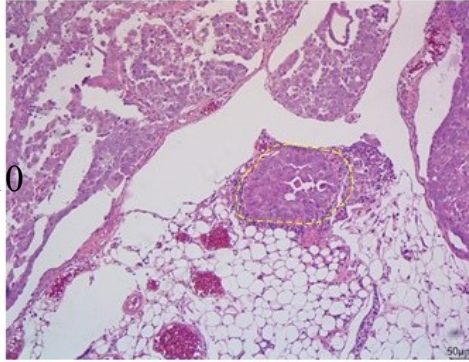


**Figure 23.** Animals injected with high load PEO14 cells showed high invasiveness to different organs within the peritoneal cavity. **(A)** Lymph nodes (square) are heavily infiltrated by the tumor growth (yellow dashed line). **(B)** Gastric wall muscle (square) is invaded by large growth of tumor (yellow dashed line). **(C)** Tumor growth (yellow dashed line) is invading the fatty tissue around the intestine (square). The tumor is surrounded by an inflammatory reaction composed mainly of lymphocytes. **(D)** The liver parenchyma (square) was almost entirely replaced by the tumor. **(E)** The skeletal muscle of the abdominal wall (square) was infiltrated by the tumor (yellow dashed line). **(F)** The pancreatic parenchyma (square) was infiltrated by the tumor (yellow dashed line).

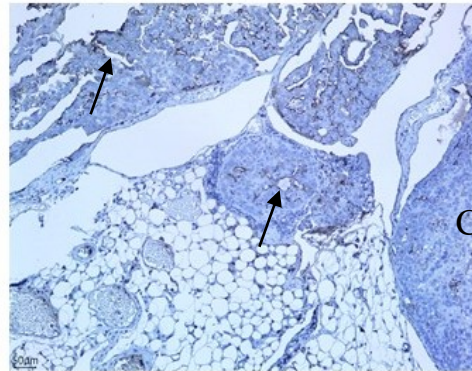
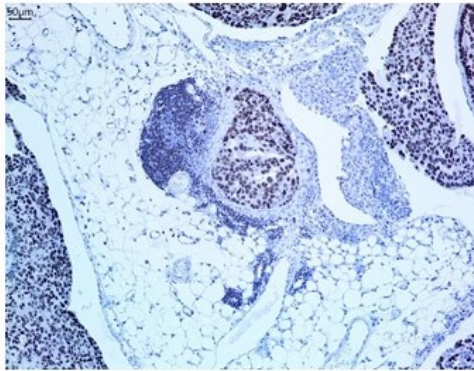
A

H & E x10



P53

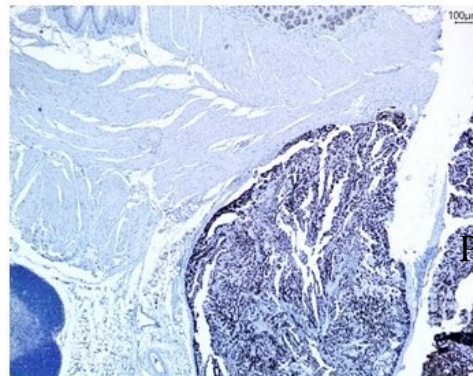
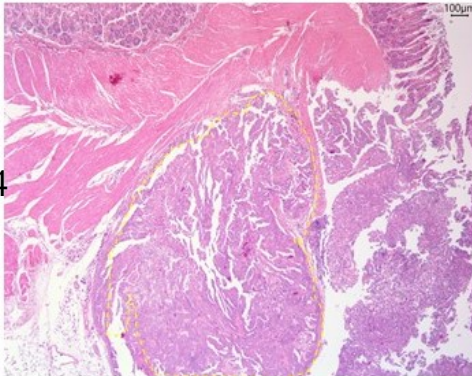
PAX8



CA125

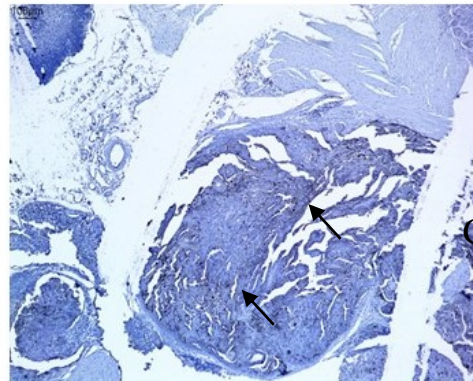
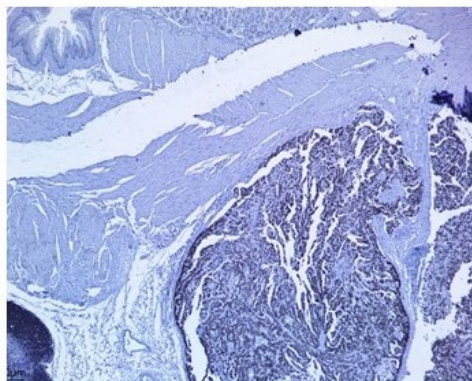
B

H & E x4



P53

PAX8



CA125

**Figure 24.** Immunohistochemical evaluation of the tumor developed within animals receiving high load PEO14 cells. **(A)** Mesenteric fat infiltrated by the tumor as observed by H&E (dashed yellow line). Dark nuclear stains are seen in case of **P53** and **PAX8**; whereas membranous expression in the open spaces between the tumor cells is observed for **CA125**. **(B)** Gastric wall invasion as observed via H&E staining (dashed yellow line). Dark nuclear stains for **P53** and **PAX8**. Membranous expression in the open spaces between the tumor cells in the case of **CA125** (arrows).

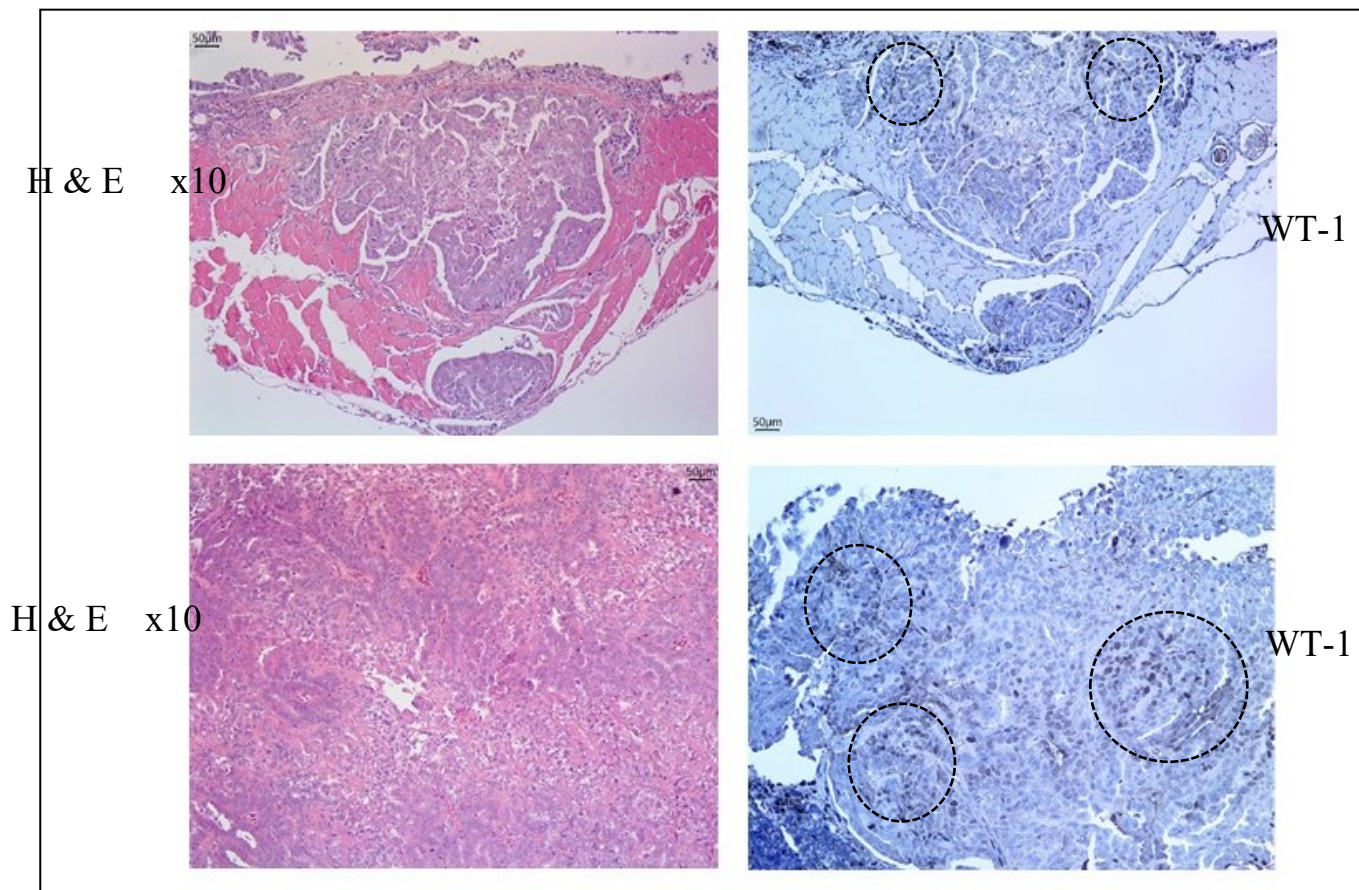
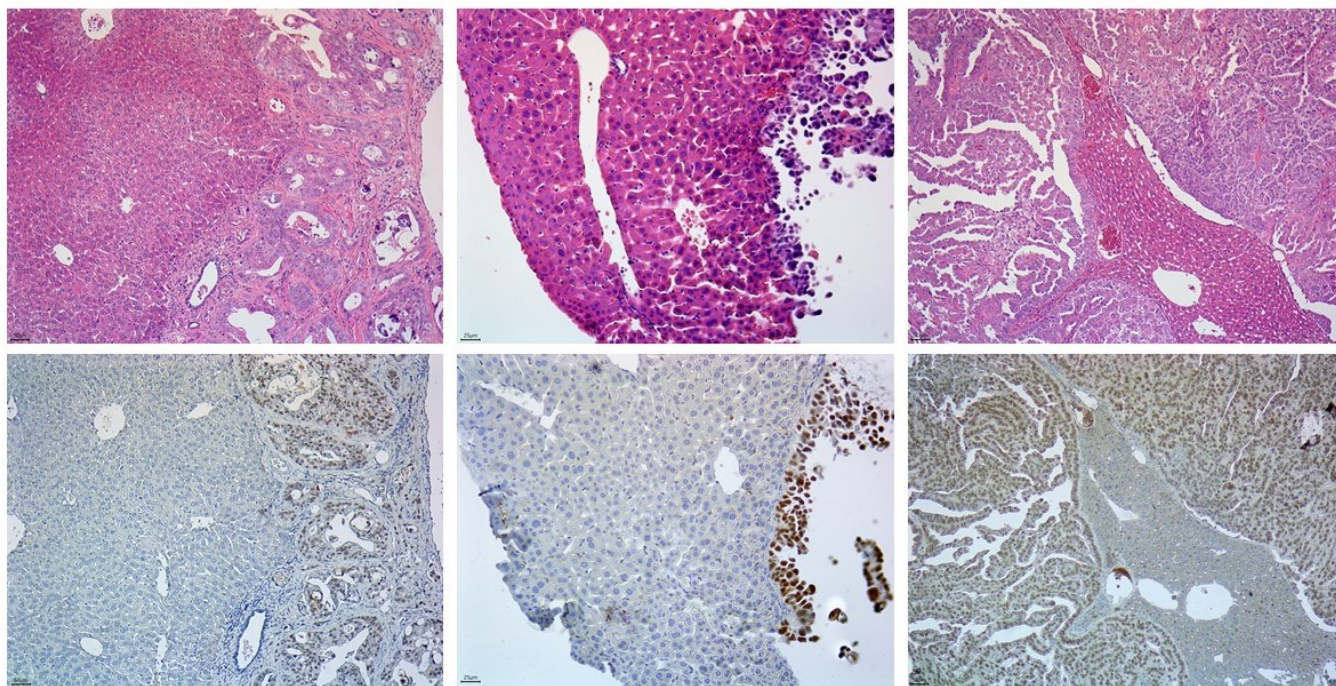
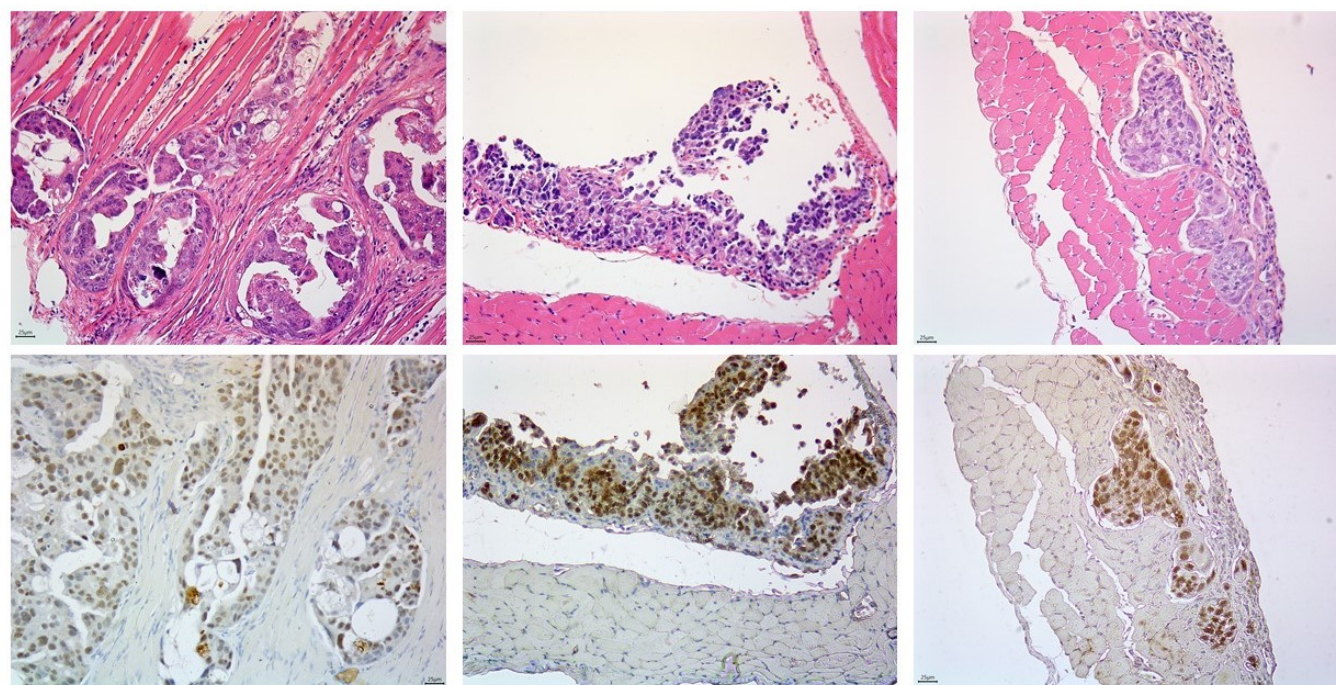


**Figure 25.** Unlike the low load of PEO14, higher load showed pockets of nuclear WT-1 expression within the tumor and the tumor invasions (dashed black line).

A



B



C

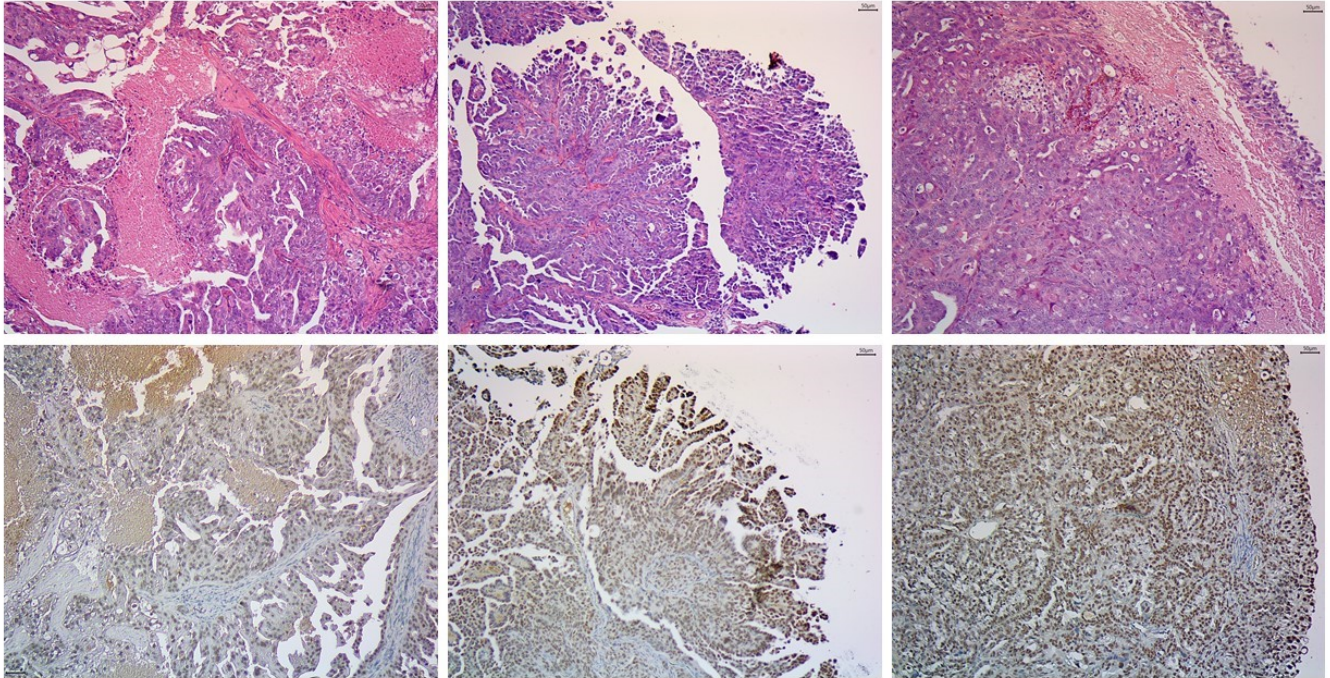


**Figure 26.** To prove that the tumor growth and infiltrates within the mouse organs are of human origin, we tested the tumors for the expression of a human nuclear antigen in the (A) liver, (B) diaphragm, and (C) a tumor mass. The tumor cells showed positive nuclear staining indicating that they are from human origin while the tissues formed around the tumor do not show any reactivity indicating the mouse nature of such cells.

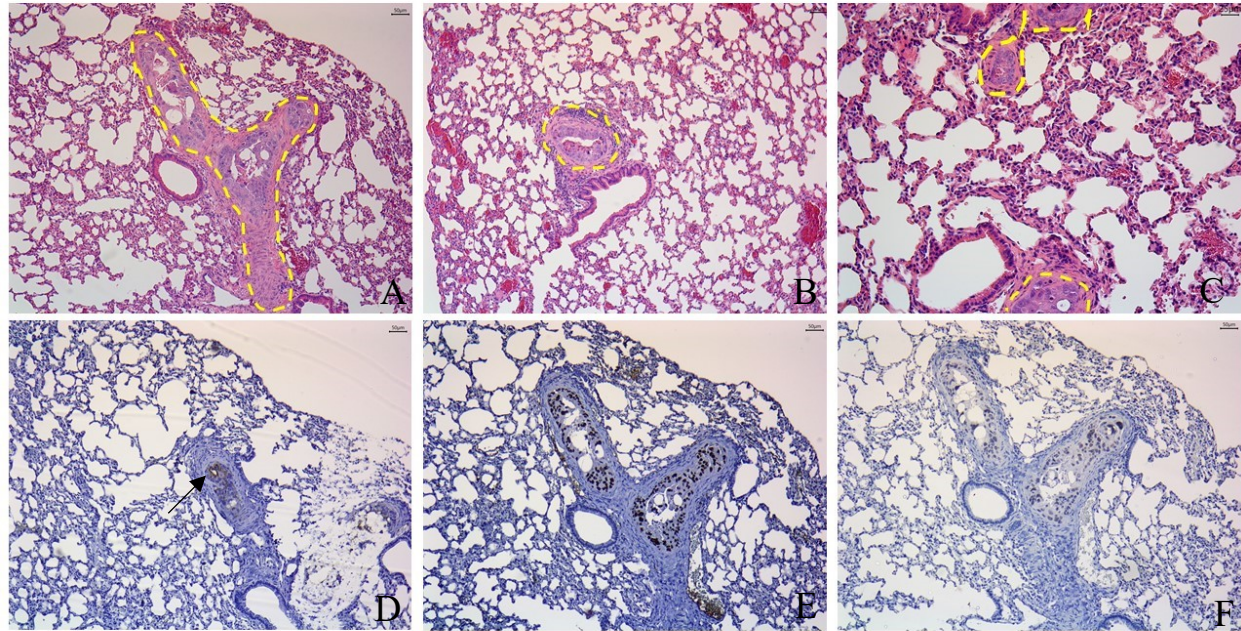
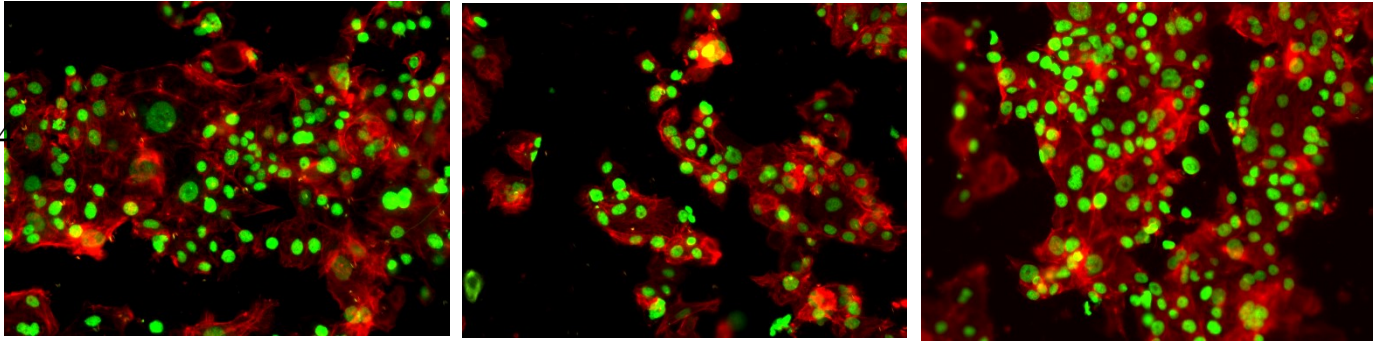


**Figure 27.** Unique metastatic site in the lung.  $2 \times 10^6$  OVCAR-4 cells injected i.p. uniquely showed microscopic disease within the lung. The upper panel, with H&E staining, shows three different lung sections collected from different animals. Notice the foci of malignant cells invading the lung parenchyma (yellow dashes). **(A)** The malignant invasiveness shows desmoplastic reaction around the tumor. This feature is not depicted in other lungs **(B and C)**. Lower panel shows the expression of CA125, P53 and PAX8 in the malignant growth. **(D)** CA125 is a membranous marker that is focally expressed in some cells (arrow). **(E)** P53 is homogenously and strongly expressed. **(F)** PAX8 is homogenously expressed in the malignant growth.

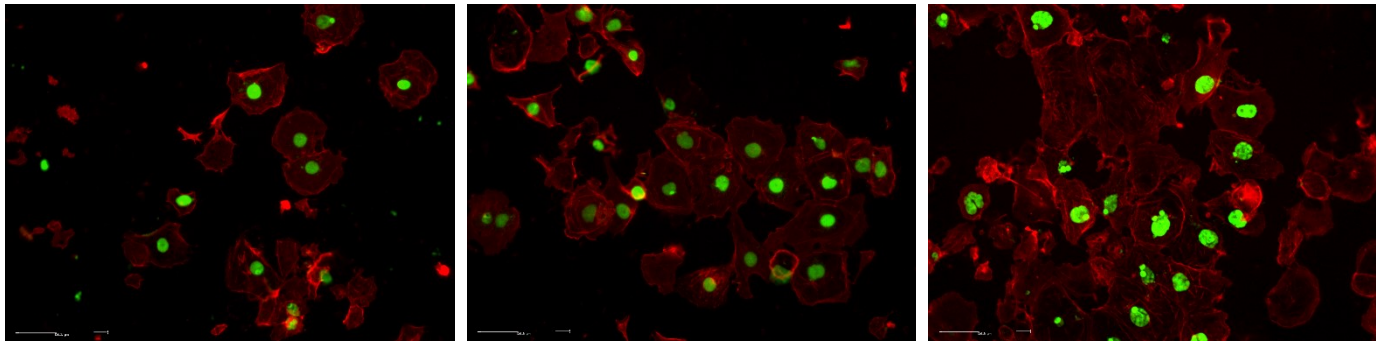
#### 4.4 In vitro functional characterizations of the OC cell lines

The ability of the five OC cell lines used in this study to migrate and invade was investigated using Boyden chambers with transwell membranes to enable the cells to migrate toward a chemoattractant with (invasion) or without (migration) adding extracellular matrix gel. Among the three cell lines that represent HGSOV, in invasion and migration assays, OVCAR-4 had the maximum number of cells and the OVSAHO had the least number of cells moving to the other side of the barrier membrane. There were significant differences of the mean values between the cell lines ( $P < 0.0001$ ) (**Fig. 28**) and (**Fig. 30**). When compared to the other two cell lines that least represent HGSOV (i.e. A2780 and SKOV-3), OVCAR-4 still showed more moving cells in migration and invasion assays among all the cell lines tested. SKOV-3 cells did not show a statistically significant difference in migration capacity when compared to PEO14 cells, but they were significantly more migratory than A2780 and OVSAHO cells (**Fig. 29**). In invasion assays, A2780 cells did not show a statistically significant difference from SKOV-3 and OVSAHO cells, but it was significantly less invasive than OVCAR-4 and PEO14 cells (**Fig.31**).

OVCAR-4



PEO14



OVSAHO

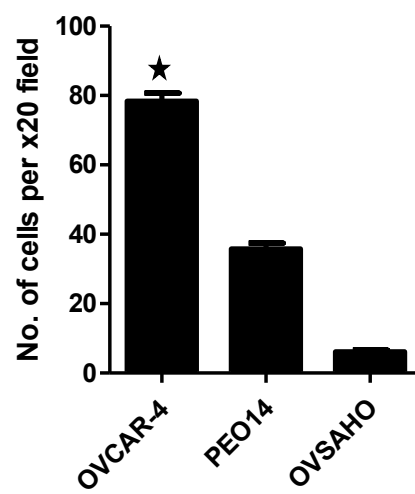
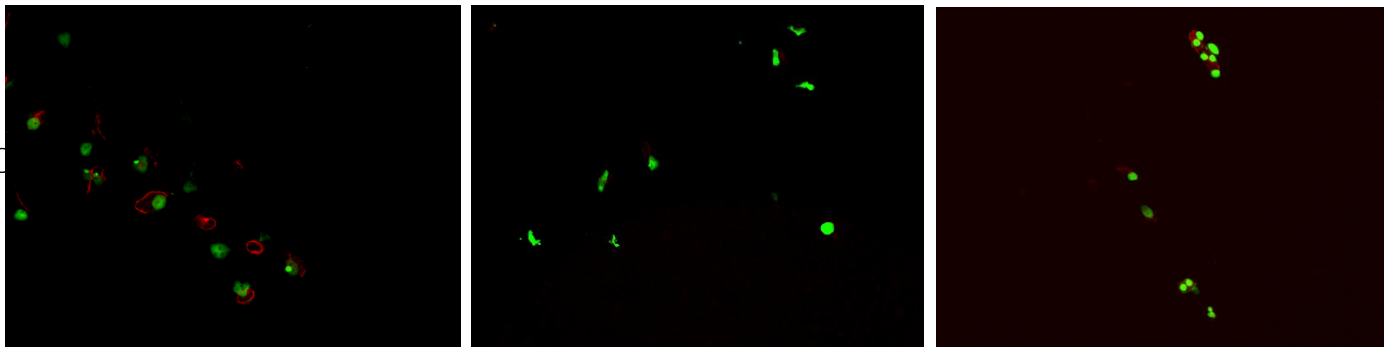
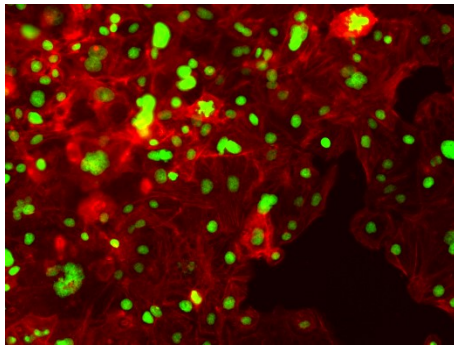


**Figure (28.** Comparison of migratory capacity among three cell lines that represent HGSOC.

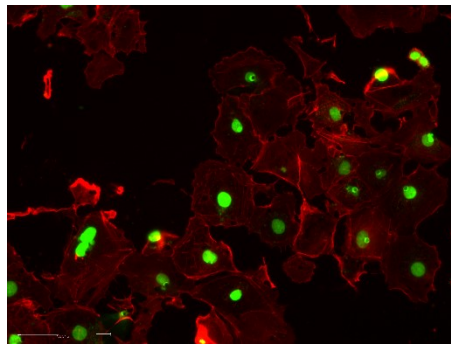
Images are representative of the migration assays after double staining of the migratory cells with Alexa Fluor 594 Phalloidin and Sytox Green. All pictures were taken at x20 magnification.

Qualitatively, OVCAR-4 cells showed many more migratory cells compared to PEO14, whereas the least migratory were OVSAHO. Quantitatively, OVCAR-4 was significantly higher than PEO14 and OVSAHO in terms of migratory capacity. There were significant differences between the means across the cell lines ( $P < 0.0001$ ).

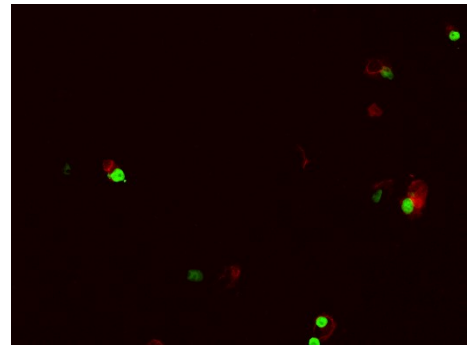
OVCAR-4



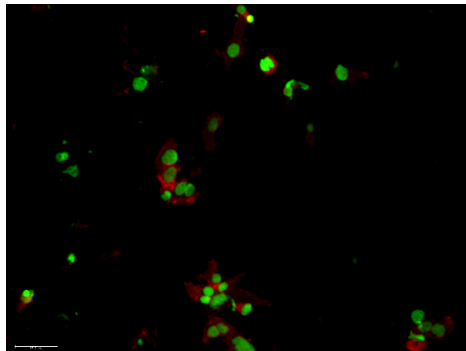
PEO14



OVSAHO



SKOV-3



A2780

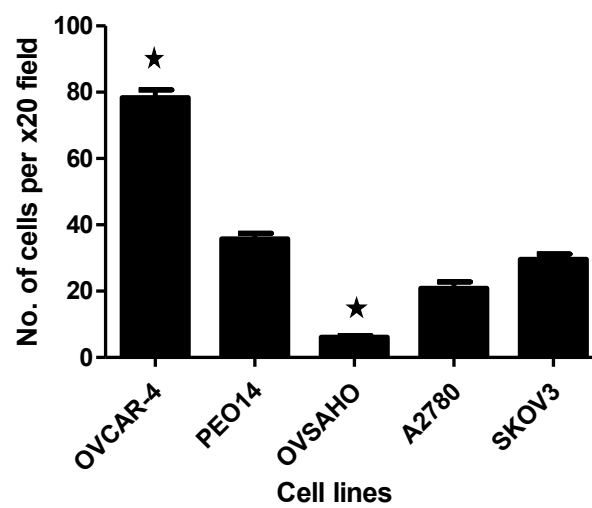
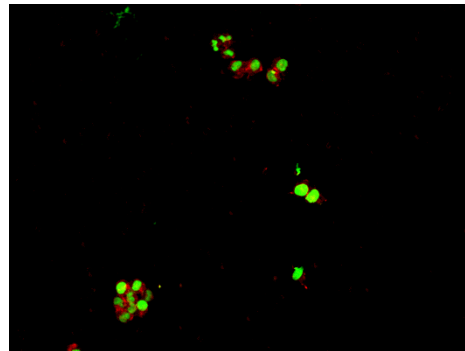
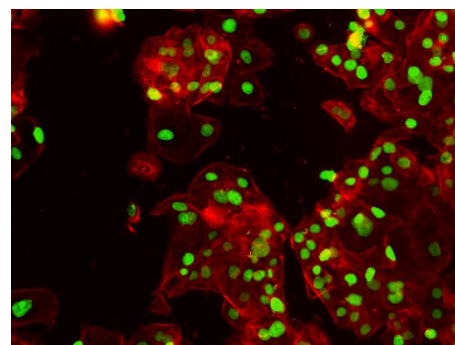
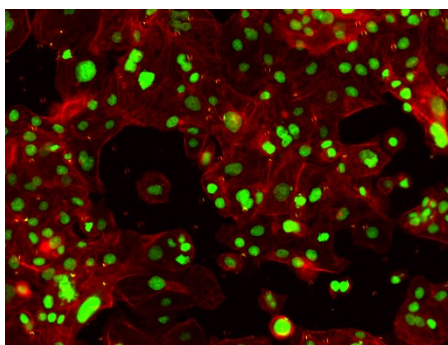
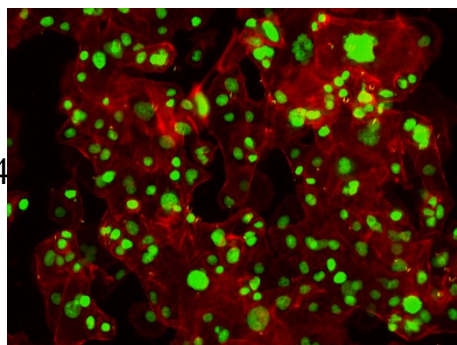
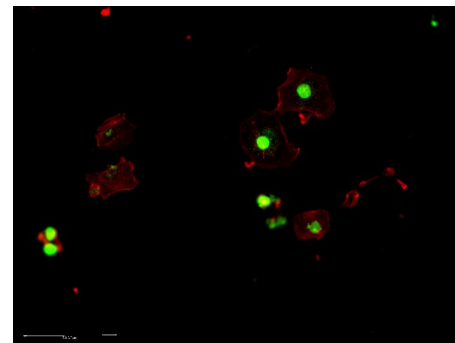
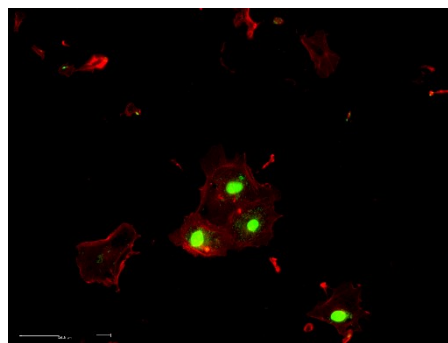
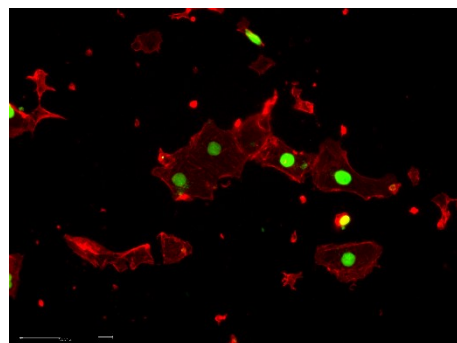


**Figure 29.** Comparison of the migratory capacity between the five OC cell lines. Representative images of the migration assays after double staining with Alexa Fluor 594 Phalloidin and Sytox Green are shown. All pictures were taken with x20 magnification. Qualitatively OVCAR-4 showed many migratory cells compared to the others cell lines. Quantitatively, OVCAR-4 was the most migratory and OVSAHO was significantly the least migratory. There were significant differences between the means across the cell lines ( $P < 0.0001$ ).

OVCAR-4



PEO14



OVSAHO

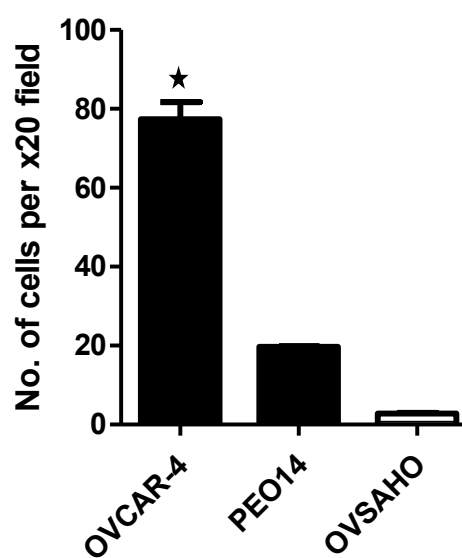
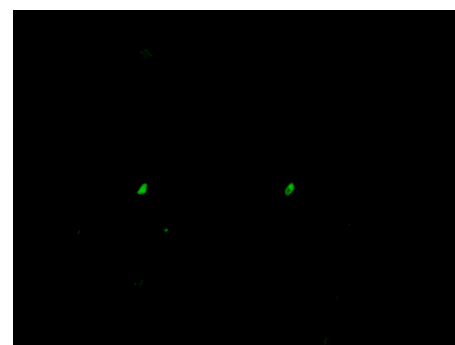
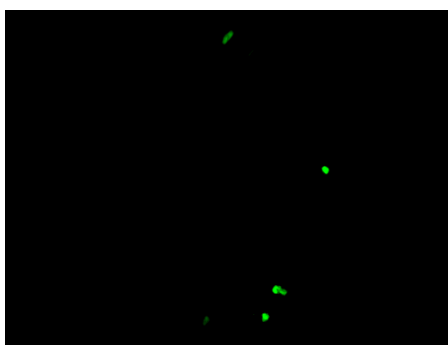
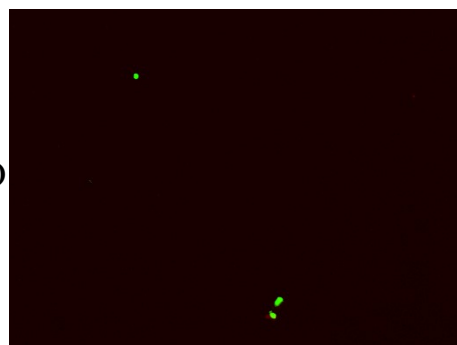


**Figure 30.** Comparison of the invasion capacity among the three cell lines that represent HGSOC.

Representative images of the invasion assays after double staining with Alexa Fluor 594

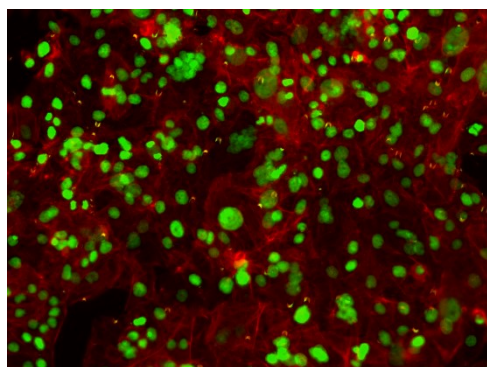
Phalloidin and Sytox Green are shown. All pictures were taken at x20 magnification.

Qualitatively, OVCAR-4 showed many more invading cells when compared to PEO14 and

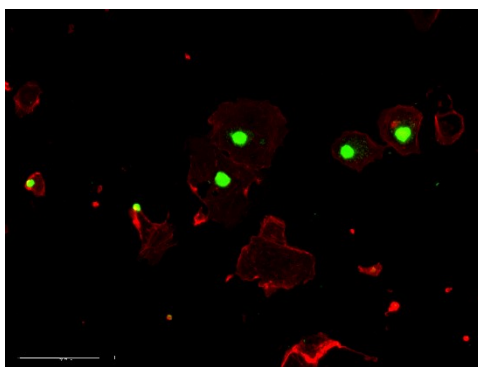
OVSAHO. Quantitatively, OVCAR-4 invasion was significantly higher than PEO14 and

OVSAHO. OVSAHO significantly showed the lowest potential for invasion. ( $P < 0.0001$ ).

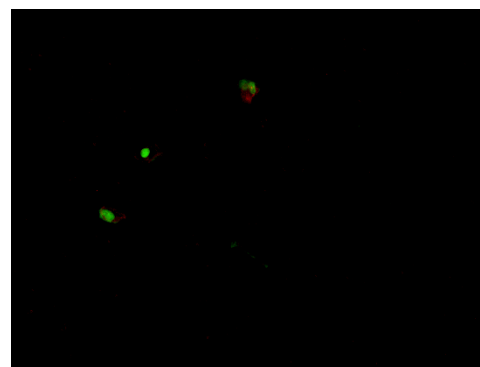
OVCAR-4



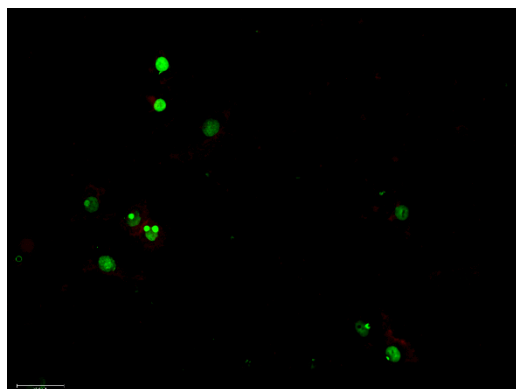
PEO14



OVSAHO



SKOV-3



A2780

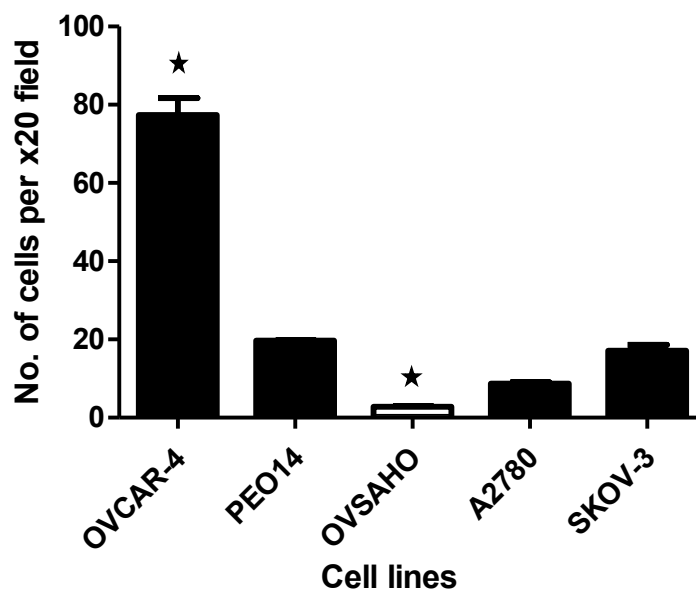
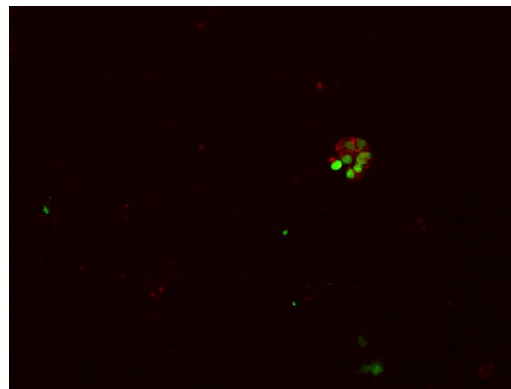


**Figure 31.** Comparison between the five OC cell lines in terms of their invasive capacities

Representative images of the invasion assays after double staining with Alexa Fluor 594 Phalloidin and Sytox Green are shown. All pictures were taken at x20 magnification. Qualitatively, OVCAR-4 showed many more invasive cells compared to the other cell lines. Quantitatively, the invasiveness of OVCAR-4 was significantly the highest, whereas OVSAHO cells showed the least invasiveness. There were significant differences between the means across the cell lines ( $P < 0.0001$ ).

## ***5. Discussion***

High grade serous ovarian carcinomas remain the most lethal gynecological malignancy. Most of the cases (up to 80%) present with late-stage disease when the tumor is already beyond the confines of the pelvic cavity (i.e. within the peritoneal cavity) (60). Despite many years of working in the field of ovarian cancer research, the outcomes of these investigations have not changed substantially the prognosis of the disease. One of the major problems, specifically in the field of high-grade serous ovarian carcinoma, is the absence of well-characterized and comprehensive models that resemble the disease in its late-stage when it has already reached the abdominal cavity. Comprehensive characterization of a model involves a meticulous choice of the cells that closely represent the disease as it develops in patients; it also must rely on the type of mouse to be used, and in the protocol to follow from the cellular injection into the animals until the point the mice require to be euthanized. A model that represents the heterogeneity of the disease will play an important role in preclinical drug studies in addition to its role in understanding the disease biology.

One of the major challenges that researchers face is the selection of the cell lines. Cell lines can be immortal or patient-derived, either primary or from patient-derived xenografts (PDXs) generated in mice. As they have infinitive ability to proliferate, immortal cell lines have been used for years as a fundamental tool in the area of scientific research. These types of cells allow equal accessibility for researchers and have large available genomic data (72). However, the major limitation is the cross contamination or misidentification (73) and the changes in phenotypes and genotypes over serial passages (74). Primary cell lines are cells isolated from solid tumors in the laboratory under a microenvironment similar to the physiological environment (75). Due to the variations of clinical responses to drugs, personalized medicine

using primary cell lines could help to create agents directly targeted at unique molecular features of a cell line, and here is where the primary cell lines allow comparisons between different clinical-based drug responses (76, 77). PDXs are tumor fragments from patients directly injected in vivo into a mouse. The PDX model maintains the histological structures of the tumor including the stromal components (78). One of the major advantages of this model is that the responses to drugs -chemotherapy- seems correlated with what is observed clinically in patients from which the PDX is derived(79). However, there are several limitations when using PDXs. The main concern is the use of severely immunocompromised mice, which limits the contribution of immune cells and the failure of PDXs to metastasize away from the injection site (80). We used the least immunocompromised animal model available, the nude mouse. In our model, and to overcome the challenges of using immortal cell lines, all the cell lines we used were authenticated in May 2017 using autosomal short tandem repeat [STR] profiling markers showing a  $\geq 80\%$  match between the cells used in this study and the original cell lines with profiles suitable for verification in reference databases.

While some reports characterized particular cell lines having high-fidelity to the HGSOC genetic background (70, 81), these characterizations were conducted from in vitro studies, which, sometimes, do not reflect the actual behavior of the disease (82). No matter how many in vitro studies can be done to characterize any given cell line, it is only the use of in vivo studies that allows a study of the cell line's tumorigenicity. Mouse xenografts are well described in the literature, yet the most used cell lines do not truly carry the genetic background representing HGSOC (2). For instance, SKOV3 and A2780 are two of the most studied lines in mouse xenografts, yet their genetic background is unlikely to represent HGSOC (2). While some may prefer to develop models using patient-derived cells or primary cell models, cell lines have some

advantages over primary cells. Table 9 highlights the advantages and limitations for both types of materials (2, 83, 84).

Table 9. Advantages and limitations for patient-derived cells and cell lines

|                    | <b>Patient-derived cells</b>   | <b>Cell lines</b>   |
|--------------------|--|---|
| <i>Advantages</i>  | <ul style="list-style-type: none"> <li>- Directly derived- minimum genomic changes</li> <li>- Allow for personalized cancer therapy</li> <li>- Provide almost complete reflection of the disease</li> </ul>  | <ul style="list-style-type: none"> <li>- Accessible for researchers</li> <li>- Consistent results</li> <li>- Rich resources for characterization</li> <li>- Easy to culture</li> <li>- Easy to obtain study approval</li> </ul> |
| <i>Limitations</i> | <ul style="list-style-type: none"> <li>- Difficult accessibility for researches <ul style="list-style-type: none"> <li>– results are usually not generalized</li> </ul> </li> <li>- Not-well genomically characterized in the literature</li> <li>- Difficult to culture; slowly proliferate and have limited life-span</li> <li>- Difficult to obtain study approval</li> <li>- More expensive</li> </ul> | <ul style="list-style-type: none"> <li>- Process of immortalization may cause cellular change genetically and morphologically</li> <li>- Cannot be used for personalized medicine</li> </ul>                                    |

Despite the information that we gained from the in vitro assays, in vivo studies using animal models that can recapitulate the human disease remain a worthy tool to study the tumor biology, to closely follow up the tumor metastasis and to further study the genetic and molecular alterations and test different therapeutic options (85, 86). Literature shows more than one type of mouse model has been used to study ovarian cancer. Every model came with several advantages and limitations that make them suitable for some studies and not for others. The main two types of mouse models are xenografts and genetically engineered mouse models (Table 10). A xenograft involves the transfer of human or murine cancer cells into the mouse and it aims to follow the disease growth, progression and follow up with diagnostic tools; it was established in the 1980s (87). Genetically engineered mouse models involve genetic manipulations of mouse genes to study the starting point of the disease that cannot be determined in the xenograft model. Since the genetic mutations causing ovarian cancer are very complex and the disease is very heterogeneous, xenografts models are the most commonly reported in the literature with different choices of cell types or mouse types (88, 89). Cells – which can be either patient derived or immortal as mentioned before- can be injected subcutaneously (s.c.), intraperitoneally (i.p.) or intrabursally (i.b.); each method has its pros and cons. For example, s.c. xenografts can be used for imaging testing studies but neither allow assessment of metastasis nor face a “true” tumor microenvironment (88). On the other hand, i.p. models are effective in studying tumor growth, proliferation and eventually treatment response. For our purpose, we used xenograft i.p. models to follow up the disease growth and progression over a period of time; we were able to observe the clinical signs of the disease that could be seen in patients carrying late stage HGSOC. For instance, reports in human patients showed that advanced stage HGSOC is significantly associated with accumulation of ascites, abdominal distention, omental cake

formation and distant metastasis (9, 90). These features are seen in our animal model using different cell lines; all of them developed distant metastasis, OVCAR-4 caused massive ascites, PEO14 developed variable size abdominal masses, and OVSAHO created an omental cake (see Figures 11 and 12 in the result section).

Table 10. comparison between xenograft model and genetically engineered model

|                      | <i>Xenograft mouse model</i>  | <i>Genetically engineered model</i>   |
|----------------------|---|---|
| <i>Advantages</i>    | <ul style="list-style-type: none"> <li>- Allows effective follow up for the tumor growth and metastasis</li> <li>- Allows testing the therapeutic response to specific drugs</li> </ul> | <ul style="list-style-type: none"> <li>- Allows study of the initial transformational step of the disease</li> <li>- Allows study of the genetic mutations responsible for the disease</li> </ul> |
| <i>Disadvantages</i> | <ul style="list-style-type: none"> <li>- Does not capture the initial steps in the development of the disease (precursor lesions)</li> </ul>  | <ul style="list-style-type: none"> <li>- Difficult to generate, especially in OC, where the genetic mutations are complex</li> </ul>  |

When modeling any kind of cancer, special attention should be drawn to the type of cells used -as mentioned before- and the mouse type employed for this purpose. Different mouse subtypes may serve as good candidates for one experiment and not for another. Immunodeficient mice have been used for years as a model for human diseases and helped create new therapeutic options and set new preventive measures (69). Different strains of immunodeficient mice are used for different purposes based on the type of study, the follow up measurements, and the outcomes to be expected. For instance, nude mice have Foxn1 gene

mutation which leads to block of the thymic-derived T cells; these mice have immunity limited to B-cells, complement activity and natural killer (NK) cells (91) (92). These features make the nude mice good candidates for xenograft models in the area of biomedical research. On the other hand, SCID mice lack both T and B lymphocytes due to different mutations. These mice are widely used and are particularly good candidates for modeling organ transplant, however, variation of the immune responses within the mice may be considered one limitation (93) in addition to the higher cost. Table 11 lists some advantages and limitations for two types of immunodeficient mice: nude and SCID. For our project, and because orthometastatic HGSOC models are poorly described in the literature, we used nude mice, the ones with the least disturbance in their immune system, having intact B-cells, complement and NK cell functions that closely mimic the physiological environment around the tumor. Our model is also cost-effective when compared to SCID mice, and has a long history as a model for therapeutic testing (94) .

Table 11. Main advantages and limitations for two types of immunodeficient mice

|                   | <b>Nude mice</b>   | <b>SCID mice</b>   |
|-------------------|--|--|
| <i>Advantages</i> | <ul style="list-style-type: none"> <li>- Closely mimics the physiological environment: presence of B-cells, NK cells and intact complement functions.</li> <li>- Cheapest among the immunodeficient mice.</li> <li>- Used for human xenografts.</li> </ul> | <ul style="list-style-type: none"> <li>- Serves as good model for organ transplantation and fetal hematopoietic tissue transplantation.</li> </ul> |

|                    |  |   |
|--------------------|--|---|
| <i>Limitations</i> | <ul style="list-style-type: none"> <li>- High NK cell activity can limit the percentage of successful tumor growth.</li> <li>- Lack functional T cells.</li> </ul> | <ul style="list-style-type: none"> <li>- Expensive.</li> <li>- Does not reflect the physiological environment.</li> </ul> |
|--------------------|--|---|

The ability of the highly ranked HGSOC cell lines, from a genetic standpoint (2), to form tumors in nude mice, is poorly described in the literature. Our project is the first to extensively evaluate the tumorigenicity of HGSOC cell lines that have genetic fidelity to the disease in adequate time allowing to accurately compare tumor latency, tumor formation, and tumor characteristics among the cell lines tested. Among the three cell lines chosen as a model of the disease, OVCAR-4, OVSAHO, and PEO14 cells, the tumor latency was at least four and half months compared to less than the three months reported for SKOV-3 and A2780 when injected into the abdominal cavity of nude mice. Even with increased load of cells – in the case of PEO14 – to 20 times, it took 6 months for the animals to reach one of the end-of-wellness endpoint criteria. This result questions the conclusions from other publications that report a lack of tumorigenicity in some HGSOC cell lines in experiments conducted for a maximum of 3 months (95, 96).

Our results showed variable clinical presentations among the cell lines tested, which are characteristic features of HGSOC as it presents in patients. Although most of the advanced cases reported have peritoneal disease presented with abdominal symptoms, there are some cases reported that presented predominantly with lymphadenopathy. Metastasis of the disease can even reach to the supradiaphragmatic lymph nodes without having supradiaphragmatic parenchymal organ metastasis (97). In our model, OVCAR-4 and high load PEO14 were able to invade and replaced many lymph nodes within different sites of the animal. However, it was difficult to

assess which comes first: the lymph node invasion or the organ invasion; this is probably because we were waiting for the animals to reach one of the end-of-wellness endpoint criteria without analyzing them longitudinally. Consistent with the histopathological features of the disease and a pathologist's opinion, the tumors developed formed structures with papillary configuration lined by highly atypical cells showing high nuclear/cytoplasmic ratio, atypical nuclei that have prominent nucleoli and display massive mitotic activity. All these features highly suggest the diagnosis of HGSOC. Although all the tumors developed from the cell lines homed to the omentum-spleen-pancreatic area, there were variations in their ability to migrate and invade different organs within the abdominal cavity emphasizing the heterogeneity of HGSOC. Thus, the in vivo variations in tumor phenotypes observed in our three model systems- the aggressive capacity for migration and invasion seen in OVCAR-4, compared to the ability of PEO14 to form masses of different sizes, versus the discrete disease developed by OVSAHO cells, could represent the heterogeneity of HGSOC. For instance, OVCAR-4 showed the highest level of aggressiveness among the three lines studied; two million cells loaded into the abdominal cavity caused invasion to almost all the abdominal organs and, interestingly at the microscopic level, it reached and invaded the lung parenchyma forming desmoplastic reactions around foci of the tumor. This cell line, we can argue, allows development of stage IV tumors as the cells reach the lungs. This would make this model suitable to test new drug responses in a very advanced stage of the disease. PEO14 cells, on the other hand, formed variable size tumor masses that pushed the organs but without visible invasion. OVSAHO cells developed into very slowly growing tumors and needed higher load to display the disease within a shorter time. However, the experiment was repeated using high load of OVSAHO cells – twenty and forty

times- and the animals still reached the end-of-wellness endpoint around five months after injection (data not shown).

Our results demonstrated significant variabilities among the five OC cell lines when identified using immunohistochemical markers. The consistent observation was that the three cell lines that represent HGSOc showed intense expression of mutant P53 and of PAX8. Interestingly, SKOV-3, characterized as a likely clear cell carcinoma (at least in vivo), showed complete absence of expression of P53 whereas A2780, likely representing an endometrial histotype, showed wild-type p53 expression. The other seven biomarkers used displayed various degrees of expression (see Table 6 in the result section). This provides additional evidence of the heterogeneity of the disease and could work as a starting point for eventually identifying more molecular targets.

All the three models tested and that highly represent HGSOc in our study, showed abundant nuclear expression for mutant P53 and PAX8 in agreement with previous reports (95, 96). The results are also consistent with the in vitro testing of these biomarkers using immunohistochemistry as mentioned before. The in vivo tumors were able to reproduce the nuclear expression of WT-1 in cases of OVCAR-4 and OVSAHO. OVCAR-4 derived-tumor showed heterogeneous expression of WT-1 in which small portions of the cells showed nuclear expression, while the rest were negative. Interestingly, the tumor developed from the low load cells of PEO14 (2 millions) did not show any nuclear expression of WT-1; however, a small population of cells started to show WT-1 nuclear expression when the tumor developed from the high load of cells (40 millions). This observation may highlight the presence of a proportion of cells with more tumorigenic capacity within a heterogeneous population of cancer cells present within the tumor before the chemotherapy (65).

The antigen CA-125 was predominantly expressed in the empty spaces –slit like spaces— within the tumor, and did not show any expression in the areas of glandular complexity. Thus, the results suggest that CA-125 could be a factor that is secreted by the tumor cells only in the areas where spaces open such as those of the slit-like areas.

Table 12. Comparison between in vivo and in vitro biomarker expression using immunohistochemistry

|                   | P53               |                   | PAX8              |                   | WT-1              |                   | CA 125       |                  |
|-------------------|-------------------|-------------------|-------------------|-------------------|-------------------|-------------------|--------------|------------------|
|                   | In vitro          | In vivo           | In vitro          | In vivo           | In vitro          | In vivo           | In vitro     | In vivo          |
| OVCAR-4           | Strongly positive | Strongly positive | Strongly positive | Strongly positive | ~50% is positive  | ~50% is positive  | + in pockets | + in slit spaces |
| OVSAHO            | Strongly positive | Strongly positive | Strongly positive | Strongly positive | Strongly positive | Strongly positive | + in pockets | + in slit spaces |
| PEO14 (low load)  | Strongly positive | Strongly positive | Strongly positive | Strongly positive | ~30% in pockets   | Negative          | + in pockets | + in slit spaces |
| PEO14 (high load) | Strongly positive | Strongly positive | Strongly positive | Strongly positive | ~30% in pockets   | ~20% in pockets   | + in pockets | + in slit spaces |

There are scant reports in the literature (82, 95, 96) testing the functional properties of some of the top HGSOc cell line candidates mentioned by *Domcke et al* (2). In our study, we compared, among five cell lines chosen, their capacity to migrate and invade in Boyden chamber assays. This method allows us to better compare among the cell lines themselves and between their behavior in culture and contrast the information with the data obtained in vivo. It is

interesting to note that the three cell lines, OVCAR-4, OVSAHO and PEO14, showed different behaviors in the functional studies (i.e. migration and invasion). We found that OVCAR-4 cells were the most aggressive in terms of migration and invasion in vitro and tumorigenic capacity in vivo. The other cell lines showed different ranges of migratory and invasion capacities from the lowest potent OVSAHO passing through the intermediate PEO14 to the highest OVCAR-4. We also noticed no significant difference when comparing the migration capacity of PEO14 versus that of SKOV-3 or when comparing the invasion capacities of A2780 and OVSAHO. Moreover, it was difficult to clearly correlate the behavior of the cells in vitro to their behavior in vivo. Therefore, we conclude that the functional studies conducted in vitro to characterize specific cell lines might not necessarily relate to their in vivo behavior in terms of tumorigenic capacity. Thus, it is of high importance to take these concepts into consideration when planning to correlate in vitro assays and in vivo studies.

The selection of the cell lines to represent the HGSOC is a vital step before attempting to model the disease. We provided a model using mice with the least disrupted immunity to develop a highly heterogeneous disease using several cell lines genetically resembling HGSOC. (OVCAR-4, PEO14 and OVSAHO). We compared such tumorigenicity vs. less likely cells to resemble HGSOC (i.e. SKOV3 and A2780). Despite having used three cell lines with high genetic fidelity of HGSOC, they still were heterogeneous in terms of disease progression when implanted intraperitoneally in nude mice and when tested in vitro using immunohistochemical markers and functional studies. Researchers and health care providers may work together and use this conclusion to further explore the biology and genomic properties of the disease. Moreover, diversities in the presentations and behaviors of the HGSOC cell lines that were seen in this

project may raise the possibility of introducing personalized medicine (or precision medicine) for HGSOC patients in the future.

## ***6. Conclusion and future directions***

Upon utilization of in vivo models of HGSOC, special attention should be given to the heterogeneity of the disease. The models highlight this heterogeneity and extensively describe the macroscopic and the microscopic facets of the pathology, which closely mimics what is usually seen in patients carrying advanced stage HGSOC. This work clarifies and adds to what has been published in this area while providing crucial data to help further develop preclinical therapeutic testing studies in order to document new molecular targets as well as preventive measures.

Further experiments using primary cell lines, i.e. patient derived, could be done to expand this work when studying new preventive or therapeutic approaches. Further genetic analysis for the cell lines and their corresponding tumor growth is also necessary to determine the discordance – if present – between them.

## ***References:***

1. Prat J, Oncology. FCoG. Staging classification for cancer of the ovary, fallopian tube, and peritoneum. *international Journal of Gynecology and Obstetric* 2014;124(1):1-5.
2. Domcke S, Sinha R, Levine DA, Sander C, Schultz N. Evaluating cell lines as tumour models by comparison of genomic profiles. *Nature Communications*. 2013;4(2126).
3. Vaughan S, Coward JI, Jr RCB, Berchuck A, Berek JS, Brenton JD, et al. Rethinking ovarian cancer: recommendations for improving outcomes. *Nature Review;Oncology*. 2011;11:719-25.
4. Young B, Lowe JS, Stevens A, Heath JW. *Functional Histology* Philadelphia: Elsevier; 2006. 437 p.
5. Auersperg N, Wong AST, Choi K-C, Kang SK, Leung PCK. Ovarian surface epithelium: biology, endocrinology, and pathology. *Endocrine Reviews*. 2001;22(2):255–88.
6. Society CC. Canadian Cancer Society's Advisory Committee on Cancer Statistics. *Canadian Cancer Statistics* 20162016.
7. Abell MR. The nature and classification of ovarian neoplasms. *Canadian Medical Association Journal* 1966;94:1102-24.
8. Reid BM, Permuth JB, Sellers TA. Epidemiology of ovarian cancer: a review. *Cancer Biology and Medicine* 2017;14(1):9–32.
9. Lurie G, Wilkens LR, Thompson PJ, Matsuno RK, Carney ME, Goodman MT. Symptom presentation in invasive ovarian carcinoma by tumor histological type and grade in a multiethnic population: a case analysis. *Gynecologic Oncology*. 2010;119(2):278–84.
10. Kurman RJ, Shih I-M. The dualistic model of ovarian carcinogenesis; revisited, revised, and expanded. *The American Journal of Pathology* 2016;186(4):733-47.
11. Chen VW, Ruiz B, Killeen JL, Cote TR, Wu XC, Correa CN. Pathology and classification of ovarian tumors. *American Cancer Society* 2003;97(10 ):2631 - 42
12. Ayhan y, Chakrabarti I, Ehdaivand S, Gupta N, Kuhn E, Malliah R, et al. Ovary tumor 2018 [Available from: [www.pathologyoutlines.com/ovarytumor.html](http://www.pathologyoutlines.com/ovarytumor.html)].
13. Vang R, Shih I-M, Kurman RJ. Ovarian low-grade and high-grade serous carcinoma pathogenesis, Clinicopathological and molecular biologic features, and diagnostic Problems. *Advances in Anatomica Pathology*. 2009;16(5):267–82
14. Seidman JD, Horkayne-Szakaly I, Haiba M, Boice CR, Kurman RJ, Ronnett BM. The histologic type and stage distribution of ovarian carcinomas of surface epithelial origin. *International Journal of Gynecological Pathology*. 2003;23:41–4.
15. bel MK, Kalloger SE, Huntsman DG, Santos JL, Swenerton KD, Seidman JD, et al. Differences in Tumor Type in Low-stage Versus High-stage Ovarian Carcinomas. *International Journal of Gynecological Pathology*. 2010;29:203–11.
16. Ulbright TM, Roth LM, Stehman FB. Secondary ovarian neoplasia. A clinicopathologic study of 35 cases. *Cancer* 1984;53(5):1164-74.
17. Cathro HP, Stoler MH. Expression of cytokeratins 7 and 20 in ovarian neoplasia. *American Journal of Clinical Pathology* 2002;117:944-51.
18. Gemignani ML, Schlaerth AC, Bogomolnii F, Barakat RR, Lin O, Soslow R, et al. Role of KRAS and BRAF gene mutations in mucinous ovarian carcinoma. *Gynecologic Oncology*. 2003;90:378–81.
19. Anglesio M, Kommoss S, Tolcher MC, Clarke B, Galletta L, Porter HM, et al. Molecular characterization of mucinous ovarian tumours supports a stratified treatment approach with HER2 targeting in 19% of carcinomas. *The Journal of Pathology* 2013;229(1):111-20.
20. Perren TJ. Mucinous epithelial ovarian carcinoma. *Annals of Oncology*. 2016;27:53-7.

21. Anglesio MS, Carey MS, Köbel M, Mackay H, Huntsman DG. Clear cell carcinoma of the ovary: a report from the first Ovarian Clear Cell Symposium, June 24th, 2010. *Gynecologic Oncology*. 2011;121(2):407-15.
22. Yamamoto S, Tsuda H, Takano M, Hase K, Tamai S, Matsubara O. Clear-cell adenofibroma can be a clonal precursor for clear-cell adenocarcinoma of the ovary: a possible alternative ovarian clear-cell carcinogenic pathway. *Journal of Pathology* 2008;216(1):103-10.
23. Okamoto A, Sugiyama T, Hamano T, Kim JW, Kim BG, Enomoto T, et al. Randomized phase III trial of paclitaxel/carboplatin (PC) versus cisplatin/irinotecan (CPT-P) as first-line chemotherapy in patients with clear cell carcinoma (CCC) of the ovary: A Japanese Gynecologic Oncology Group (JGOG)/GCIG study. *Journal Of Clinical Oncology*. 2014;32(5s).
24. Tsuchiya A, Sakamoto M, Yasuda J, Chuma M, Ohta T, Ohki M, et al. Expression profiling in ovarian clear cell carcinoma: identification of hepatocyte nuclear factor-1 beta as a molecular marker and a possible molecular target for therapy of ovarian clear cell carcinoma. *American Journal of Pathology*. 2003;163(6):2503-12.
25. Fujiwara K, Shintani D, Nishikawa T. Clear-cell carcinoma of the ovary. *Annals of Oncology*. 2016;27:50-2.
26. Sekizawa A, Amemiya S, Otsuka J, Saito H, Farina A, Okai T, et al. Malignant transformation of endometriosis: application of laser microdissection for analysis of genetic alterations according to pathological changes *Medical Electron Microscopy*. 2004;37(2):97–100.
27. Tavassoli FA, Devilee P. World Health Organization Classification of Tumours. Pathology and Genetics of Tumours of the Breast and Female Genital Organs: (World Health Organization 2003.
28. Prat J. New insights into ovarian cancer pathology. *Annals of Oncology*. 2012;23:111-7.
29. Obata K, Morland SJ, Watson RH, Hitchcock A, Chenevix-Trench G, Thomas EJ, et al. Frequent PTEN/MMAC mutations in endometrioid but not serous or mucinous epithelial ovarian tumors. *Cancer Research* 1998;58:2095–7.
30. Catasús L, Bussaglia E, Rodriguez I, Gallardo A, Pons C, Irving JA, et al. Molecular genetic alterations in endometrioid carcinomas of the ovary: Similar frequency of beta-catenin abnormalities but lower rate of microsatellite instability and PTEN alterations than in uterine endometrioid carcinomas. *Human Pathology* 2004;35:1360–8.
31. Austin RM, Norris HJ. Malignant Brenner tumor and transitional cell carcinoma of the ovary: a comparison. *international Journal of Gynecological Pathology*. 1987;6(1):29-39.
32. Cuatrecasas M, Catusus L, Palacios J, Prat J. Transitional cell tumors of the ovary: a comparative clinicopathologic, immunohistochemical, and molecular genetic analysis of Brenner tumors and transitional cell carcinomas *American Journal of Surgical Pathology*. 2009;33(4):556-67.
33. Shih I-M, Kurman RJ. A Proposed Model Based on Morphological and Molecular Genetic Analysis. *American Journal of Pathology*. 2004;164(5):1511–8.
34. Rathod S, Vijayalakshmi S. A Giant Ovarian Cyst: A Rare Case Of Mucinous Cystadenocarcinoma Of The Ovary In A Teenage Girl *Journal of Postgraduate Gynecology & Obstetrics* 2015;2(5).
35. Zannoni GF, Improta G, Pettinato A, Brunelli C, Troncone G, Scambia G, et al. Molecular status of PI3KCA, KRAS and BRAF in ovarian clear cell carcinoma: an analysis of 63 patients. *Journal of clinical pathology*. 2016.
36. Ketabi Z, Bartuma K, Bernstein I, Malander S, Grönberg H, Björck E, et al. Ovarian cancer linked to Lynch syndrome typically presents as early-onset, non-serous epithelial tumors. *Gynecologic Oncology*. 2011;121(3):462-5.
37. Olsen CM, Green AC, Whiteman DC, Sadeghi S, Kolaheidoz F, Webb PM. Obesity and the risk of epithelial ovarian cancer: a systematic review and meta-analysis. *European Journal of Cancer* 2007;43(4):690-709.

38. Rauh-Hain JA, Krivak TC, Carmen MGd, Olawaiye AB. Ovarian Cancer Screening and Early Detection in the General Population. *Diagnostic Review*. 2011;4(1):15 - 21
39. O'Brien T, Beard J, LowellUnderwood, Dennis RA, Santin AD, York L. The CA 125 gene: an extracellular superstructure dominated by repeat sequences. *Tumor Biology*. 2001;22(6):348-66.
40. Moss EL, Hollingworth J, Reynolds TM. The role of CA125 in clinical practice. *Journal of Clinical Pathology*. 2005;58(3):308–12.
41. Henderson JT, Webber EM, Sawaya GF. Screening for Ovarian Cancer: Updated Evidence Report and Systematic Review for the US Preventive Services Task Force. *JAMA*. 2018;319(6):595-606.
42. Rojas V, Hirshfield KM, Ganesan S, Rodriguez-Rodriguez L. Molecular characterization of epithelial ovarian cancer: implications for diagnosis and treatment. *International Journal of Molecular Sciences*. 2016;17:1-23.
43. LE T, FAUGHT W, HOPKINS L, FUNG MFK. Primary chemotherapy and adjuvant tumor debulking in the management of advanced-stage epithelial ovarian cancer. *international Journal of Gynecological Cancer* 2005;15:770–5.
44. Elattar A, Bryant A, Winter-Roach BA, Hatem M, Naik R. Optimal primary surgical treatment for advanced epithelial ovarian cancer. *Cochrane Database Systematic Review*. 2011;10(8).
45. Liu J, Matulonis U. Treatment of Advanced Epithelial Ovarian Cancer. *US Oncological Disease*. 2006:57-61.
46. Jaaback K, Johnson N, Lawrie TA. Intraperitoneal chemotherapy for the initial management of primary epithelial ovarian cancer. *Cochrane Database Systematic Review*. 2014;11:1-64.
47. Kehoe S, Hook J, Nankivell M, Jayson GC, Kitchener H, Lopes T, et al. Primary chemotherapy versus primary surgery for newly diagnosed advanced ovarian cancer (CHORUS): an open-label, randomised, controlled, non-inferiority trial. *The Lancet*. 2015;386(9990):249–57.
48. Vergote I, Trope CG, Amant F, Kristensen GB, Ehlen T, Johnson N, et al. Neoadjuvant chemotherapy or primary surgery in stage IIIC or IV ovarian cancer. *New England Journal of Medicine*. 2010;363:943-53.
49. Ozols RF, Bundy BN, Greer BE, Fowler JM, Clarke-Pearson D, Burger RA, et al. Phase III Trial of Carboplatin and Paclitaxel Compared With Cisplatin and Paclitaxel in Patients With Optimally Resected Stage III Ovarian Cancer: A Gynecologic Oncology Group Study *Journal Of Clinical Oncology*. 2003;21(17):3194-200
50. Herzog TJ, Pothuri B. Ovarian cancer: a focus on management of recurrent disease. *Nature Clinical Practice Oncology* 2006;3:604–11
51. Markman M, Rothman R, Hakes T, Reichman B, Hoskins W, Rubin S, et al. Second-line platinum therapy in patients with ovarian cancer previously treated with cisplatin. *Journal Of Clinical Oncology*. 1991 9(3):389-93.
52. Coleman RL, Monk BJ, Sood AK, Herzog TJ. Latest research and treatment of advanced-stage epithelial ovarian cancer. *Nature Reviews;Clinical Oncology* 2013;10:211-24.
53. Schmitt J, Matei D. Targeting angiogenesis in ovarian cancer. *Cancer Treat Review* 2012;38(4):272-83.
54. Karamysheva A. Mechanisms of angiogenesis. *Biochemistry (Mosc)*. 2008;73(7):751-62.
55. Burger RA, Brady MF, Bookman MA, Fleming GF, Monk BJ, Huang H, et al. Incorporation of bevacizumab in the primary treatment of ovarian cancer. *New England Journal of Medicine* 2011;365:2473–83
56. Perren TJ, Swart AM, Pfisterer J, Ledermann JA, Pujade-Lauraine E, Kristensen G, et al. A phase 3 trial of bevacizumab in ovarian cancer. *New England Journal of Medicine*. 2011;365:2484–96
57. Alsop K, Fereday S, Meldrum C, deFazio A, Emmanuel C, George J, et al. BRCA Mutation Frequency and Patterns of Treatment Response in BRCA Mutation–Positive Women With Ovarian

- Cancer: A Report From the Australian Ovarian Cancer Study Group. *Journal Of Clinical Oncology*. 2012;30(21):2654 - 63.
58. Luvero D, Milani A, Ledermann JA. Treatment options in recurrent ovarian cancer: latest evidence and clinical potential. *Therapeutic Advances in Medical Oncology* 2014;6(5):229–39.
  59. Mariappan L, Jiang XY, Jackson J, Drew Y. Emerging treatment options for ovarian cancer: focus on rucaparib. *international Journal of Women health* 2017;9:913–24.
  60. Verhaak RGW, Tamayo P, Yang J-Y, Hubbard D, Zhang H, Creighton CJ, et al. Prognostically relevant gene signatures of high-grade serous ovarian carcinoma. *Journal Of Clinical Investigation*. 2013;123(1):517–25.
  61. Jones PM, Drapkin R. Modeling high-grade serous carcinoma: how converging insights into pathogenesis and genetics are driving better experimental platforms. *Frontiers*. 2013;3(217):1-10.
  62. Lengyel E. Ovarian Cancer Development and Metastasis. *American Journal of Pathology*. 2010;177(3):1053–64.
  63. Wozzfeld T, Strandmann EPv, Huber M, Adhikary T, Wagner U, Reinartz S, et al. The unique molecular and cellular microenvironment of ovarian cancer. *frontiers in Oncology* 2017;7(24):1 - 23.
  64. Kulbe H, Thompson R, Wilson JL, Robinson S, Hagemann T, Fatah R, et al. The inflammatory cytokine tumor necrosis factor- $\alpha$  generates an autocrine tumor-promoting network in epithelial ovarian cancer cells. *American Association for Cancer Research* 2007;67(2):585-92.
  65. Cooke SL, Ng CK, Melnyk N, Garcia MJ, Hardcastle T, Jillian Temple, et al. Genomic analysis of genetic heterogeneity and evolution in high-grade serous ovarian carcinoma. *Oncogene*. 2010;29:4905–13.
  66. Anderson R. Multiplex fluorescence in situ hybridization (M-FISH). *Methods in Molecular Biology* 2010;659:83-97.
  67. Network TCGAR. Integrated genomic analyses of ovarian carcinoma. *Nature* 2011;474:609-15.
  68. Grusby MJ, Hugh Auchincloss J, Lee R, Johnson RS, Spencer JP, Zijlstra M, et al. Mice lacking major histocompatibility complex class I and class II molecules. *Proceeding of the National Academy of Science of the USA*. 1993;90(9):3913–7.
  69. Belizário JE. Immunodeficient Mouse Models: An Overview. *The Open Immunology Journal*. 2009;2:79-85.
  70. Anglesio MS, Wiegand KC, Melnyk N, Chow C, Salamanca C, Prentice LM, et al. Type-specific cell line models for type-specific ovarian cancer research. *PLOS ONE* 2013;8(9):1-13.
  71. Freeburg EM, Goyeneche AA, Seidel EE, Telleria CM. Resistance to cisplatin does not affect sensitivity of human ovarian cancer cell lines to mifepristone cytotoxicity. *Cancer Cell International* 2009;9(4).
  72. Barretina J, Caponigro G, Stransky N, Venkatesan K, Margolin AA, Kim S, et al. The Cancer Cell Line Encyclopedia enables predictive modelling of anticancer drug sensitivity. *Nature*. 2012;483(7391):603–7.
  73. Hughes P, Marshall D, Reid Y, Parkes H, Gelber C. The costs of using unauthenticated, over-passaged cell lines: how much more data do we need? *BioTechniques*. 2018;43(5).
  74. Pan C, Kumar C, Bohl S, Klingmueller U, Mann M. Comparative Proteomic Phenotyping of Cell Lines and Primary Cells to Assess Preservation of Cell Type-specific Functions. *Molecular and Cellular proteomics* 2009;8(3):443–50.
  75. HM M, GW L. Long-term culture of primary breast cancer in defined medium. *Breast Cancer Research and Treatment* 1996;39(3):247-59.
  76. Mitra A, Mishra L, Li S. Technologies for deriving primary tumor cells for use in personalized cancer therapy. *Trends Biotechnology* 2013;31(6):347–54.
  77. Schilsky R. Personalized medicine in oncology: the future is now. *Nature revision Drug discovery* 2010;9(5):363-6.

78. Tentler J, Tan A, Weekes C, Jimeno A, Leong S, Pitts T, et al. Patient-derived tumour xenografts as models for oncology drug development. *Nature Review;Clinical Oncology*. 2012;9(6):338-50.
79. Topp M, Hartley L, Cook M, Heong V, Boehm E, McShane L, et al. Molecular correlates of platinum response in human high-grade serous ovarian cancer patient-derived xenografts. *Molecular Oncology* 2014;8(3):656-68.
80. Pompili L, Porru M, Caruso C, Biroccio A, Leonetti C. Patient-derived xenografts: a relevant preclinical model for drug development. *Journal of Experimental and clinical cancer research* 2016;35(189).
81. Beaufort CM, Helmijr JCA, Piskorz AM, Hoogstraat M, Ruigrok-Ritstier K, Besselink N, et al. Ovarian cancer cell line panel (OCCP): clinical importance of in vitro morphological subtypes. *PLOS ONE*. 2014;9(9):1-16.
82. Haley J, Tomar S, Pulliam N, Xiong S, Perkins SM, Karpf AR, et al. Functional characterization of a panel of high-grade serous ovarian cancer cell lines as representative experimental models of the disease. *Oncotarget*. 2016;7(22):32810-20.
83. Srivastava P, Kumar M, Nayak PK. Role of Patient Derived Cell Lines and Xenograft in Cancer Research *The Pharmstudent* 2016;27:40-8.
84. Goodspeed A, Heiser LM, Gray JW, Costello JC. Tumor-derived Cell Lines as Molecular Models of Cancer Pharmacogenomics. *Molecular Cancer Research* 2016;14(1):3-13.
85. Yee NS, Ignatenko N, Finnberg N, Lee N, Stairs D. Animal Models of Cancer Biology *Cancer Growth Metastasis*. 2015;8(1):115–8.
86. Hasan N, Ohman AW, Dinulescu DM. The promise and challenge of ovarian cancer models. *Translation Cancer Research* 2015;4(1):14-28.
87. Selby PJ, Thomas JM, Monaghan P, Sloane J, Peckham MJ. Human Tumour Xenografts Established and Serially Transplanted in mice Immunologically Deprived by Thymectomy, Cytosine Arabinoside and Whole-Body Irradiation. *British Journal of Cancer* 1980;41:52-61
88. Bobbs AS, Cole JM, Dahl KDC. Emerging and Evolving Ovarian Cancer Animal Models. *Cancer Growth Metastasis*. 2015;8(1):29–36.
89. Orsulic S, Li Y, Soslow RA, Vitale-Cross LA, Gutkind JS, Varmus HE. Induction of ovarian cancer by defined multiple genetic changes in a mouse model system. *Cancer Cell*. 2008;1(1):53–62.
90. Ohsuga T, Yamaguchi K, Kido A, Murakami R, Abiko K, Hamanishi J, et al. Distinct preoperative clinical features predict four histopathological subtypes of high-grade serous carcinoma of the ovary, fallopian tube, and peritoneum. *BMC Cancer*. 2017;17.
91. SZADVARI I, KRIZANOVA O, BABULA P. Athymic Nude Mice as an Experimental Model for Cancer Treatment. *Physiological Research* 2016;65:441-53.
92. Herberman R. Natural cell-mediated cytotoxicity in nude mice. Fogh J, Herberman B, editors 1979.
93. SOMASUNDARAM R, JACOB L, ADACHI K, CLASS R, SCHECK S, MARUYAMA H, et al. Mouse Model for Study of Human B-Cell Responses. *SCANDINAVIAN journal of immunology* 1995;41(4).
94. Meyerrose TE, Herrbrich P, Hess DA, Nolta JA. Immune-deficient mouse models for analysis of human stem cells. *BioTechniques*. 2003;35(6):1262-72.
95. Elias KM, Emori MM, Pappe E, MacDuffie E, Konecny GE, Velculescu VE, et al. Beyond genomics: Critical evaluation of cell line utility for ovarian cancer research. *Gynecologic Oncology*. 2015;139:97–103.
96. Mitra AK, Davis DA, Tomar S, Royc L, Gurler H, Xie J, et al. In vivo tumor growth of high-grade serous ovarian cancer cell lines. *Gynecologic Oncology*. 2015;138:372–7.
97. Euscher ED, Silva EG, Deavers MT, Elishaev E, Gershenson DM, Malpica A. Serous Carcinoma of the Ovary, Fallopian tube, or Peritoneum Presenting as Lymphadenopathy *American Journal of Surgical Pathology*. 2004;28(9):1217- 23.

## *Appendix*

I was the first student who joined Dr. Telleria's laboratory at McGill in May, 2016. Since I came from a very clinical background, the laboratory work was new for me. Dr. Goyeneche took me step by step to teach me ABC laboratory and I am so grateful to have had a teacher like her. I joined her in many laboratory activities and I tried to document every procedure in my notes. I realized that every lab has its own style and maybe it would be of great help for the incoming students joining us if I share my notes with them, helping them to become involved in the work more easily and quickly. For that reason, I revised my notes and added some additional tips from different webpages to create an easy, relevant student manual to serve as a guidance/reference for the most common activities we encounter in the laboratory. I hope that others can derive significant benefits from it and this manual can be used as an educational gift from me to Dr. Telleria's laboratory and McGill University.

# 2016



Sarah Alghamdi  
Dr. Telleria's research laboratory  
McGill University

## Index:

|   |    |
|---|----|
| <b><i>Section 1: Introduction</i></b>                         |    |
| 1.1 Why this manual -----                                     | 3  |
| 1.2 Purpose and scope -----                                   | 3  |
| 1.3 Before you start -----                                    | 3  |
| <b><i>Section 2: Cell culture in brief</i></b>                |    |
| 2.1 History -----   | 4  |
| 2.2 Definition -----  | 4  |
| 2.3 Cell culture application -----                            | 5  |
| 2.4 Types of cultures and cells in culture-----               | 6  |
| <b><i>Section 3: Cell culture facilities</i></b>              |    |
| 3.1 Cell culture laboratories -----                           | 7  |
| 3.2 Minimum requirement for cell culture laboratories-----    | 7  |
| 3.3 Basic equipment-----                                      | 8  |
| 3.4 Basic supplies-----                                       | 11 |
| <b><i>Section 4: Cell culture media</i></b>                   |    |
| 4.1 Different types of media -----                            | 12 |
| 4.2 Basic component of media-----                             | 13 |
| 4.3 To add serum or not to add? -----                         | 14 |
| 4.4 Different media for different purposes -----              | 14 |
| 4.5 Preparing media in our laboratory -----                   | 18 |
| <b><i>Section 5: Working with the cell line</i></b>           |    |
| 5.1 Retrieve the cells from the liquid nitrogen -----         | 19 |
| 5.2 Choosing the growth surfaces -----                        | 20 |
| 5.3 Follow up and assessment of cells-----                    | 22 |
| 5.4 Planning for sub-culturing, fixation or preservation----- | 23 |
| <b><i>Section 6: Safety</i></b>                               |    |
| 6.1 Safety practice for personnel-----                        | 28 |
| 6.2 Working in a sterile environment-----                     | 28 |
| <b><i>Cell culture full protocol summary</i></b> -----        | 29 |
| <b><i>References</i></b> -----                                | 34 |

## Symbols:



*Expand your knowledge by reading in this topic*



*Technique you have to practice it in the laboratory*



*Extra information lights up your brain for more exploration*



*Warning! You should pay full attention to this topic*

## ***Section 1: Introduction***

### *1.1 Why this manual?*

This manual contains all the essential information in a very easy language for the students as well as anyone who is working in the field of science dealing with cell culture. The manual is divided into many sections allowing readers to organize their approaches to cell culture. It includes a brief introduction to the cell culture world; then, it will take you to the cell culture technique step by step insuring that your work is of proper technique and safety. Beyond the technical part, you will be enriched with a lot of information about different reagents, enzymes and many materials and tools you might deal with during your practice.

### *1.2 Purpose and scope:*

This manual has been designed primarily for students at the novice level to facilitate their work with cell culture.

### *1.3 Before you start!*

Always remember that working with cell culture requires a high level of precision, care and patience. But it is FUN!

## Section 2: Cell culture in brief

### 2.1 History

The history of cell culture goes back to the late nineteenth century when *Wilhelm Roux* managed to maintain living cells from the neural plate of chick embryo in saline buffer for a few days. Until the late 30's, many experiments were conducted by various scientists to develop models for cell culture but all were failures. At that time, cell culture was too difficult to manage. However, in the early 40's, *Earle* established the first cell line, consisting of fibroblasts in culture media. Then in 1995, *Dr. Jones* diagnosed *Henrietta Lacks* with cervical cancer. He sent a sample of her tumor to *Dr. Gey* who cultivated the cells and discovered that the cell line was durable and would undergo cell division every twenty hours. This cell line (called HeLa, after the patient (Henrietta Lacks), gave him the best means to develop the poliovirus, allowing the development of Salk vaccine.

### 2.2 Definition

Cell culture refers to the process of removal of cells from a source (human, animal or plant) and their subsequent growth in an artificial environment.

RECOMMENDED  
ARTICLE IN THIS  
TOPIC:

*International Journal of  
Current Research and academic  
Review: **Cell Culture: History,  
Development and Prospects***

[http://www.academia.edu/10071919/Cell\\_Culture\\_History\\_Development\\_and\\_Prospects](http://www.academia.edu/10071919/Cell_Culture_History_Development_and_Prospects)



Can we culture an organ or a whole tissue?

### 2.3 Cell culture applications

The great advancement in the realm of technology and cell biology allowed us to provide standardization of cell cultures from the media development, the sophisticated incubators, the adhesion surface, etc. Extensive and varied applications of cell culture have been developed and used.

---

*more applications and detailed uses are well explained in the following article:*

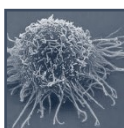
---

*International Journal of Current Research and academic Review: **Cell Culture: History, Development and Prospects***  
[http://www.academia.edu/10071919/Cell\\_Culture\\_History\\_Development\\_and\\_Prospects](http://www.academia.edu/10071919/Cell_Culture_History_Development_and_Prospects)



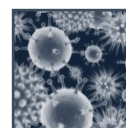
Cell culture to study cell morphology and physiology

- cell culture provides excellent model to study the normal physiological changes of the cells including the effect of different toxic compound and drugs.
- It provides also a clear method to study the morphology and the characteristics of cells.



cell culture in basic and Cancer research

- Intracellular activities: DNA transcription and protein synthesis.
- Biomolecular intracellular flow as RNA processing, protein transport, assembly and disassembly of microtubules
- Used to Study the function of various chemicals, viruses & radiation to convert normal cultured cells to cancerous cells



Cell culture to study Virology and toxicology

- Cell culture is a necessary tool to study virology and furthermore, vaccination and biotechnology.
- Used to study the effects of new drugs



Have you heard about tissue engineering?

Many things can be done for humanity. Read about it!

## *2.4 Types of cultures and cells*

### **A- Primary Culture**

It means the cultured cells came directly from the parental tissue.

### **B- Secondary Culture**

When the primary culture is sub-cultured. Other name is “passage,” the process described to transfer the cells from one culture vessel to another one.

*In culture the cells can grow in two ways:*

### **A- Adherent Cells**

Also called dependent cells because they need attachment to enhance growth. The growth is limited by the surface area.

### **B- Suspension Cells**

Other name is independent cells, in contrast to adherent cells; they do not need a surface to enhance the growth. Growth is limited by the concentration of cells.

## *Section 3: Cell culture facilities*

### *3.1 Cell culture laboratories*

Cell culture laboratories may differ based on the type of research conducted. However, all of them share some basic equipment and supplies.

### *3.2 Minimum requirements for a cell culture room*

In addition to the aseptic environment – to be discussed later-, there are basic equipment and supplies that should be provided in every tissue culture facility room:

#### Basic equipment

- Cell culture hood
- Incubators
- Centrifuge
- Water bath
- Inverted microscope
- Refrigerator or freezer ( usually -20 °C )
- Cryostorage container
- Air filter

#### Basic supplies

- Aspiration pump
- Pipettes and pipettors
- Syringes and needles
- waste container
- Cell culture vessels (e.g., flasks, Petri dishes, roller bottles, multiwell plates)
- cells
- cell cryovials

#### Extended equipment

- pH meter
- Roller racks (for scaling up monolayer cultures)
- Confocal microscope
- Flow cytometer
- EG bioreactors
- Autoclave

### 3.3 Basic equipment

#### A- Cell culture hood

Also called laminar-flow hood or biosafety cabinet. It is an enclosed ventilated laboratory workspace for safely working with material that requires a defined biosafety level. All exhaust air is filtered as it exits from the cabinet providing highly safe environment for the worker and the samples. Usually the hood is provided with an ultraviolet lamp to ensure high standards of disinfection as germicide or to avoid DNA contamination (if PCR is used).



Cell culture hood. Picture was taken from LABCONCO



There are three classes of biosafety cabinets – they vary depending on the protection they provide. Read about it!

#### B- Incubator

An incubator is an enclosed device that maintains specific temperature, carbon dioxide and oxygen levels within the inside environment. The purpose of this device is to provide the appropriate environment for cell growth. The temperature and the level of CO<sub>2</sub> should be frequently measured and adjusted.



Incubator. Picture was taken from Thermo Scientific



Dry versus humidified incubator. Read about it!



**Measuring the CO<sub>2</sub> within the incubator:** for the tissue culture purpose the CO<sub>2</sub> should be within 5%, mimicking physiological levels. FYRITE is used to measure CO<sub>2</sub> concentration with a simple method that depends on a chemical reaction.



### How to use FYRITE to measure CO<sub>2</sub>?

- 1- Hold the FYRITE in upright position.
- 2- Press the plunger valve to vent FYRITE and then release. Adjust the fluid level to the zero line on the scale.
- 3- Insert the end of the tube (the one with rubber adapter) into the gas port of the incubator.
- 4- Press the upper valve firmly and pump using the aspirator bulb 18 times.
- 5- Invert the FYRITE until fluid drains into the upper reservoir then turn upright.
- 6- Wait for few seconds until stabilized and read the percentage on the scale

**N.B. Practice this technique many times until you master it!**



FYRITE. Picture was taken from Department of animal science UOF.

### C- Centrifuge

It is a device that spins samples at high speed and thus creates a strong centripetal force causing the denser materials to travel towards the bottom of the centrifuge tube more rapidly than they would under the force of normal gravity.



Centrifuge. Picture was taken from Thermo Scientific

### D- Water bath

It is a container filled with heated water. Uses include warming of reagents, melting of substrates or cell culture incubation. It can be used also for certain chemical reactions that need high temperature.



---

A water bath is a major source of bacterial growth. Many methods can be used to prevent contamination. Methods include use of disinfectants and/or rising the temperature to 90°C more than once a week.

---

## E- Inverted microscope

It is a special type of microscope with its light source and condenser on the top, while the objectives are below. It is used mainly to observe the living cells under natural conditions.



Inverted microscope. Picture was taken from vision engineering

## F- Cryostorage (liquid nitrogen)

It is a process of preserving the cells by cooling to very low temperatures (typically  $-196^{\circ}\text{C}$ ). This very low temperature is enough to stop any enzymatic or chemical reaction which might cause damage to the cells.



Cryostorage . Picture was taken from Thermo Scientific



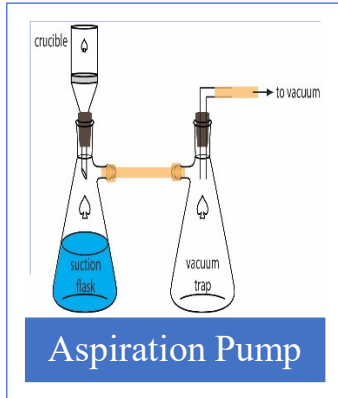
---

Nitrogen gas is odorless, colorless, tasteless, and nonirritating, nitrogen has no warning properties. Humans possess no senses that can detect the presence of nitrogen. Although nitrogen is nontoxic and inert, it can act as a simple asphyxiant by displacing the oxygen in air to levels below that required to support life. Inhalation of nitrogen in excessive amounts can cause dizziness, nausea, vomiting, loss of consciousness, and death. Death may result from errors in judgment, confusion, or loss of consciousness that prevents self-rescue. At low oxygen concentrations, unconsciousness and death may occur in seconds and without warning.

For more information: <http://www.airproducts.com/~media/files/pdf/company/safetygram-7.pdf>

---

### 3.4 Basic supplies



As you practice you will see other supplies and instruments. Write down here what are the new things you learn:

- 1- .....
- 2- .....
- 3- .....
- 4- .....

## Section 4: Cell culture media

### 4.1 Different types of media

Choosing the appropriate medium to cultivate the cells is a crucial step in cell culture. A growth medium provides a major source of energy and nutrient supplies to regulate the cell cycle.

There are two major types of media:

- a- Natural media: usually derived from a biological fluid, tissue extract or clots. Examples include: serum, extract of liver or spleen and plasma clots, respectively. Although it is very convenient in cell culture, its poor reproducibility limits its uses.
- b- Artificial media: usually it is a complex media that contains many nutrients and essential elements. It has four major categories:

#### ❖ Serum containing media:

Fetal bovine serum (FBS) is the most common supplement. Serum is a major source of nutrients, hormones and growth factors. However, the use of FBS is controversial for many reasons. The seasonal variation in the serum composition which leads to variation in results, the unnecessary suffering of the unborn calf and the unignorable percentage of virus-positive FBS are among the major disadvantages of using FBS containing media.

#### ❖ Serum free media:

It is recommended now by guidelines for good cell culture practice (GCCP) and ECVAM scientific advisory committee (ESAC) to use serum-free

### *Recommended Articles in this topic:*

1-Cell culture media: A Review: A comprehensive review of cell culture media and Labome survey results on cell culture media from 750 formal publications.

<http://www.labome.com/method/Cell-Culture-Media-A-Review.html>

2-Optimization of chemically defined cell culture media- Replacing fetal bovine serum in mammalian *in vitro* methods

<http://www.sciencedirect.com/science/article/pii/S0887233310000809>

substitutes for current and new *in vitro* methods. These media are formulated to support the culture of a single cell type and contain defined amounts of purified growth factors, lipoproteins and other proteins. It is also called *defined culture medium* as its components are known.

#### ❖ Chemically defined media

This type of medium does not contain proteins or any other unknown chemical component. Highly purified hormones or growth factors can be added.

#### ❖ Protein-free media

Protein-free medium does not contain high molecular weight proteins, but may contain peptide fractions.

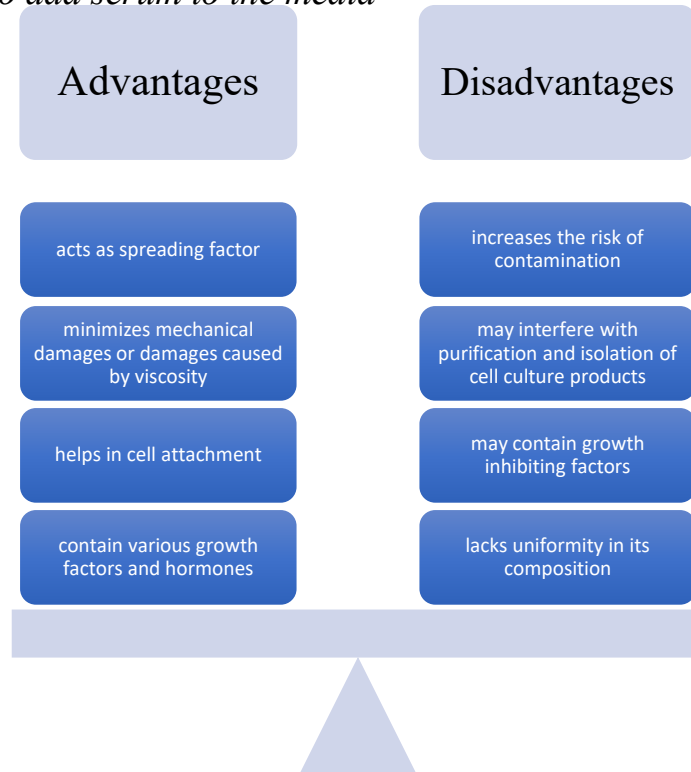
### 4.2 Basic components of culture media

| Component                    | Function   | Example   |
|------------------------------|--|---|
| <b>Buffering systems</b>     | Control PH within physiological range  | HEPES   |
| <b>Amino acid</b>            | Building unit of proteins, important for cell proliferation; secondary source of energy. | L-glutamine   |
| <b>Carbohydrates</b>         | Major source of energy.  | Glucose   |
| <b>Proteins and peptides</b> | Extremely essential in serum-free media.   | Albumin has binding capacity which enables it to remove toxic substance and transport essential elements between cells. |
| <b>Vitamins</b>              | Growth and proliferation of cells. Important in serum-free media.                        | Vitamin B group   |
| <b>Trace elements</b>        | Essential in serum-free media. Play role in maintenance of enzymatic activities          | Copper, Zinc  |
| <b>Media supplements</b>     | Maintaining normal cell growth and metabolism  | Hormones and growth factors   |
| <b>Antibiotics</b>           | Used to control the growth of bacterial and fungal contamination.                        | Penicillin, streptomycin  |
| <b>Fatty acid and lipid</b>  | Essential in serum-free media.   |   |



The use of antibiotics is **not recommended**. Read about the rationale behind that!

#### 4.3 To add or not to add serum to the media



#### 4.4 Different media for different purposes

As we mentioned before, choosing the appropriate media for the experiment is a crucial step. In general, start with MEM for adherent cells and RPMI-1640 for suspension cells.

#### 4.5 Preparing the media in our laboratory

Preparing the media is the first step! And it has to be done accurately under aseptic conditions.



Let's prepare media for our cells, we will choose RPMI 1640.. from the 500 ml bottle remove 100 ml and put the following components together:

- a- 10 mM of HEPES
- b- 4mM of glutamine
- c- 100 IU penicillin, 100 µg/ml streptomycin
- d- 0.01 mg/ml insulin
- e- 1 mM of sodium pyruvate
- f- 100 ml of FBS



##### *Why HEPES?*

HEPES is known to be a good buffer that maintains physiological PH despite changes in the CO<sub>2</sub> concentration. It keeps PH values ranging from 6.8 to 8.2 at a working concentration of 10 mM.

*Write your observation when you add HEPES to the fetal bovine serum (FBS)*

.....

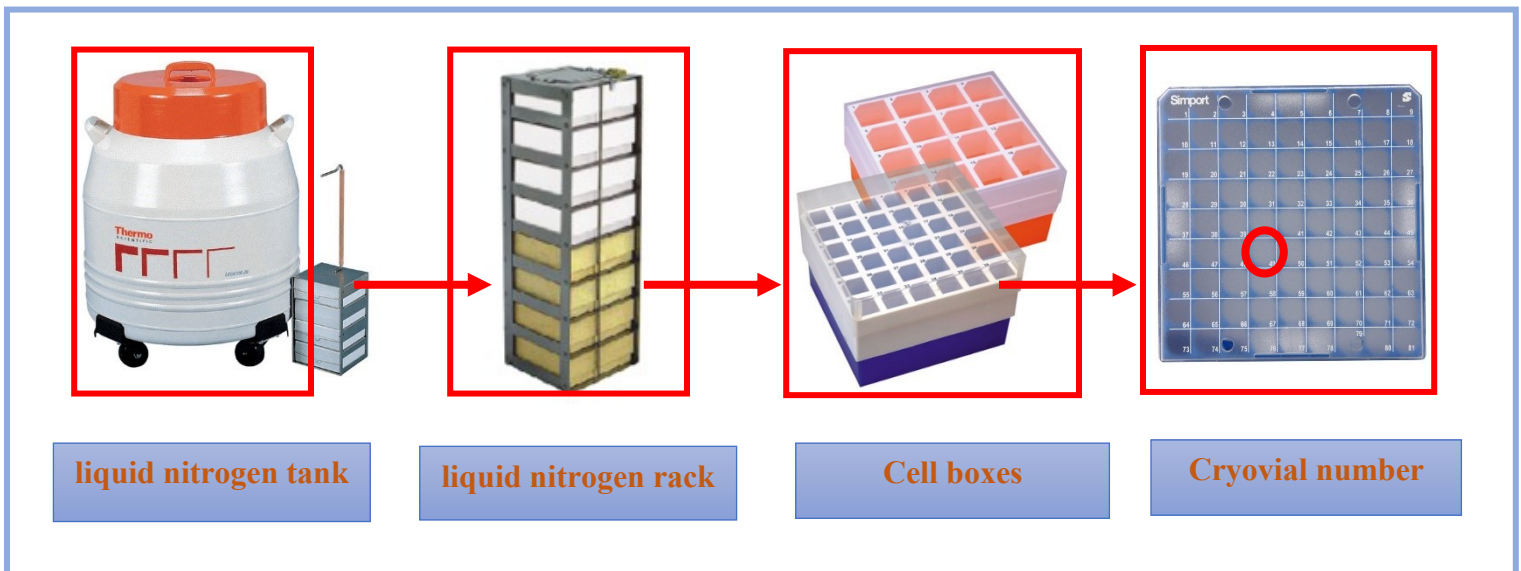
## Section 5: Working with cell lines

After the medium has been prepared, it is time for cell cultivation. A process that needs high level of precision, care and a lot of patience. Before you start your work:

- Warm up your media in the water bath
- Check the pump (rinse it with ethanol 70%)- Section 6
- Check the incubator (CO<sub>2</sub> concentration and temperature) – Section 3.3

### 5.1 Retrieve the cells from the liquid nitrogen

- ❖ Do it quickly, ideally in less than one minute!
- ❖ Check the number of the rack, box and cell vial.
- ❖ Warm up the vial immediately in a 37 °C water bath.



*When retrieving the cells from liquid nitrogen, thaw it **quickly!** And store it back in liquid nitrogen **slowly** after pre-cooling overnight at -80°C.*

## 5.2 Choosing the surface for cultivation

### 5.2.A Brief history

During the past 100 years, the surfaces used for growing cells have evolved as the needs of researchers have changed. The first surfaces used to cultivate cells were glass flasks and Petri dishes. The PYREX Povitsky flask was the first one used for commercial purposes; it was successfully used to produce the Polio virus vaccine. Due to the difficulty many cells had to attach to the glass surface and the careful cleaning procedures required by glass flasks, researchers began experimenting with disposable plastic culture flasks. By the 1960s, plastic flasks, dishes and well plates were all available commercially. The polystyrene used for flasks was treated to be hydrophilic, even though treated polystyrene has its limitations, especially for growing cells in serum free media. For that reason, researchers have developed coatings for culture vessels surfaces to improve cell attachment and performance. Various biological materials have been used for this purpose including extracellular matrix, collagen, fibronectin, etc. There are several types of surfaces used in cell culture, depending on the amounts and types of cells

### 5.2.B Flasks

As mentioned before, polystyrene treated flasks were developed years ago and were commercially available in the 1960s. Initially, D-flasks were used with D referred to their diameters. “T”-flasks then introduced in 1947 with hexagonal or rectangular shape; “T” referred to the total surface area of the flask that is available for cell growth; thus, a T-25 flask means it contains 25 cm<sup>2</sup> of growth area. Flasks were developed with several cap styles; vented caps are highly recommended to reduce the contamination within the CO<sub>2</sub> incubators. Several advantages make the flasks superior to use especially with adherent cells:

- ✓ Traditional and easy to use
- ✓ Easy pipette access
- ✓ Easy access to see the cells by the microscope
- ✓ Reduce media spills and culture contamination





---

Vent caps contain a 0.2  $\mu\text{m}$  pore, hydrophobic membrane sealed to the cap, providing consistent, sterile gas exchange while minimizing the risk of contamination. These caps are highly recommended for use in all CO<sub>2</sub> incubators, especially for long-term use. The vent cap was a Corning innovation that first appeared in 1988.

---



---

Choosing a flask shape is usually a matter of personal preference:

---

- 1- Low profile flask
  - 2- Triangle and modified triangle flask
  - 3- Rectangular flasks
  - 4- Angled neck and traditional straight neck flask
  - 5- U-shape flask
- 



***Cell culture surfaces with their properties, advantages and disadvantages are discussed in the following articles:***

- 1- [http://csmedia2.corning.com/LifeSciences/Media/pdf/lp\\_cellculture\\_selection\\_guide\\_3\\_02\\_lslp\\_cc\\_006.pdf](http://csmedia2.corning.com/LifeSciences/Media/pdf/lp_cellculture_selection_guide_3_02_lslp_cc_006.pdf)
  - 2- [https://www.corning.com/media/worldwide/cls/documents/cc\\_scale\\_up\\_guide.pdf](https://www.corning.com/media/worldwide/cls/documents/cc_scale_up_guide.pdf)
-

### 5.3 Follow up and assessment of cells

Daily follow up and record of cell observations are highly important. Every day make a checklist with the parameters you have to examine. You can make your own notes or you might use the following checklist to ensure you complete your observations.

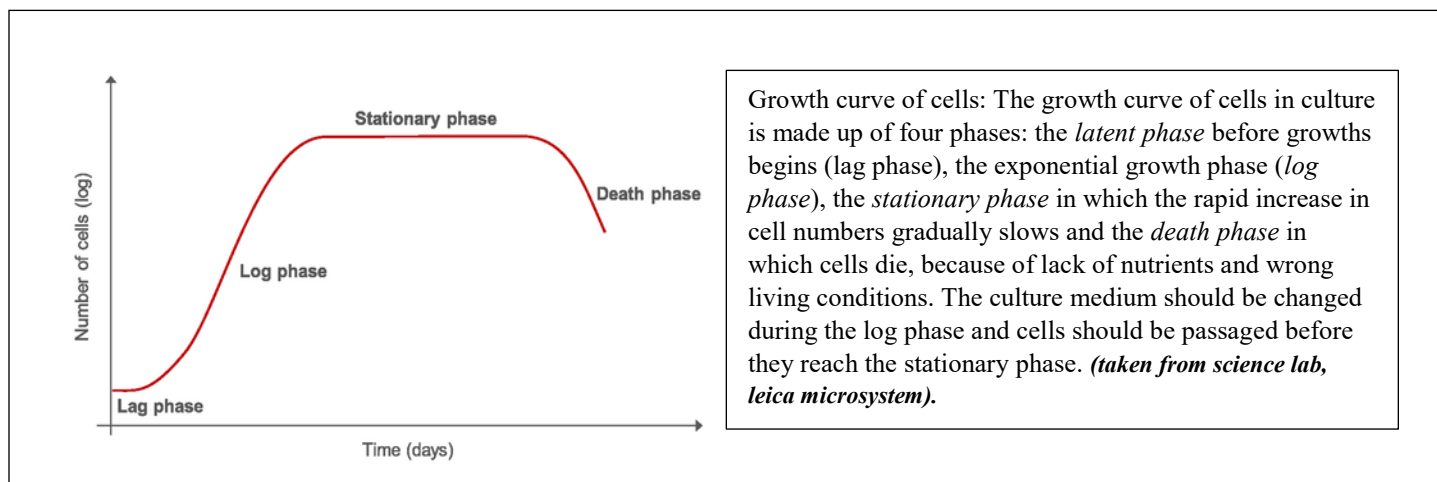
|                                |   |   |
|--------------------------------|---|---|
| <i>Gross examination</i>       | Color   | <input type="radio"/> Pink-orange<br><input type="radio"/> Yellow |
|                                | Comment:  |   |
|                                | Appearance  | <input type="radio"/> Clear<br><input type="radio"/> Cloudy       |
|                                | Comment:  |   |
| <i>Microscopic examination</i> | Adherent component  | <input type="radio"/> Present<br><input type="radio"/> Absent     |
|                                | % of confluency   | <input type="radio"/> .....                                       |
|                                | Dead cells  | <input type="radio"/> Present<br><input type="radio"/> Absent     |
|                                | Floating component  | <input type="radio"/> Present<br><input type="radio"/> Absent     |
|                                | Comment:  |   |
|                                | Shape of the cells  | <input type="radio"/> Elongated<br><input type="radio"/> Round    |
|                                | Comment:  |   |
| <i>Decision- plan</i>          | <input type="radio"/> Change media and continue growing<br><input type="radio"/> Grow more without changing the media<br><input type="radio"/> Stop culturing either for fixation or preservation |   |



*confluency means the percentage of the surface of a culture vessel that is covered with cells.*

#### 5.4 Planning for sub-culturing, fixation or preservation

“In cell culture, cells stop growing when they reach confluence (contact inhibition)”.



Sub-culturing, planning for fixation or preservation are two steps required before detaching the cells from the vessel surface and counting them.

Sub-culturing:

It means “passaging” and it refers to transfer the cells from the previous culture to a new flask containing fresh medium. This process enables more propagation in cell growth.

Fixation:

Is the process of preserving the cells permanently. It plays a critical role in immunohistochemistry studies as the fixation stabilizes the cell morphology and architecture, disables proteolytic enzymes, and protects against contaminations. There are two types of fixation: chemical and physical fixation. The most common chemical fixative used is formaldehyde.

Formaldehyde, Paraformaldehyde and formalin. Aren't they the same?

| Formaldehyde  | Formalin  | Paraformaldehyde                           |
|---|---|--|
| Prepared with paraformaldehyde dissolved in distilled water with ethanol added to stabilize the aqueous status. | Contains around 37% of formaldehyde – 15% of methanol – around 50% water. | It is the powder polymerized formaldehyde. |



- Preparing 4% formaldehyde solution
  - ⇒ Reagents: Deionized water – HCL – NaOH (1N) – Paraformaldehyde powder – 1XPBS
  - ⇒ Material: Filter unit – Glassware and stir bar – hot plate with magnetic stirrer – thermometer
  - ⇒ Procedure:
    - ✓ For 1 L of 4% Formaldehyde, add 800 mL of 1X PBS to a glass beaker on a stir plate in a ventilated hood. Heat while stirring to approximately 60 °C (do not boil!)
    - ✓ Add 40 g of paraformaldehyde powder to the heated PBS solution.
    - ✓ The powder will not immediately dissolve into solution. Slowly raise the pH by adding 1 N NaOH dropwise from a pipette until the solution clears.
    - ✓ Once the paraformaldehyde is dissolved, the solution should be cooled and filtered.
    - ✓ Adjust the volume of the solution to 1 L with 1X PBS.
    - ✓ Recheck the pH, and adjust it with small amounts of diluted HCl to approximately 6.9.

*(procedure was taken from R&D systems-biotechne brand)*



*Formaldehyde is highly toxic and carcinogenic. Full personnel protection should be taken in place including: wearing gloves, safety glasses and gown. The solutions should be stirred in the hood.*



*Formaldehyde is not the only fixative; other fixatives are available with different compositions.*

[http://link.springer.com/protocol/10.1007%2F978-1-59745-324-0\\_8](http://link.springer.com/protocol/10.1007%2F978-1-59745-324-0_8)



**PBS (Phosphate-buffer saline):** it is a water based salt solution, commonly used in biological research. It is isotonic and non-toxic. Major uses: substance dilution and cell rinsing. The PH of 1x PBS is 7.4

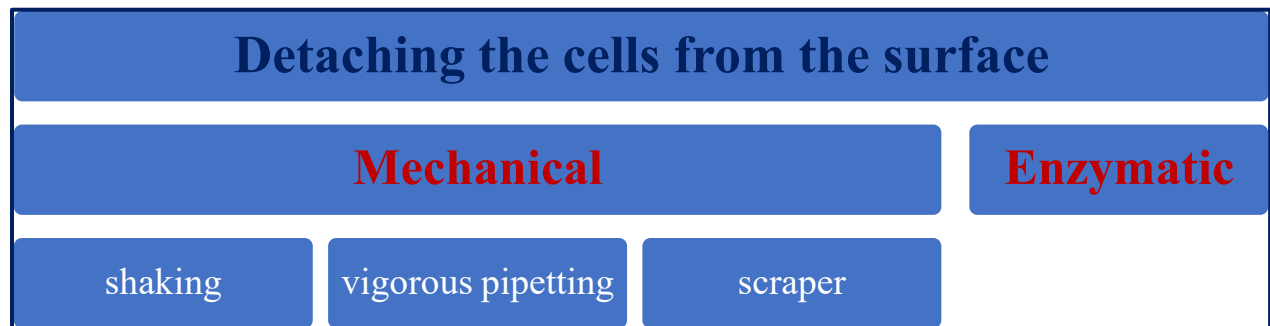


**Preparing 1x PBS:**

1. Dissolve the following in 800ml distilled H<sub>2</sub>O.
  - 8g of NaCl
  - 0.2g of KCl
  - 1.44g of Na<sub>2</sub>HPO<sub>4</sub>
  - 0.24g of KH<sub>2</sub>PO<sub>4</sub>
2. Adjust pH to 7.4 with HCl.
3. Adjust volume to 1L with additional distilled H<sub>2</sub>O.

### *Detaching the cells from the vessel surface:*

Detaching cells from the surface is done by either enzymatic or mechanical techniques. In general, shaking and vigorous pipetting are used for the loosely adherent cells, while cell scraping and enzymatic means are used for adherent cells. Cell scrapers may cause damage to some cells. Trypsin is a commonly used enzyme for cell dissociation. Other enzymes may be used: collagenase, dispase and TrypLE dissociation enzymes.



**Trypsin:** it is a protease enzyme found in the digestive tract of many vertebrates. It is formed in the small intestine as the enterokinase converts the trypsinogen (inactive form produced by the pancreas) to the active enzyme trypsin. In the duodenum, trypsin catalyzes the hydrolysis of peptide bonds, thus the protein breaks into small peptides. In the laboratory, Trypsin can be purified and used in biotechnological processes; it is not stable at room temperature.



TrypLE dissociation enzymes: they are microbial- produced cell dissociation enzymes, which share many similarities in kinetics with trypsin. They are superior to trypsin as they are completely free of animal and human derived components. Other advantages are their stabilization at room temperature for at least six months and that they do not require inactivation.

## Cell counting:

Cell counting is one of the skills that you have to master. You will need to do it prior to sub-culturing, fixation or preservation. A hemocytometer is the tool used to count cells manually. Trypan blue is the dye used and it is called dye exclusion method as it is picked up by the dead cells, not the live ones (the dye cannot penetrate an intact cell membrane).



*The name Trypan comes from the ability of the dye to kill the trypanosomes – the parasites causing sleeping sickness. An analog to trypan called suramin was developed to treat trypanosomiasis.*

## Hemocytometer:

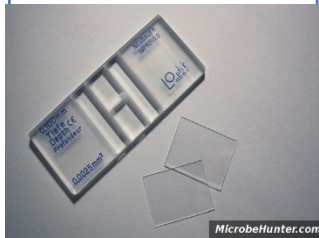
It was originally designed to count red blood cells. It consists of a thick microscope glass slide with rectangular indentations that form the chambers.



### Cell counting in practice:

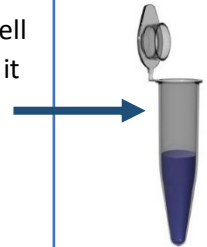
#### Preparing the hemocytometer:

- 1- Clean the surface of the hemocytometer with 70% methanol.
- 2- Moisten the cover slip with some water and fix it to the hemocytometer



#### Preparing the sample:

- 1- Take 100  $\mu$ l of the cell suspension and put it into an Eppendorf tube.
- 2- Add 100  $\mu$ l of the trypan blue solution
- 3- Mix it gently using the ninette



#### Counting:

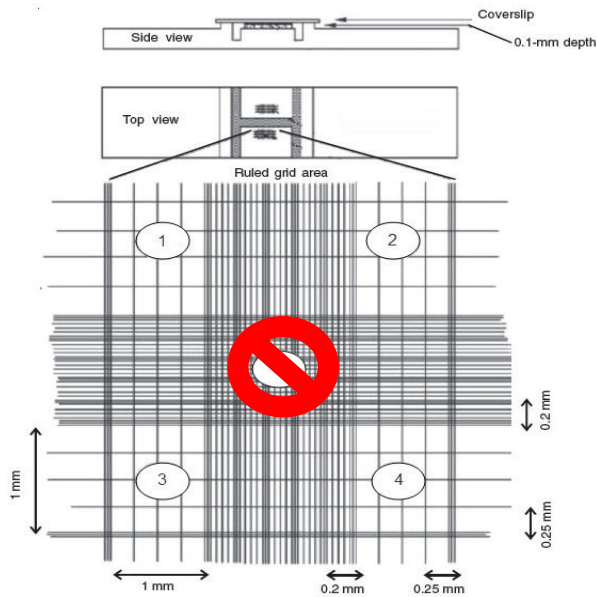
- 1- After mixing, take 100  $\mu$ l of the mixed suspension of cells and trypan blue and fill the chamber underneath the cover slip.
- 2- Using the microscope 10X power, start counting the live cells.
- 3- Move the hemocytometer in an appropriate manner so you don't miss any square.



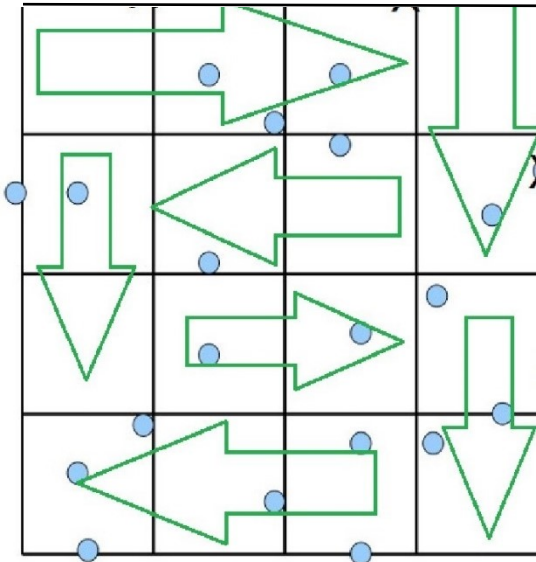
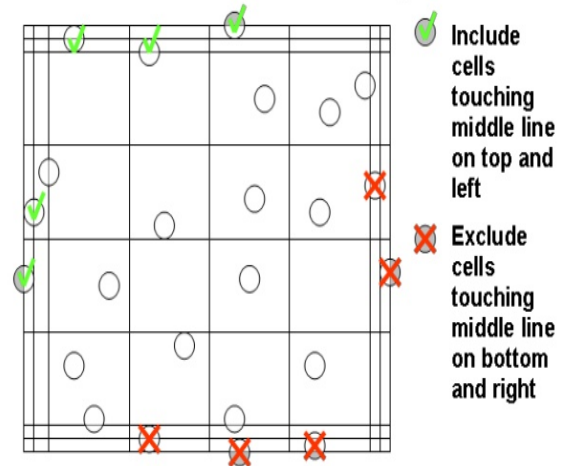


## Cell counting in practice- Cont'd:

### Counting under the microscope:



### Counting system to ensure accuracy and consistency



### Calculation of cell density:

- 1- Take the average of the four squares.
- 2- Cell density =  
Average x dilution factor x  $10^4$
- 3- The result will be the number of cells/ml
- 4- If you have for example 10 ml then you multiply the number of cells x 10, so you will have the total number of cells in 10 ml.



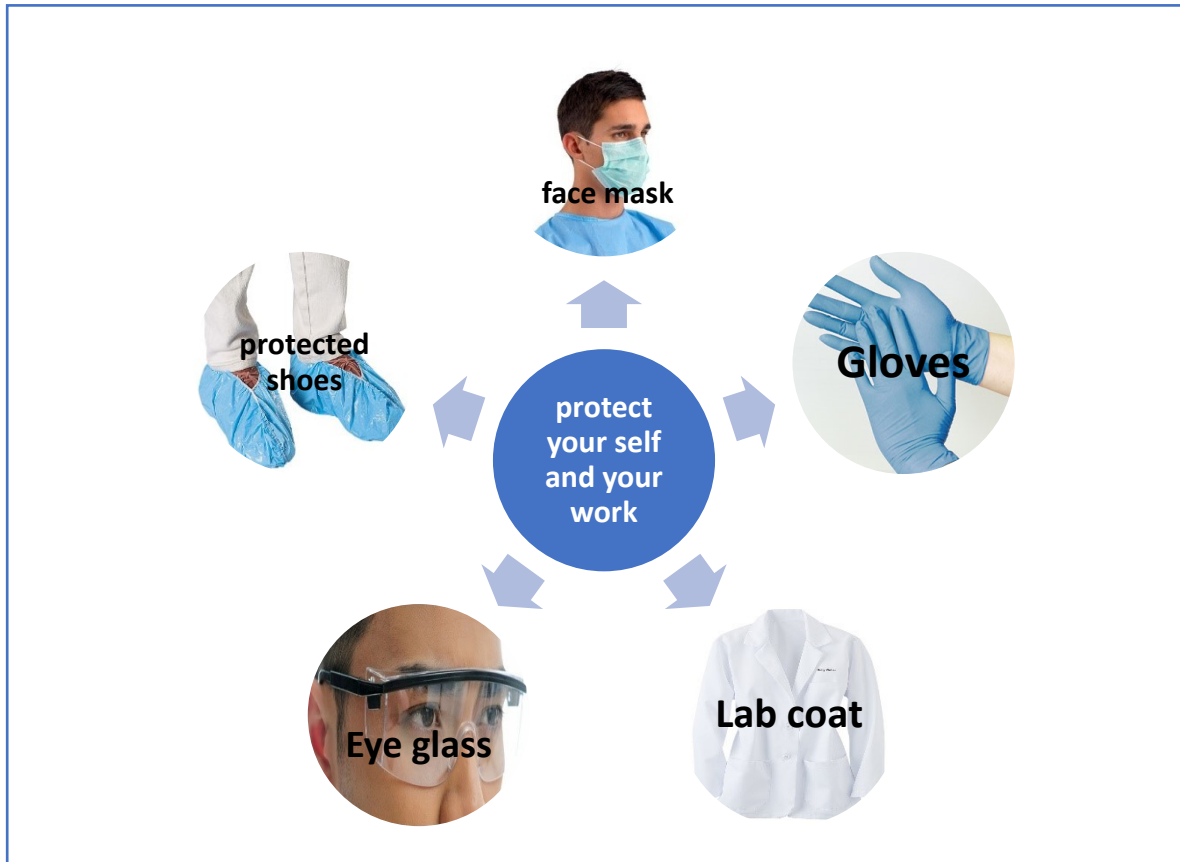
### Fan of I-phone application?

You can try “hemocytap”. Very easy application that helps you with calculation.



## ***Section 6: Safety***

### *6.1 Safety practice for personnel*



### *6.2 Working in a sterile environment*

- 1- Always wipe the hood surface with 70% ethanol before you start and after you finish.
- 2- Turn on the UV light 15 – 20 minutes before start working in the hood.
- 3- Wash your hands before you start and after you finish.
- 4- Wear the personal protective devices (mentioned above).
- 5- Wipe the outside surface of any bottle or flask you wish to use.
- 6- Make sure all the tubes, bottles and flasks are capped before using them.
- 7- Make a habit to rinse the pump at the end of the day with bleach and 70% ethanol.
- 8- Before placing the flasks into the incubator, wipe them with 70% ethanol.
- 9- Always check the water bath for possible contamination.



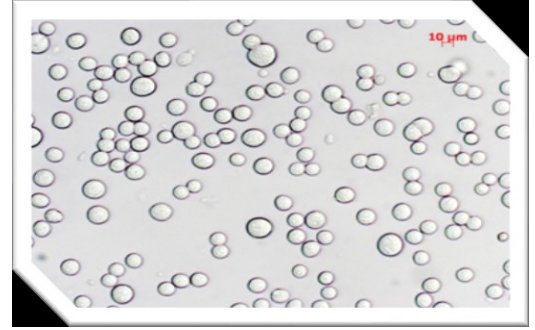
## *Cell culture full protocol technical part*



We will take PEO1 as an example of an adherent cell line we want to cultivate.

➤ *First day:*

- 1- Warm up your media (put it in water bath to reach 37°C).
- 2- Check the pump function and rinse it with ethanol 70%.
- 3- Check the incubator temperature and the CO<sub>2</sub> and adjust them if needed.
- 4- Switch on the UV light for 15-20 minutes and wipe the surface with ethanol 70%.
- 5- Wipe your gloves with ethanol 70%.
- 6- Fill a 15 ml tube with media.  
(Note: carefully label the tube with the type of cell, passage number, and date)
- 7- Take out the cyrovial containing the cells from the liquid nitrogen and quickly thaw it in 37°C water bath (section 5).
- 8- Aspirate the cells and transfer them to the 15 ml tube that contains media.
- 9- Centrifuge for 3 minutes.  
(Note: place tubes in balance before centrifugation to assure equal weight distribution among them)
- 10- Aspirate the media slowly and carefully and leave the small pellet of cells in the bottom.
- 11- Add 5 ml of new media to the cell pellet and mix it well.
- 12- Aspirate the 5 ml mixture of the media and cells and transfer it to the flask (in this case we will use a T-25 flask).
- 13- Watch the cells with the inverted microscope.
- 14- Place the flask inside the incubator and make sure you close the door.



➤ Second day:

- 1- Warm up your media (place it in a water bath to reach 37°C).
- 2- Check the pump function and rise it with ethanol 70%.
- 3- Check the incubator temperature and CO<sub>2</sub> and adjust it if needed.
- 4- Switch on the UV light for 15-20 minutes and wipe the surface with ethanol 70%.
- 5- Wipe your gloves with ethanol 70%.
- 6- Take the flasks out of the incubator.
- 7- Examine the media grossly for: color and appearance
- 8- Watch the cells under the microscope and make your comment (Section 5.3).

An example of writing a comment on your cells:

Grossly the media is orange in color, not clear and covering the whole flask surface. Under the microscope there are a lot of tiny floating cells which are most likely dead cells. Cells that are adherent to the surface look healthy with around 35-40% confluency (it means the cells cover 35-40% of the surface). Cells are all adherent, no floating component is seen, oval to polygonal in shape closely attached to each other.

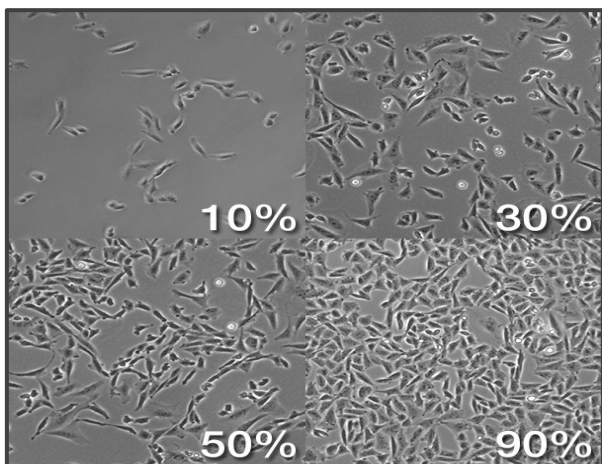
My plan is: change the media and let the cells grow more. Daily follow up.

9- Changing the media:

- a- Carefully aspirate the old media using the pump (try to move the flask and to aspirate away from the adherent surface so you don't hurt the cells).
- b- Take 5 ml of new fresh media with a sterile pipette and add it to the flask (use the same technique: i.e. add it opposite to the adherent surface).

10- Watch the cells with the inverted microscope.

11- Place the flask inside the incubator and make sure you close the door.



➔ A microscopic view of cultured cells shows different percentages of confluency. Note the shape of cells here are spindle.



Third day:

- 1- Warm up your media, PBS or any other reagent you might need (place them in a water bath to reach 37°C)
- 2- Check the pump function and rinse it with ethanol 70%.
- 3- Check the incubator temperature and CO<sub>2</sub> and adjust values if needed.
- 4- Switch on the UV light for 15-20 minutes and wipe the surface with ethanol 70%.
- 5- Wipe your gloves with ethanol 70%.
- 6- Take the flasks out of the incubator.
- 7- Examine the media grossly for: color and appearance.
- 8- Watch the cells under the microscope and make your comments (Section 5.3).

An example of writing follow up notes for your cells:

Grossly the media is orange in color, not clear and covering the whole flask surface. Under the microscope there are a lot of tiny floating cells which are most likely dead cells. Cells that are adherent to the surface look healthy with around 90% confluency (it means the cells cover 90% of the surface). Cells are all adherent, no floating component is seen, oval to polygonal in shape closely attached to each other.

My plan is: Stop growing, fix some of the cells and store the rest.

#### 9- Trypsinization:

- a- Carefully aspirate the old media using the pump (try not to move the flask and to aspirate away from the adherent surface so you don't hurt the cells).
- b- Take 5 ml of sterile PBS and add it to the cells, shake it gently and carefully aspirate the PBS (aspirate away from the adherent surface!).
- c- Repeat (B)
- d- Take 5 ml of trypsin solution and add it to the cells; wait for 3-5 minutes (you can wait longer or shorter according to the type of cells- judge by your observation).
- e- Observe the cells under the inverted microscope for detachment. The cells look round after detachment.  
(Note: you can apply also some gentle shaking as a mechanical way of detachment. You could also incubate the cells for two minutes to enhance the reaction).
- f- Stop the reaction when 50% of the cells or more are floating → by adding 7 ml of fresh media.
- g- Aspirate the whole volume and transfer the cell suspension to a 15 ml tube.
- h- Centrifuge for 3 minutes. (Note: balance tubes before centrifugation).
- i- Back to the hood: Carefully discard the supernatant volume and keep the pellet of cells



*Trypsin is a proteolytic enzyme.  
Excessive trypsinization will  
break the cells and kill them.*



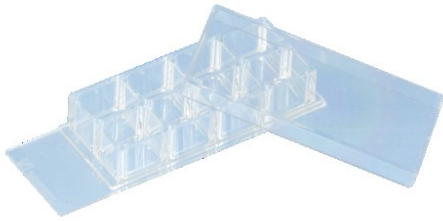
*FBS contains alpha-1-  
antitrypsin which inhibits  
trypsin*

- 10- Resuspend the cells in 10 ml of fresh media containing FBS
- 11- Count the cells (Section 5.4)
- 12- Repetitive pipetting is recommended to ensure good cell distribution

1-

A- Fixing some cells for staining and studying:

- Decide the volume of cells in each well of the eight well slide.



media suspension.

- Observe under the microscope.
- Place it inside the incubator.
- You could wait from 1-3 days to ensure good confluency. Everyday do the same follow up:
  - a- Assess the media: appearance and amount
  - b- Assess the cell growth
- If the cells covered the whole surface you can stop the growth and fix the cells.

B- Store the cells back in cryostorage:

Remember to do it slowly

- Centrifuge the rest of the media and cells for 3 minutes.
- In the hood: Aspirate the supernatant and keep the small pellet of cells.
- Divide the number of cells to number of vials you wish to use.
- Re-suspend the cells in the freezing media containing DMSO: 1ml of freezing media per vial.
- Mix the suspension well.
- Freeze at -80°C overnight
- Transfer the vials to the liquid nitrogen tank next day.



*Pre-freezing examination for bacterial  
and fungal contamination should be done.  
Examine the cells under the microscope.*

#### Steps to fix the cells in formaldehyde:

- 1- Remove the media from the slide without suction. Discard it.
- 2- Wash twice with PBS 300 µl/well. Add the PBS to the corner of the well (Don't stress the cells directly).
- 3- After removing the PBS (without suction), add 300 µl of formaldehyde to each well. *(Wait for 20 minutes)*
- 4- Remove the formaldehyde, fill each well with PBS gently, close with slide cover properly and keep it at 4°C.

## **You are done!**

Work with the cell culture with the passion that you are serving humanity by studying the cells that cause suffering for many humans. In our scope of research, we are dealing with cell lines that come from ovarian cancer, a devastating illness that kills thousands of women each year. The scientific community, health care providers, and health organizations still need a lot of information to discover the mysteries behind this disease. Be part of the solution!

## ***References:***

1- The Internet is a rich source of good references that might expand your knowledge. Some good articles are mentioned before, here are some website that might help you as well:

- <http://www.sigmaaldrich.com/canada-english.html>
- <https://www.thermofisher.com/ca/en/home.html>
- [http://www.abcam.com/index.html?pageconfig=popular\\_protocols](http://www.abcam.com/index.html?pageconfig=popular_protocols)

2- The technical part was written based on our work and facilities available in our research laboratory. You might find small differences between the procedures done in our laboratory versus others.